Diploma Thesis

Use of Sensors and sensor for Assessment of the Structural Condition of Road pavements

Submitted in satisfaction of the requirements for the degree of
Diploma Engineer
of the TU Wien, Faculty of Civil and Environmental Engineering

---

Diplomarbeit

Einsatz von Sensorik zur Bewertung des strukturellen Zustands von Straßenaufbauten

ausgeführt zum Zwecke der Erlangung des akademischen Grads
Diplom-Ingenieur / Diplom-Ingenieurin
eingereicht an der TU Wien, Fakultät für Bau- und Umweltingenieurwesen

von

Mohammad Hadi Mahmoudi Hashemi
Matr.Nr.: 01228566

Betreuung: Univ. Prof. Dipl.-Ing. Dr. techn. **Ronald Blab**
Assistant Prof. Dipl.-Ing. Dr.techn. **Lukas Eberhardsteiner**
Univ.Ass. Dipl.-Ing. **Martin Johannes Peyer**
Institut für Verkehrswissenschaften
Forschungsbereich Straßenwesen
Technische Universität Wien,
Karlsplatz 13, 1040 Wien, Österreich

Baden, 01.06.2024

Ich habe zur Kenntnis genommen, dass ich zur Drucklegung meiner Arbeit unter der Bezeichnung

Diplomarbeit

nur mit Bewilligung der Prüfungskommission berechtigt bin.

Ich erkläre weiters an Eides statt, dass ich meine Diplomarbeit nach den anerkannten Grundsätzen für wissenschaftliche Abhandlungen selbstständig ausgeführt habe und alle verwendeten Hilfsmittel, insbesondere die zugrunde gelegte Literatur, genannt habe.

Weiters erkläre ich, dass ich dieses Diplomarbeitsthema bisher weder im In- noch Ausland (einer Beurteilerin/einem Beurteiler zur Begutachtung) in irgendeiner Form als Prüfungsarbeit vorgelegt habe und dass diese Arbeit mit der vom Begutachter beurteilten Arbeit übereinstimmt.

Baden, im June 2024 Mohammad Hadi Mahmoudi Hashemi

Acknowledgements

This project provided me with comprehensive practical knowledge of various concepts in pavement monitoring with a particular focus on the use of sensors for assessment within this monitoring.

At this juncture, I want to convey my sincere appreciation to those who have played a significant role in shaping both my personal and professional development during my diploma semester and throughout my academic path.

First and foremost, I would like to express my gratitude to Univ. Prof. Dipl.-Ing. Dr. techn. Ronald Blab for the opportunity to conduct this diploma thesis at the Institute of Transportation Sciences, in the Research Division for Road Engineering.

I would also like to extend my sincere thanks to Assistant Prof. Dipl.-Ing. Dr. techn. Lucas Eberhardsteiner for providing me with the opportunity to conduct this diploma thesis at the Institute of Traffic Sciences, Department of Highway Engineering.

First and foremost, I would like to express my gratitude to Assistant Prof. Dipl.-Ing. Dr.techn. Lucas Eberhardsteiner for providing me with the opportunity to conduct this diploma thesis at the Institute of Traffic Sciences, Department of Highway Engineering.

Furthermore, I would like to thank Univ.Ass. Dipl.-Ing. Martin Johannes Peyer for the continuous guidance and support throughout this project timeline. I am very grateful for his valuable guidance, constructive and detailed advice that helped me find the right path towards the completion of this thesis.

Lastly, I would like to thank my wife for her patience and motivation throughout my degree, and my family for their continuous support.

Baden, June 2024

Mohammad Hadi Mahmoudi Hashemi

Abstract

Effective pavement health monitoring is crucial for the analysis and management of road infrastructure. The assessment of road condition provides an objective foundation for justifying decisions within the framework of action planning. This proactive approach can yield substantial cost and time savings by detecting pavement wear and damage at their incipient stages.

Recent years have witnessed a growing emphasis on in situ pavement health monitoring due to its effectiveness. The focus of this work is on describing some widely used sensor types and sensor systems, as well as summarizing promising installation and application concepts for these sensors within the structural health monitoring of road pavements. These methodologies encompass, among other aspects, the calculation of horizontal and vertical strains within pavement and the determination of layer stiffnesses based on measured acceleration of longitudinal waves from vehicle loads. These techniques are often complemented by data collected from moisture, temperature, and traffic-related sensors.

The review also addresses crucial issues surrounding sensor selection, installation and protection during road construction and throughout the service life to minimize damage. Valuable insights and experiences gained from literature reviews and field demonstrations are synthesized.

By strategically integrating these sensor technologies, engineers can forecast the optimal timing for pavement rehabilitation, potentially resulting in substantial cost savings during infrastructure reconstruction. The principal aim of this thesis is to furnish a comprehensive and up-to-date critical literature review of some of the most diverse sensors employed in pavement health monitoring. It considers accumulated experiences as a foundational reference point and outlines the methodology employed for literature collection and analysis. Additionally, it provides descriptions and insights into key sensor characteristics for pavement monitoring, particularly for damage detection purposes. These characteristics encompass elements such as energy supply, detection methods, hardware and network architecture as well as performance validation procedures.

Zusammenfassung

Die effektive Überwachung des Straßenzustands stellt eine wichtige Grundlage für die Analyse und Verwaltung der bestehenden Straßeninfrastruktur dar und bildet mit der darauf aufbauenden Zustandsbewertung eine objektive Grundlage zur Rechtfertigung von Entscheidungen im Rahmen des kosten- und maßnahmenoptimierten Erhaltungsmanagements. Dieser proaktive Ansatz kann erhebliche Kosteneinsparungen und Zeitersparnisse ermöglichen, indem er den Verschleiß und die Schäden an der Fahrbahn in ihren Anfangsstadien erkennt, wodurch frühzeititig entsprechende Maßnahmenplanungen zielgerichtet initiiert werden können.

Aufgrund ihrer Effektivität und ihrer Leistungsfähigkeit kommt der messtechnischen in-situ-Überwachung eine immer größere Bedeutung bei der Zustandserfassung von Straßenaufbauten zu.Während einige in-situ-Verfahren zur messtechnischen Zustandserfassung bereits flächendeckend angewendet werden (z.B. FWD), befinden sich viele andere Verfahren noch in der Entwicklungsphase. Mehrere vielversprechende Ansätze nutzen im Straßenaufbau eingebettete Sensoren und Sensorsysteme um Dehnungen, Beschleunigungen, Temperaturen, etc. zu messen und durch Anwendung unterschiedlicher Auswertealgorithmen entsprechende Zustandsgrößen zu bestimmen.

Im Rahmen dieser gegenständlichen Literaturrecherche wird zunächst auszugsweise auf einige allgemeine Ansätze bzw. angewendete Strategien zum Erhaltungsmanagement von Straßen eingegangen. Der Hautpteil dieser Arbeit beschäftigt sich jedoch mit einer Erfassung und Beschreibung von einigen der am häufigsten angewendeten Sensorarten bzw. Sensortypen sowie der Beleuchtung entsprechender Kriterien für die Auswahl, die Installation und Nutzung der Sensoren und der zugehörigen Devices sowie verschiedener Aspekte zu den Themen Einbaueignung, Energieversorgung, Hardware- bzw. Netzwerkarchitektur, Erfassungsmethoden und Auswertealgorithmen. Anschließend werden einige vielversprechende Ansätze bzw. Forschungsprojekte hinsichtlich der Anwendung eingebetteter Sensoren zur strukturellen Zustandserfassung von Straßen im Rahmen einer umfassenden Literaturübersicht zusammengefasst und diskutiert.

Contents

Chapter 1: Introduction

1.1. Introduction

As a method for assessing the structural integrity of structures like bridges, buildings, towers, dams and offshore facilities SHM is extensively applicable. Traditional SHM systems have monitored and recorded external conditions and the resulting structural responses using wired sensors strategically placed within the structures. Bridges and buildings have been the most frequently used SHM applications in civil infrastructure among these structures. Dynamic behaviour of bridges under unpredictable mechanical and environmental loads that might lead to unexpected behaviour has been characterized using SHM [1].

Moreover, in the realm of road infrastructure, Structural Health Monitoring (SHM) continues to assume a significant and growing role, offering essential insights into structural conditions impacted by a combination of vehicle and environmental loads.Under continuous traffic and/or environmental loads, pavements have a tendency to degrade over time. Early pavement distress and damage detection enables transportation authorities to create more efficient pavement maintenance and rehabilitation plans, resulting in considerable cost and time savings. The structural health monitoring (SHM) idea may be thought of as a methodical approach for determining the structural health of pavement infrastructure systems and its state [2].

For example, Zonzini et al. [3] compared a piezoelectric sensor to a MEMS sensor for vibration-based SHM, illuminating the viability of MEMS as a SHM technology with a notable cost decrease. Another illustration is provided by Girolami [4], which is the original source and has been verified in production. It employs Wi-Fi, a short-range wireless technology that consumes 0.5 W of electricity for data transmission. It is not battery-operated and does not require power cabling.

Currently, non-invasive and intrusive technologies make up the majority of sophisticated sensing technology for pavement monitoring. The non-intrusive techniques which are particularly practical since they are non-destructive and simple to use include visual inspection, pneumatic tubes, cameras, light barriers, falling weight deflectometer test (FWD) and radar systems among others. They are however, partly susceptible to the effects of the weather and have some other disadvantages.

The structural health of pavements under repeated traffic loads and other environmental conditions may be observed using invasive technologies such as sensors placed in the

pavement. However, there are drawbacks to using connected sensors for long-term SHM as well as additional financial and security issues, especially when using conventional piezoelectric sensors. They are very expensive and susceptible to failures or damages due to certain environmental or installation conditions (high temperatures, high loads due to compaction, …). Micro-electromechanical sensors (MEMS) are cheaper than conventional sensors and they are smaller, more compact and have low energy consumption.

Therefore the use of more cost-effective MEMS sensors and sensor systems that are both long-lasting and affordable in favour of pricy piezoelectric ones is a significant trend in SHM [2].

Subsequently in many of the before mentioned application fields, research work has been conveyed on the development of suitable MEMS sensors and sensor systems as well as on their applicability.

This paper first provides an overview of health monitoring and maintenance of road pavements. It describes the different types of road damages, the methods for monitoring and damage detection, experimental approaches, and road-condition evaluation and management systems. Chapter 3 is the main focus of this work and provides an overview of the different sensors and sensor systems used in assessing the structural conditions of roads. It describes accelerometers, strain sensors, temperature sensors, and moisture sensors, among others, as well as the algorithms for analysing the measured signals. Chapter 4 provides an overview of various research projects that focus on the condition monitoring of road pavements using instrumented test tracks or test sections. It describes specific projects and their results, which have contributed to the development and validation of monitoring technologies and methods The concluding chapter summarizes the key findings of the work and provides an outlook on future research opportunities and practical applications. It emphasizes the importance of integrating modern sensor technology into road infrastructure management to improve efficiency and safety.

Chapter 2: Overview of Health Monitoring and Maintenance Concepts Used for Road Pavements

2.1. Health Monitoring in General

There are four levels as part of health monitoring according to Plankis and Heyliger as follows.

a. Determining the existence of damage

b. Pinpointing the site of damage

c. Assessing the damage of health monitoring

d. Estimating how long the structure will continue to function

To address the initial three levels, methods for health monitoring can be categorized into global and local health monitoring. the idea behind global health monitoring is to employ technology to identify changes in stiffness, mass and other dynamic global qualities brought on by serious structural damage. It is often not necessary to know the precise site of harm or where it could occur for purposes of monitoring global health. Resonant frequencies, mode shape vectors, mode-shape curvatures, a dynamic flexibility matrix, update of modal parameters and acoustic characteristics are significant modal attributes for global health monitoring. In conclusion, global damage detection approaches try to find damage that is large enough to change the attributes of significant portions of the structure or the structure as a whole. These techniques track how structures react to unnatural or intentional excitations and detect deterioration by examining changes in the dynamic characteristics of the structure that is being assessed [7]. Local health monitoring involves monitoring the progression of damage and assessing the extent of damage at predetermined or anticipated locations. The investigation of particular faults found in a chosen location or structural component is the main objective of local approaches. Technically, traditional Structural Health Monitoring (SHM) based on wired sensors represents a form of local health monitoring technology [7].

2.2. Types of Distresses Occurring in Road Pavements

Damages and defects are categorized into groups of characteristics and subsequently specific individual characteristics are assigned to these characteristic groups depending on the type of covering. Damages are defined as undesirable changes to the intended condition of the track covering caused by material loss or material breakage. Conversely, defects are undesired alterations to the intended condition of the track covering that occur without any loss of

material substance in the track covering. Damages in pavement vary significantly based on the type and load of the road structure [8].

Preservation measures for asphalt pavements typically fall into two categories: surface and structural damage. Additionally, based on their appearance, these issues can be further classified as longitudinal unevenness, transverse unevenness, crack formation, and surface damage [11].

Concrete pavements primarily experience irregularities such as breakouts, spalling, step formation, corner breakouts, and edge breakouts, as well as cracks such as longitudinal cracks, transverse cracks, map cracking, edge cracks, and joint cracks in the roadway.

Block pavements may experience ruts, settling, bulging, as well as issues like faults, patching, and breakage of cobblestones [11].

The condition characteristics can be fundamentally divided into crack formation, surface damage, flatness defects, and Skid resistance or friction. The following selected characteristics are defined below. [9].

- Crack damage: During the condition assessment, a crack damage is documented either as a single crack (longitudinal, transverse or diagonal) or as an extensive crack (irregular crack or network crack).

Single cracks can range from fine to gaping fractures. They can be classified as transverse, longitudinal or diagonal based on their position and orientation on the road. Cryogenic tensile stresses caused by limited thermal contraction at low temperatures dissipate slowly. Rapid cooling rates can lead to the material's strength limit being exceeded. The result is transverse cracks that occur at regular intervals on the road surface. Longitudinal cracks are caused by the combination of thermal and traffic-induced tensile stresses on the underside of the pavement layer in the wheel track and/or on the top of the layer adjacent to the wheel track, occurring at a distance of 0.5 to 0.9 meters. A single crack is classified as a diagonal crack when the line connecting its two ends is neither clearly parallel nor perpendicular to the lateral edges of the track covering. If there is uncertainty, the crack should be recorded as a diagonal crack. Cracks allow water penetration, leading to progressive damage as the water freezes during frost conditions. When the crack width reaches around 2.0 cm, road safety may be affected.

Network cracks are interconnected cracks caused by fatigue. Material fatigue is essential for determining the structural lifespan of the road surface and for designing layer thicknesses.

Radial tensile stresses are generated on the underside of the sub-base layer, subjected to repeated traffic loads, lead to the formation of fine cracks and a gradual decrease in stiffness and load-carrying capacity. The accumulated cracks eventually migrate to the surface, where they become visible. Since addressing network cracks requires significant preservation measures, it is recommended to delay the occurrence of this type of damage by using a more robust design, thus prolonging its appearance over time [9].

- Surface damages:

Surface damages refer to material losses in the wearing or base layers, such as thinning, breakouts, spalling and a lack of skid resistance due to binder bleeding. Surface damages may occur relatively early compared to other characteristics, but they are generally not critical for the overall lifespan of the road structure due to their gradual or linear progression. Furthermore, certain damages are fixed during regular maintenance, while others are commonly addressed using surface layer measures within the Road Management System.

- Evenness:

Longitudinal evenness is utilized to evaluate the unevenness along the length of the roadway and has effects on road safety, driving comfort and structural stress on the road. Uneven road surfaces can cause wheel lifting, leading to a loss of traction between the tire and the road. This is more evident during curves which poses a risk to driving safety. The longitudinal evenness of a road is influenced by various factors, including road construction (materials and execution), climatic conditions (heat, frost, water), traffic and the uniformity of the underlying surface.

Unevenness in the transverse direction is primarily represented by ruts, which are vertical deviations from the intended cross-section within the wheel tracks, running continuously along the length of the roadway. Ruts have an impact on driving safety and offer insights into the deformation of the road structure. In rainy conditions, water collects in the ruts heightening the risk of aquaplaning or loss of control over the vehicle particularly at higher speeds. The causes of rut formation include wear due to mechanical stress, plastic deformation from traffic loads and high temperatures. Its compaction after traffic is accumulated on the road. Ruts can develop in the surface layer, the base layer or the unbound layers of the pavement [9].

- Skid resistance or friction:

Skid resistance refers to how the road surface influences the transfer of driving, braking and lateral forces between the tire and the road. Skid resistance measurements are performed globally on wet road surfaces due to the generally high skid resistance level on dry roads. Additionally, the friction values are heavily influenced by the vehicle's motion state or slip condition. Slip refers to the percentage difference between the circumferential speed of the wheel and the vehicle's speed. Force transmission reaches its peak at a slip value of 10-20% (in wet conditions) and decreases with increasing slip until it reaches the sliding friction coefficient at 100% slip (locked wheel) Due to road safety concerns. Skid resistance plays a vital role in identifying and mitigating accident-prone hazardous locations [9].

2.3. Existing Pavement Monitoring and Damage Detection Methods

Data collection on pavement condition is often a costly and time-consuming task. Any Pavement Management System (PMS) must have the proper pavement assessment methodology. While the development of new reference and visualization tools as well as a large increase in computational power has led to a steady improvement in Maintenance and repair models, progress in improving the data gathering of a PMS in an accessible way has lagged. Since 1970s, obsolete and low-resolution condition data have frequently limited PMS forcing them to make a lot of assumptions and extrapolations. There are two primary categories that may be used to categorize current pavement examination techniques [10]. Manual inspection (visual status recording), namely Pavement condition data collecting through techniques where individuals are actively engaged in the inspection or measurement of pavement characteristics [10]. Assessments of the state of a location distresses can be done either while walking on the pavement (on-foot surveys) or while driving (windshield surveys).

Automated Technical Inspection is the process of gathering information on the state of the pavement using image technology or other sensor devices. In the following sections, some exemplary methods for damage detection will be explained:

2.3.1. Visual Inspection

The visual assessment of road surfaces is an ongoing and dynamic procedure, systematically conducted to assess the state of road infrastructure, ensuring timely actions are taken to uphold road safety and durability. Qualified professionals and engineers are responsible for conducting this visual inspection, with various organizations and authorities undertaking these assessments based on their jurisdiction and specific regional responsibilities. To perform visual condition assessments effectively, it is advisable to create a data collection form that allows recording all pertinent information. When documenting damages and deficiencies, the following approach can be employed.

- Determination of location / stationing: The first step in inspecting a damage or deficiency is to determine the location and document it in the data collection form.
- Determination of the position in the cross-section
- Determination of the pavement type (Asphalt pavement, concrete pavement and block pavement)
- Condition assessment

The approach to data collection varies based on the type of pavement and the characteristics of the damage or deficiency [2].

In visual condition assessments, sections are defined based on a minimum length of 25 to 50 meters, depending on the actual damages. On the other hand, measurement-based assessments involve continuous recording of damages, typically requiring mathematical delineation using various algorithms, such as calculating a moving average and forming condition classes [11].

2.3.2. Falling Weight Deflectometer

Falling Weight Deflectometer (FWD) is globally recognized as the most reliable and effective non-destructive testing (NDT) method for measuring pavement deflection and bearing capacities [12]. The operating principle of the falling weight deflectometer consists of applying a load pulse to the road surface and measuring the resulting elastic deformation. The load pulse is generated by dropping a weight from a certain height onto a spring system consisting of rubber buffers, which transmit the load into the road construction via a circular load plate with a diameter of 30 cm. The magnitude of the applied load depends on the drop height and the mass of the falling weight and can be controlled using these two variables. The maximum value of the elastic deformation (deflection) is measured using a deflection gauge located at the centre of the load and a number of radial deflection sensors (geophones). By connecting the measured

values of the individual sensors, the so-called deflection is obtained. Depending on the magnitude of the applied load pulse, the measured deflections provide information about the structural condition of the road construction [12]. The standard load of 50 kN with a load duration of approximately 25 ms corresponds to the load of a heavy vehicle traveling at 50 km/h. FWD measurements allow for determining the load-bearing capacity of all layers of the road surface. Comparing the load-bearing capacity of different measurement sections, detecting structurally invisible damages. It also captures load-bearing behaviour, identifying potential causes of damage and selecting suitable measures within the framework of maintenance planning. FWD measurements are typically carried out every 25 m, and up to 50-100 m is possible in homogeneous conditions [11].

2.3.3. Image-Based-Monitoring

Since pavement surface cracking is one of the pavement distresses that may be easily documented by imaging, image-based health monitoring technologies have been around for more than 30 years. The Distress Identification Manual, created by the Long-Term Pavement Performance Program (LTPP) of the U.S. Federal Highway Administration (FHWA), offers a consistent and standard means of gathering and reporting pavement distress data for the LTPP. Every state highway agency basically uses this manual, while there may be minor differences in how each agency collects PMS distress data. It started as a manual or windshield survey and developed into the taking of analogue photos or videotapes, which were subsequently processed to extract information on pavement cracking. The present state-of-the-art involves employing high-speed cameras installed on a customized data gathering van travelling at highway traffic speed to capture 2D digital photographs of pavements. A compression subsystem is used to reduce the size of the high-resolution digital photographs of the pavement surfaces without reducing quality before they are saved. Images are subsequently analysed by a variety of algorithms to get summary statistics and information on cracking, which is then stored in the surface distress database (can be linked to PMS) [13].

2.3.4. RoadStar (Österreich)

The RoadStar Device is a dynamic measurement system used for the acquisition of the most important surface properties as well as tracing parameters. The installed grip measurement device allows for continuous determination of the friction coefficient in the longitudinal direction. RoadSTAR is built on a 2-axle truck. Above the rear axle is a water tank and at the rear in the right wheel track is the grip measurement device, a modified Stuttgart friction meter.

RoadSTAR can perform grip measurements in flowing traffic at measurement speeds ranging from 30 km/h to 120 km/h. There are currently only two of these measuring systems in use worldwide, both of which are deployed on the road network in Austria [11].

The RoadStar vehicle can determine various characteristics of the road, including skid resistance (grip), transverse evenness (rut depth), theoretical water depth in ruts, longitudinal evenness, macrotexture, curve radius, curve curvature, cross slope, longitudinal slope, road environment objects (traffic signs, road markings, etc.), as well as road cracks of 1 mm and potholes.

The mobile mapping system RoadSTAR is also used for capturing road surface images in Austria which uses a line scan camera in combination with permanent lighting devices. Both mapping systems allow continuous capturing of road surface images even at high velocities (about 80 km/h). Images of the mapping device are transformed to have a fixed metric correspondence to comply with federal regulations. Therefore, standardized images in Austria correspond to a metric resolution of 4 meters in width and approx. 3 meters in height. RoadSTAR images are captured with roughly 900 pixels per meter. This system is also carrying out data acquisition in Switzerland [12].

Due to the size of the RoadSTAR measurement system, it can mainly be used on main roads with flowing traffic or on airstrips (runways). Its high daily mileage makes it perfect for capturing large road networks [11].

2.3.5. Ground Penetrating Radar (GPR)

Ground-penetrating radar (GPR) as a non-destructive technique and is widely employed for infrastructure condition assessment due to its high effectiveness. This geophysical method operates by utilizing electromagnetic waves to detect objects located within the shallow subsurface. Electromagnetic waves are transmitted into the survey medium by GPR, which subsequently captures reflected signals from various layers and objects. The properties of the received signal are determined by the electromagnetic characteristics, depth and shape of the reflecting object. GPR equipment is capable of investigating several meters below the surface, even in materials that are non-homogenous and have the ability to absorb radar signals [12]. Frequencies in the range of 100 MHz to 2 GHz are frequently employed in civil engineering applications. GPR systems utilize antennas with frequencies ranging from 10 MHz to 1000 MHz to examine road pavements, tunnel liners and utilities on a meter-scale. On the other hand, antennas with frequencies between 900 MHz and 2.0 GHz are utilized to obtain data regarding

the upper 0.3 to 1 meter layer of the pavement [14]. Depending on the depth of application, there are two main GPR system types: ground-coupled and air-coupled GPR systems. Typically, air-coupled antennas (ranging from 1 to 2 GHz) are mounted on mobile vehicles and positioned at a distance of approximately 0.5 to 0.6 meters above the surface. Conversely, ground-coupled antennas (ranging from 10 MHz to 2 GHz) are typically used in contact with the surface or positioned just above it at a distance of 2 to 5 centimetres. One of the advantages of GPR in infrastructure condition assessment is its ability to acquire data reliably and rapidly at driving speeds by utilizing air-coupled antennas.

GPR is primarily utilized in pavement assessment for the following applications:

Detecting cracks, measuring pavement layer thickness, assessing moisture damage, identifying voids, Detecting subsidence and sinkholes [12].

2.3.6. Infrared Thermography

Infrared thermography (IRT) is also a non-destructive evaluation technique employed in the assessment of infrastructure condition. The information can be gathered by a camera affixed to a tripod, Unmanned Aerial Vehicles (UAVs) or installed at top of a vehicle. These benefits facilitate quick inspections without disrupting traffic. Infrared thermography identifies surface and subsurface flaws and damages by detecting the emitted radiation in the infrared range of the electromagnetic spectrum. The defects are pinpointed by detecting the thermal contrast of the surfaces being inspected. IRT can be performed using either an active or passive approach, depending on the heat source. The active approach involves introducing an artificial heat/cooling source to supplement the object of interest with extra energy, followed by detecting changes in the thermal signature at various locations. On the other hand, the passive approach entails the collection of radiation emitted from the surface of the object, utilizing natural heat sources like solar heating. The drawback of IRT is its inability to provide details about the depth of the defects, as it only records radiation from the surface [12].

IRT is primarily used for pavement evaluation in applications like delamination detection, segregation, cracking detection and debonding detection.

2.3.7. Ultrasonic Pulse-Echo Test

Ultrasonic test involves transmitting ultrasonic waves through a substance, which are subsequently identified and examined. The very small stresses generated within the tested

medium enable us to presume a linear correlation between stresses and strains. Additionally, the velocity of ultrasonic waves at a specific temperature and pressure serves as a distinctive material attribute. The ultrasonic testing apparatus comprises a display unit (oscilloscope), a pulser-receiver, and transducers. The pulser-receiver generates electrical pulses that are transformed into a sound wave by the transducer (as a sender) [15]. This sound wave travels through the sample and is subsequently reconverted into an electrical signal by the transducer (as a receiver) at the opposite end of the specimen. The key result of the ultrasonic assessment for determining stiffness is the time it requires for waves to pass through the specimen, a measurement that necessitates determination for both longitudinal and transverse waves. To achieve accurate flight times for the specimen, it is essential to measure the system delay time (t_0) and subsequently deduct it from the total travel time (t_{tot}). The system delay time encompasses the travel duration in the absence of the specimen. In the following, the fundamental equations used to quantify the elastic stiffness properties through ultrasonic testing are presented. Velocities of the longitudinal (V_L) and transverse waves (V_T) can be calculated by utilizing the respective arrival times ($t_{L,tot}$and $t_{T,tot}$) and the specimen's length, which is equivalent to the travel distance (L) as shown below:

$$V_i = \frac{L}{t_i} = \frac{L}{t_{i,tot} - t_{i,0}} \qquad (2-1)$$

Wavelength (λ_i) can be calculated based on the frequency (f) using the following equation:

$$\lambda_i = V_i / f \qquad (2-2)$$

Longitudinal bulk waves exhibit similarity to waves propagating through infinite media, where lateral deformation is constrained. Longitudinal bar (extensional) waves resemble waves propagating through slender rods, allowing lateral deformation [15]. In contrast to these two categories, propagation of transverse waves is notably less influenced by the geometric attributes of the tested specimen. Hence, in the case of an isotropic and homogeneous elastic material, the velocity of longitudinal bulk waves (V_l) as well as the velocity of transverse waves (V_T) can be connected to the stiffness tensor component C_{1111} (C_{1212}) and the mass density ρ through the following relationship:

$$V_l = \sqrt{\frac{C_{1111}}{\rho}} \qquad V_T = \sqrt{\frac{C_{1212}}{\rho}} \qquad (2-3)$$

Elastic modulus (E), the Poisson's ratio (ν), the bulk modulus (K) and the shear modulus (G) can be obtained by:

$$E = \rho \times \frac{V_T^2 \times (3 \times V_L^2 - 4 \times V_T^2)}{V_L^2 - V_T^2} \qquad (2-4)$$

$$\nu = \frac{V_L^2 - 2 \times V_T^2}{2 \times (V_L^2 - V_T^2)} \qquad (2-5)$$

$$K = \frac{\rho}{3} \times (3 \times V_L^2 - 4 \times V_T^2) \qquad (2-6)$$

$$G = \rho \times V_T^2 \qquad (2-7)$$

Ultrasonic pulse-echo (UPE) inspection technique is widely recommended for the in-situ and full-field evaluation of rigid pavements and concrete structures as a non-destructive testing method. This method employs a pulsed or Q-switched laser to generate ultrasonic waves in a remote and non-contact manner [12]. The pulse-echo apparatus is composed of a scanning head with two lasers for scan detection, which is affixed to a two-axis translation stage. By utilizing the aforementioned stage, the inspector can automate the scanning of the inspection area. The pulse-echo method has been employed to detect and survey interface defects in pavement structures. The inspection is conducted at high speeds of up to 1600 points per second with a specific interval rate of 0.25 mm.

The primary applications of ultrasonic waves for road transportation assessment are:

Concrete thickness, Steel reinforcement mapping, Delamination/debonding, Joint diagnostics of concrete deterioration and spalling, Flaw detection and defects, Detection of urban sinkholes, Material properties and asphalt compaction [12].

2.3.8. Profilometer

Inertial Profilers (IP) or Road Surface Profilers (RSP) are non-destructive testing methods that provide measurements of the International Roughness Index (IRI) and rut depth. IRI is metric used to assess pavement quality and quantify pavement roughness in terms of vertical deviations. On the other hand, pavement texture can be characterized by the use of rut depth. Various indices are utilized to describe these characteristics, including MPD (Mean Profile Depth), MTD (Mean Texture Depth) and RMS (Root Mean Square). Typically, the profilometer is mounted on a vehicle that must continuously move along the road at a specific

velocity to meet the required standards. The equipment comprises laser-based sensors used for profile measurement [12].

The primary purpose of utilizing this technique is to identify following surface damages in flexible pavements:

Cracking detection, Disintegration such as potholes, ravelling and bumps and sags, Deformation. It can also be used to determine shoving and corrugation, depressions, Segregation and roughness, Cross-sectional profile slope and texture of the lane [12].

2.3.9. Electrical Resistivity Tomography

There are various and unique fields of application for Electrical Resistivity Tomography (ERT), ranging from civil engineering to hydrology and geology [12]. The ability to accurately identify anomalies in terms of their geometry both vertically and horizontally is greatly limited by very low resolutions. Consequently, this constraint is taken into consideration when attempting to detect small or shallow cracks on a surface or at shallow depths. The foundation of ERT lies in the transmission of electrical current through metal poles, also as current electrodes into the soil which is then detected as energy by the potential electrodes. The most intricate aspect of ERT is the typical need to insert metal electrodes into the medium. Consequently, in both concrete and asphalt it is necessary to drill holes to introduce the electrodes and establish contact with the material. Air cannot conduct electric current effectively due to its high electrical resistivity, as a result poor contact between the electrodes and the medium will impede the downward flow of electrical current. Asphalt acts as an electrical insulator which renders the measurement of electrical resistivity values impossible. Four distinct scenarios were simulated by Park et al. [16] including a field ground with and without a cavity as well as concrete pavement with and without a cavity. The outcome demonstrated that all present cavities were detected and precisely outlined. ERT is a highly effective method for evaluating pavement condition, particularly in distinguishing between cavities filled with air or water.

The principal uses of the ERT technique in road inspection include:

Road pavement instability such as bedrock fractures and depressions, Cavities and sinkholes, Stratified layers, Grouting injection and Degradation of concrete slab [12].

2.3.10. Stuttgart Friction Tester (Stuttgarter Reibungsmesser SRM)

This grip measurement system consists of a truck with a water tank and a longitudinally mounted measuring wheel on the rear that is attached to a parallelogram suspension. Measurements are performed using a locked towed wheel on a wetted road surface. SRM has been the standard measurement method in Austria and Germany for a long time but was later replaced by RoadSTAR. Currently, the Stuttgart Friction Tester is only used as a standard measurement method in Switzerland [17]. Originally, SRM was operated only with a locked towed wheel. However, there are now modified versions (such as RoadSTAR) that allow measurements with various slip conditions and simultaneous measurements in both the right and left wheel tracks. By default, SRM simulates full braking without an anti-lock braking system (ABS) by intermittently blocking the measuring wheel during constant speed measurement. The cycle length is 25 m, with 20 m being measured in a blocked state and 5 m allowed to roll freely. The average coefficient of friction is determined from the last 15 m of the blocked distance. The braking torque is measured during the blocked state. With knowledge of the measuring wheel's half-wheel radius, the braking force transmitted between the tire and the road can be calculated from the braking torque. Dividing the braking force by the known wheel load yields the coefficient of friction μSRM, in accordance with Coulomb's friction law [17].

2.4. Experimental pavement monitoring and damage detection methods

In the field of transportation engineering, measurement and evaluation of road conditions are critical for ensuring safe and efficient mobility. Traditionally, road condition assessment has been carried out through various established methods such as visual inspections, road surveys and instrumented vehicles. However, with the advancement of technology there is growing interest in developing new approaches for road condition recording and analysis.

In this regard, several research projects have emerged that explore innovative methods for measuring and evaluating road conditions. In addition to the established measurement methods described above, some of the new techniques being developed to record road conditions are reviewed. In the following sections, some of them will be explained as examples.

2.4.1. Acoustic Signal Analysis

The implementation of a new approach for assessing health of road pavements is monitoring vibrations and noise brought on by traffic as described by Fedele et al [18]. This technique falls under the category of an acoustic technique since it is based on the idea of acoustic signals which is described in their work as the spectral content of acoustic signals emanating from a road pavement under conditions of automobile traffic. The evaluation of this signal's evolution over time offers crucial information about the ways in which roads respond to traffic, or more specifically, about the state of their structural health. In this initial stage, during rapid loading in-lab testing, acoustic signals were detected by a sensor installed in a hole drilled both in uncracked and cracked slabs of asphalt concrete (EN 12697-22:2007). These signals were captured and processed simultaneously in order to reproduce the acoustic signal of the slab being tested. The findings indicate the potential for creating a novel acoustic technique that would enable determining a road pavement's structural health state from its acoustic signature. A set of dense graded friction course (DGFC) slabs were used as a pavement sample and a wheel tracking machine also known as (WTM) was used as a source of vibration and sound. This apparatus is made to produce/compact slabs in accordance with Colorado Procedure-Laboratory 5116-10 and perform the rutting test (according to EN 12697-22) [18].

Comparative analyses were carried out to compare the data before and after the appearance of cracks. Based on the obtained results, it can be concluded that cracks seem to lead to a decrease in the peak frequency and an increase in the peak amplitude of certain vibration phenomena. These vibrations are generated at the wheel-pavement interface, propagate through the slab which are captured by the microphone. Furthermore, higher loads appear to correspond to higher peak amplitudes. However, the peak frequency does not show significant variations based on the applied load. These findings are promising as they suggest the possibility of associating a specific acoustic signature with a particular pavement condition. This approach relies on the characterization of course properties and the assessment of the pavement's structural health, enabling effective structural health monitoring [18].

2.4.2. Multispectral Pictures / Images Using Unmanned Aerial vehicle (UAV)

In order to distinguish between intact and damaged pavements, Pan, et al [19, 20] used multispectral image-based Machine Learning algorithm using photos obtained by drones. The Support Vector Machine SVM, Artificial Neural Network ANN and Random Forest (RF)

algorithms were assessed and contrasted on RGB (Red, green, blue) and multi-spectral pictures. On multispectral pictures, it was determined that RF outperforms the other two methods with a high degree of accuracy. The spatial resolution of the pavement picture was inferred to additionally have a decisive role in the classifier's performance in addition to the feature set. In order to distinguish between three different types of pavement cracks, Xhang et al. [21] built a Reliability Centred Maintenance (RCM) system based on drone photos. The proposed combination approach which was created by fusing Otsu thresholding and Canny, produced respectable results.

According to Pan, et al [22] it was suggested that low-flying UAV multispectral data be obtained together with spatial characteristics derived from Convolutional Neural Network (CNN). It was used to analyse the aging and degradation states of pavements using an SVM classifier. The UAV pavement imagery was classified using a multi-scale semantic segmentation technique. In order to classify pavement surfaces into cracks, potholes, early medium, and late aging three main components were acquired. After dimensional reduction in the multispectral, data were coupled with deep abstract spatial information from the CNN and provided as inputs to the SVM classifier. However, the multispectral image necessitates extra processing. Furthermore, low-flying UAVs might not be a suitable solution for busy roads.

In a different dynamic monitoring research, Zhang and Elaksher [23] developed a novel monitoring technique. They used a digital image acquisition system based on an unmanned aerial vehicle (UAV) to evaluate the surface condition of unpaved roads with excellent data gathering efficiency. A variety of cutting-edge techniques and image processing algorithms were used to build a 3D model of the road surface faults. A model helicopter equipped with a global positioning system (GPS) and an internal navigation system was employed in their monitoring system to direct the flying along a certain path. The view-angle, picture size and resolution of the digital camera on the helicopter were all controlled by a computer. Additionally, the receiver (computer) showed flight information including the helicopter's height, speed and the GPS signal. The outcomes might give rise to a 3D model of surface distresses. The accuracy of UAV in measuring length and height was quite great, reaching ground precision of half a centimetre. The outcomes also demonstrated high degree of measurement accuracy of the monitoring system particularly when it came to spotting potholes and rutting in the road. Benefits were minimal costs, flexibility and the ability to be utilized in many other research fields. However, this method is not appropriate for measuring all forms of distresses. Additionally, it is difficult to get the necessary equipment and 25 minutes is not

enough time for the helicopter to check the state of the road before its battery runs out. This pavement monitoring approach is comparable to the conventional method and the difference is that it uses a test car traveling at a set pace to assess the state of the unpaved road surface.

2.4.3. Laser-Scanning with Ground Devices

Zhang et al. [24] suggested a 3D laser-based pavement scanning and automatic defect identification strategy to identify micro cracks and macro deformation problems as opposed to the conventional 2D and manual approaches. To identify fracture candidate locations and deformations support points, a sparse processing approach was developed. An exact location and categorization of flaws were entirely acquired by the algorithm, with a detection accuracy of above 98 percent. A Machine Learning ML-based system for the detection and intelligent categorization of potholes and fractures in pavement surfaces was defined by Huincalef et al [25]. Pavement 3D point-cloud structures and physical characteristics were retrieved using a Kinect device. The system was able to compute the physical characteristics of pavement depressions, such as the length, breadth and depth as well as categorize cracks and potholes.

A laser scanner installed on a mobile mapping system was used by Van Der Horst et al. [26] to capture 3D photographs of the pavement in order to develop a technique for identifying road deterioration. With the aid of many ML approaches, the pavement was attempted to be segmented. In their research, Fan et al. [27] created a pothole-detection algorithm that is computationally effective and is based on disparity maps and disparity transformation methods. A comparison of actual and simulated disparity maps allowed for the eventual discovery of potholes. Following that, the pothole point clouds were extracted. The system attained an overall accuracy of 98.7 percent using the three datasets that the scientists developed for stereo vision-based pothole identification.

2.4.4. Smartphone-Based Data Acquisition

Sattar et al [28] conducted a thorough analysis of road surface damage identification using smartphone sensors, noting several problems and difficulties with the existing approach and identifying areas for more research. The effects of speed dependence, mounting position, vehicle suspension and smartphone orientation on damage detection were also studied. Five main criteria sensor data collection, pre-processing, processing, post-processing and Overall Performance and Suitability were used to compare the available methods. Instead of result-oriented techniques, the main emphasis was on data collection and processing to perform anomaly detection. Basavaraju, et al [29] used data from an accelerometer, gyroscope and GPS

to classify the state of the road surface using a smartphone-based pavement analysis. Features from all three dimensions of the smartphone sensors were used to implement multiclass supervised machine learning algorithms. Three basic categories of smooth roads, potholes and deep transverse cracks were the emphasis in this study. The outcomes showed improved performance over models using single-axis features.

Using a smartphone accelerometer and complexity invariant distance, De Souza et al [30] carried out a thorough experimental assessment on three datasets that represented various scenarios of asphalt pavement categorization. He broke down the assignment into three distinct categorization issues in his paper. The first step was to recognize ordinary asphalt pavement, the second step was to recognize cobblestone or dirt roads and the third step was to recognize bumps as well as elevated marks on the pavement surface. Samsung Galaxy A5 and Samsung S7 cell phones that were mounted inside a Hyundai i30 car using the flexible suction holder provided data in four different Brazilian towns. Assault is an Android app that runs on the cell phones. Before gathering data, specialists may input pavement conditions using this smartphone application, which also takes video. The limitation of this method was that it provided no information on the quality of pavement.

Astarita et al. [31] installed a mobile application that allowed the use of sensors to monitor the state of the road surface. The accelerometer was used to find irregularities in the pavement. The whereabouts of test cars and the location of distresses on the road surface were known thanks to the GPS. Maximum and lowest travel speeds of the test vehicle were 25 and 40 km/h. To examine how the orientation of a mobile device can impact measurement accuracy, three alternative accelerometer positions within the car were selected. It was discovered that the filters used in the signal analysis allowed detecting high percentages of bump events, but the localization of potholes was not always accurate in the case of the road test site, which was characterized by several anomalies (rubber bumps, rough pavement surface and potholes of different dimensions).

Astarita et al [31] came to the conclusion that the analysis of the acceleration signal's energy peak values revealed certain variations between the two types of bumps. The free location of the device has an amplifying influence on the peak event, according to a comparison of the original acceleration signals for the three situations of device placement. For the Via Pascoli test site, the post-processing technique was sufficient to identify 98 percent of bump occurrences in Italy. In the case of the road test, the rate of bumps that were recorded was very

high, although the rate of potholes that were recorded was quite obvious. The primary shortcoming of this study was the need for more effort to improve pothole detection.

To automate pothole identification, Wu. Et al [32] investigated the vibration-based sensors and GPS built into cell phones. A specialized mobile application set up in designated automobiles was used to collect data. To determine the most effective method, a number of image processing approaches were used and the characteristics that were collected were given to different ML (Machine Learning) classifiers. When recognizing potholes, it was found that time and frequency domain variables worked well. The RF (Random Forest) classifier beat all other classifiers when tested against different types of roads to determine its robustness.

Vittorio et al [33] concentrated on creating the system, which relied on a straightforward smartphone application that used two key mobile sensors. GPS receiver to determine the location of the vehicle and a three-axis accelerometer to gather acceleration data in response to the motion of the vehicle during road distresses. Following a real-time upload to a central server, automatic methods for signal analysis were used to analyse the data. In the study, the authors concentrated on creating a methodology for the post-processing of acceleration signals measured in terms of impulse after the usage of a vertical axis re-orientation operation. They then determined precise criteria to which the predicted impulse levels were continually compared using statistical analysis of the experimental data. Additionally, they concentrated on assessing the potential for automatic localization of road anomalies when a regular stream of occurrences exceeding the thresholds was recorded in the same area. Two test locations in the urban core of the Italian city of Rende were chosen for data collecting. Test site A contained 19 bumps whereas test site B included a few oddities on the road, including cross joints, rubber bumps, and potholes. Three distinct mobile devices were used to capture the data, each using a different frequency. The test vehicle's overall travel speed ranged from 25 to 50 km/h. The results showed that the pothole depth and the impulse appeared to be directly correlated. Nevertheless, a bigger region of distress defined a longer stress duration for the vehicle as evidenced by the number of points over the predetermined threshold that were reported and positioned near to each other. The approach enabled the detection of abnormalities on the road surface with a reasonable degree of correct positive detected occurrences (always greater than 80%). The acceleration impulse and the size of pothole measured in terms of their mean depth have a linear relationship.

2.4.5. Autonomous Object Detection (Neural Network) and Augmented Reality Solutions

For the purpose of identifying damaged pavement, Li et al. [34] suggested applying the Faster R-CNN (Region-based Convolutional Neural Network) algorithm to a customized dataset that was broken down into six different categories. This included Lateral crack, longitudinal crack, pothole and separation, alligator crack, well cover without damage and damage around the well cover. When it came to finding and recognizing the dataset's fissures, the suggested Convolutional Neural Network (CNN) architecture demonstrated good accuracy and stability. Aslan et al. [35] provided a system based on DL (Deep Learning) to automate the assessment of road condition, capitalizing on the benefits of autonomous feature extraction using CNN. Longitudinal, transverse, alligator and pothole kinds of pavement fractures were classified using a CNN and the dataset for crack identification was built using photos from search engines. The suggested overall accuracy of CNN around 76% was justified as appropriate when compared to approaches that were only capable of classifying things in binary terms.

The feasibility and precision of thermal imaging in the field of pothole detection were examined by Bhatia [36]. In order to complete the task, potholes had to be photographed in both thermal and visual form under a variety of lighting situations. After using augmentation techniques, convolutional neural networks were then applied to the photographs. ResNet101 is a powerful deep neural network architecture with 101 layers that uses residual connections to improve training and performance. It is commonly used for tasks that involve image analysis, recognition, and understanding. ResNet101 has the highest accuracy of 97.08 percent when compared to the pre-trained and customized models. By combining pictures with mobile mapping point-cloud data, Wu et al. [37] created a unique approach for pothole identification. This technique found a potential pothole in the position of the image and 2D edge first. The mean depth of the candidate pothole was then calculated using the point clouds to distinguish between potholes and patches. A simulation experiment was used to test the geometric correctness of the pothole extraction and the results showed that the accuracy ranged between 1.5 and 2.7 cm on average.

2.4.6. Invasive Sensors or Sensor systems

In recent years, there has been growing interest in the possibility of embedding sensors into road infrastructure to enhance the efficiency, safety and maintenance of transportation networks. These embedded sensors have the potential to provide real-time data on various

parameters, enabling intelligent traffic management systems and facilitating proactive maintenance strategies. In this context, there are two or three different types of sensors that have been widely explored for this purpose each offering unique capabilities and advantages. Detailed descriptions of these sensor types can be found in chapter 3 of this thesis.

Among the various applications of embedded sensors in road infrastructure, one crucial area is the detection and assessment of damages. The ability to accurately identify and quantify damages is essential for effective maintenance planning and resource allocation. Two prominent types of sensors commonly employed for damage detection in road infrastructure are conventional sensors (for example sensors using piezoelectric effect) and Micro Electro Mechanical System (MEMS) sensors.

Piezoelectric sensors are designed to convert mechanical stress or strain into electrical signals. When embedded in road structures, these sensors can detect vibrations, strains and other mechanical disturbances. This can be caused by traffic loads, environmental factors, climatic effects or structural defects. By analysing the electrical signals generated by piezoelectric sensors it is possible to identify areas of excessive stress, fatigue or potential damage in the road surface or underlying layers. This information can help in timely repairs and preventive measures minimizing the risk of further deterioration [38].

On the other hand, MEMS sensors are miniaturized devices that utilize microscale mechanical structures to measure various physical quantities such as acceleration, pressure and temperature. When integrated into road infrastructure, MEMS sensors can provide valuable data on factors that contribute to damage, such as vehicle impact forces, temperature variations, and moisture levels. By continuously monitoring these parameters, MEMS sensors enable the identification of abnormal conditions or stress patterns that may indicate potential damages. This information can guide maintenance crews in prioritizing areas for inspection and intervention, leading to more targeted and efficient maintenance strategies. The combination of piezoelectric sensors and MEMS sensors in road infrastructure allows for a comprehensive monitoring system. Piezoelectric sensors primarily focus on surface-level stresses and strains induced by traffic, while MEMS sensors provide additional insights into environmental and dynamic factors affecting road conditions. By leveraging the data from these embedded sensors, authorities and transportation agencies can gain a better understanding of the health and performance of the road network enabling proactive maintenance, reducing costs and enhancing road safety [39].

Multiple wireless sensor nodes are combined to create (Wireless) Sensor Networks (WSN). In order to continuously and in real-time monitor a specific event (such as the appearance and propagation of hidden cracks) or measure a parameter (such as temperature, pressure, etc.), a smart sensor network is an embedded WSN made of a set of sensors, called nodes, integrated into the structure of interest in pre-determined positions. Antennas for data transmission are built into sink nodes, enabling remote monitoring. Self-powered smart networks are made to maximize energy effectiveness and sensing capabilities [40]. Applications involving SHM can benefit significantly from wireless sensor networks. There are still a number of problems to be solved. These difficulties include an unreliable wireless environment, a constrained bandwidth, weak signal, hardware architecture, embedded software, energy consumption and battery life. Impact of the weather on data gathering as well as data aggregation, communication hops for huge structures and many other issues are still to be solved [41].

In order to monitor condition of pavements, Xue et al. [42] developed a sensing network using a variety of commercial sensors. The sensors in the paper comprised horizontal and vertical strain gauges, load cells, thermocouples and moisture sensors placed in the base of a reconstruction pavement. It detailed a 2011 study on Virginia State Route 114 section. To gather sensor data and transfer it to a base station via RF, all embedded sensors were linked to V-Link wireless voltage nodes close to the pavement using cables of various diameters attached to a wireless data recorder. In this system, the wired link between the V-Link nodes and the sensors was initially required. Utilizing software based on finite element analysis (FEA), numerical simulation was carried out using the gathered data to compare monitored strain response data with the observed field data. In this work, back calculations of pavement dynamic modulus were shown using data gathered from a test car. The Mechanistic-Empirical Pavement Design Guide's (MEPDG) fatigue cracking and rutting prediction models were utilized to calculate the cumulative damage from distress. This was done in order to start an early pavement degradation warning system. However, the research states that all vertical strain gauges broke after five months most likely as a result of the challenging climate and heavy load [42].

the installation of sensors in roads is a highly interesting and promising approach for future road condition assessment. These embedded sensors enable the determination of the appropriate type and timing of maintenance measures contributing to more efficient and cost-effective road management strategies. The inclusion of detailed information on sensors in Chapter 3 stems from the significance of these technologies in revolutionizing road

infrastructure management. By understanding the capabilities, functionalities and applications of different sensor types valuable insights can be gained. This can be used for their potential in monitoring road conditions, detecting damages and optimizing maintenance activities.

2.5. Index-Linked Pavement Assessment

In many countries, a range of evaluation techniques is utilized to generate evaluative indicators from the measurement data collected using the methods described in Chapter 2.3. In addition, several organizations have developed specialized grading systems that precisely match their requirements. While some are more complex, some of these rating systems simply divide the roads into three categories as good, fair and bad [45]. Localized pavement condition metrics refer to specific measurements and assessments of pavement condition at localized or individual distress locations on the road surface. The main drawbacks of these localized systems include the difficulty in comparing their ratings to those of other types of systems and the difficulty in extrapolating these ratings as little study has been conducted using those criteria. These indicators play a crucial role in Pavement Management Systems, as described in Chapter 2.6. Their purpose is to identify and execute the most appropriate maintenance measures.

The following section will provide just a few examples of globally applied evaluation approaches:

- Pavement Condition Index (PCI)
- Pavement Surface Evaluation and Rating System (PASER)
- Condition Rating Survey (CRS)
- Localized Pavement Condition Metrics
- The Austrian Evaluation Method

2.5.1. Pavement Condition Index (PCI)

The calculation of the ASTM (American Society for Testing and Materials) Pavement Condition Index (PCI) is a common practice for road evaluation in the United States. PCI is a numerical ASTM standard between 0-100 that was created in 1976 by the US Army Corps to represent the general state of pavements, with 100 being the best possible condition and 0 representing the worst possible condition [43].

Experts visually examine and grade 39 pavement distresses in three severity categories low, medium, or high to compute PCI. From these afflictions, the PCI is then determined in relation

to the severity of each of those reported distresses by subtracting points from 100 based on the expert measurements as shown in Table 1. Before calculating PCI, specialists should separate the road network into three categories: "samples", "branches" and portions with a similar construction history. As a result, the samples are examined to evaluate the degree of the pavement distresses as mentioned before.

Table 2.1: PCI Values

PCI	Maintenance Action Required
90 < PCI	Do Nothing
70 < PCI < 90	Preventive Repair
40 < PCI < 70	Rehabilitation
PCI < 40	Reconstruction

2.5.2. Pavement Surface Evaluation and Rating System (PASER)

The general state of pavements is indicated by the PASER categorization metric, which ranges from 1 to 10 with 10 being the maximum suited condition and 1 representing the worst possible condition. Based on the visual examinations of the subject-matter specialists, the PASER assessment method utilizes four major surface distresses as follows;

- Surface cracks (Ravelling, flushing, polishing)
- Surface wrinkling (Rutting, distortion)
- A crack (Transverse, Longitudinal, Alligator, Block, Reflection, Slippage)
- Potholes & patches

To determine PASER, surveyors must first determine if the pavement is typically in good, fair or poor condition. Then, using the snapshots of each rating they assess four pavement distresses as indicated above. The maintenance categories in Table 2.2 can typically be used to translate the PASER rating scale. The PASER is an estimated indicator of road quality that depends on the surveyor's assessment.

Table 2.2: PASER Ratings Related to Maintenance and Repair Strategies

PASER	Maintenance Action Required
PASER = 9, 10	Do Nothing
PASER = 8	Little Maintenance
PASER = 7	Routine Maintenance
PASER = 5, 6	Preventive Repair
PASER = 3, 4	Rehabilitation
PASER = 1, 2	Reconstruction

2.5.3. Condition Rating Survey (CRS)

Another widely used metric to assess the general state of pavements is the Condition Rating Survey (CRS). It involves the visual inspection and evaluation of various distresses and defects present on the pavement surface. The CRS is a numerical measure that ranges from 1 to 9, with 9 representing the best possible condition and 1 denoting the poorest possible condition. The specific guidelines or standards used by transportation agencies or organizations may vary, influencing the interpretation and application of these numerical ratings [44]. The maintenance categories in table 2.3 may typically be used to translate the CRS grading system.

Table 2.3: CRS Values

CRS Maintenance Action Required	CRS Maintenance Action Required
7.6 ≤ CRS ≤ 9.0	Do Nothing
6.1 ≤ CRS ≤ 7.5	Preventive Repair
4.6 ≤ CRS ≤ 6.0	Rehabilitation
1.0 ≤ CRS ≤ 4.5	Reconstruction

2.5.4. The Austrian Evaluation Method

The condition assessment approach for road pavement in Austria was developed based on the considerations of Prof. SCHMUCK [9]. The procedure essentially consists of two main steps: standardization and value synthesis. The classification of the condition variables determined from the assessment into condition classes is also standardized in the Austrian RVS standards. The determination of condition variables does not rely on constant section lengths instead, it is based on the formation of homogeneous sections using mathematical algorithms. The establishment of the normalization functions relies on statistical analyses conducted on the visual condition assessment carried out in 1995 which included observations of cracks, surface damages and ruts. Additionally, measurements were taken between 1991 and 1996 to assess

skid resistance while expert surveys were conducted in 1999 to evaluate longitudinal evenness. The determination of these functions also takes into consideration existing threshold values in Germany and the federal states of Austria. The condition variables are standardized and converted into grades on a uniform scale, ranging from 1 (excellent) to 5 (very poor). Table 2.4 provides an overview of the assessment procedure. The condition value 3.5 is referred to as a warning threshold. Reaching the warning threshold prompts the planning of necessary measures. The condition value 4.5 is known as the threshold value and represents a critical state. Reaching this threshold especially in the presence of safety-related damages requires the immediate implementation of rehabilitation measures [9].

The overall evaluation involves combining individual characteristics into partial values, taking into account upper structure details like material, age, and layer thickness. These partial values, including substance (non-safety-relevant damage characteristics) and utility assessments, are then integrated to form an overall value using an expanded maximum criterion that considers both maximum and minimum values.

The utility value (GI) focuses on elements related to traffic safety and driving comfort, treating surface damage as an exception and assessing it directly through the weighted condition size, especially for condition sizes below a specific threshold.

The substance value (SI) is composed of ceiling components and theoretical load-bearing capacity, considering structural damage indicators and deck age. The structural fatigue of the pavement is considered through the condition parameter theoretical load-bearing capacity, based on a relationship between statistically evaluated lifetimes of bituminous layers and the condition function for cracks.

The total value (GW) is formed by combining the partial values of utility and substance, with priority given to the needs of road users. This involves a reduction of the substance value by a factor determined by the road category.

Table 2.4: The Condition Assessment Approach For Road Pavement in Austria

Grade	Classification
1	Very Good
2	Good
3	Middle
4	Bad
5	Very Bad

2.6. Software Programs for Pavement and Asset Management System

A good (PMS) includes user-friendly software that can provide pavement evaluation data and carry out the required activities. The following components make up pavement management systems in general. The data needed for the PMS analyses are stored in a comprehensive database. Valuable decision-making products are produced by mathematical techniques and the system parameters are fine-tuned using the most recent field observations by calibration procedures [46]. Thus, a study of some of the most widely utilized PMS software applications now in use by transportation authorities. These are the programs:

- Micro PAVER
- Street Saver
- PAVEMENT view
- Road-Soft Geographic Information System (GIS)
- Data analysis with VIAPMS (Programs used in Austria)

2.6.1. PAVER

Micro PAVER which was manufactured by the US Army Corps in the 1980s is most likely the application used for Pavement Condition Index (PCI-based). PCI inspections can be either on-foot surveys in which professionals walk along each road and take measurements or wind-shield examinations where experts drive slowly while observing pavement distresses. Road network inventory are stored by Micro PAVER, and condition ratings are derived from them. Several decision-making tools are available in Micro paver for cost-effectively scheduling maintenance and repair activities. These technologies forecast state of the pavement in present and future recommending appropriate repair measures. Additionally, Micro paver enables users to alter some of the software presumptions and examine other financial situations [47].

Micro paver's primary inputs are PCI distresses and their related severity levels from which the application derives the PCI. For the surveyed parts, comments and pictures of the pavements can be manually entered.

Four tools are provided by Micro PAVER to assist in managing Maintenance and Repair (M&R) activities. These tools include:

- Summary charts: Summaries of pavement information layers in graphs for different distresses
- Standard reports: List of pavement branches in addition to their repair history and current conditions.
- Re-inspection reports: Reports after new inspection data has been entered into the software.
- GIS reports: Maps, tables and graphs of future condition predictions and budget needs [47].

2.6.2. PAVEMENT View

PAVEMENT view is a component of the asset management program Cartegraph (signposts, utilities, etc.). This program creates Capital improvement planning (CIP) scenarios or budget allocation plans for improving the pavement condition of the road network after a user-defined number of years by taking an inventory of the conditions and geometrical details of the pavement networks (length, breadth, etc.). PAVEMENT view offers repair advice and lets the user alter its decision-making processes. The benefit-to-cost ratio of each maintenance task is used by this program to determine the order in which repairs should be prioritized [48]. A thorough assistance manual is included with PAVEMENT view to aid surveyors performing distress inspections. After the user enters the observed pavement distresses, PAVEMENT view creates a statistic called the Overall Condition Index (OCI) which is very similar to PCI. PAVEMENT view assesses the remaining life of the pavement portions in addition to forecasting the network's future state[48].

2.6.3. street Saver

More than 350 organizations in the US alone utilize Street Saver, which was created by the Metropolitan Transportation Commission (MTC) [48]. Like Micro paver, Street Saver is built on PCI approach. Instead of the 39 pavement distresses utilized in Micro paver, the PCI used by this program is calculated using seven selected distress kinds. The original PCI distresses have been condensed into seven categories in research by Shahin et al. [49] on which these distresses are based. These distresses include longitudinal and transverse cracking, block and alligator cracking, distortions, rutting, patching and weathering for flexible pavements. Based on PCI, Street Saver recommends the necessary fixes. By saving many budget scenarios in the same session, this program enables the user to generate various budget scenarios and analyse the advantages of each. Additionally, the user can alter some of the presumptions made by

Street Saver when recommending M&R procedures. Street Saver can provide over thirty various graphs and reports about the state of the pavement and anticipated financial requirements [50].

2.6.4. Road Soft GIS

Road soft GIS (A Geographic Information System) is a Pavement Surface Evaluation and Rating System PASER-based program that has been developed by the Michigan Tech Transportation Institute and is widely utilized in towns and cities there. Road Soft holds asset management data including signpost and utility information in addition to pavement information layers. Road soft is utilized in data collecting and can compute PASER from distress sheets on laptops and tablets [48]. GIS is described as "a system of hardware and software components for recording, storing, displaying, processing and analysing all types of geographical data to assist pattern detection. It is also used to knowledge discovery and decision making [51]. Since the geographic character of road networks and the spatial analysis capabilities of GIS are complementary, GIS has long been utilized to improve pavement management operations. Many governments and towns are incorporating historical data into GIS which includes capabilities like visually presenting the pavement conditions of a network of roadways.

2.6.5. VIABASE and VIAPMS

The road database utilized in Austria, known as VIABASE_AUSTRIA contains all the essential information for systematic maintenance management and operates through the VIABASE software. The Swiss company VIAGROUP AG has assumed responsibility for distribution and support of this product for the European market while also obtaining the rights to it. The structure of a database managed with VIABASE© is divided into three hierarchically structured levels which ensure a clear and organized framework [52]. These are:

- Perspectives
- Logical Data Groups
- Database Fields

Perspectives are used to provide descriptions of the properties and occurrences of a specific object, event, or feature along the linear infrastructure. When constructing the database structure, it is possible to choose perspectives with different properties. For example, section perspectives, point perspectives, lane perspectives, historical perspectives, repeating point perspectives and more can be selected.

The logical data groups represent the second level and are always linked to a perspective. The logical data groups play a crucial role in organizing the perspectives and can only be defined after creating the respective perspective. Additionally, each perspective includes an internal logical data group (Internal) that consists of data fields facilitating the unique identification of elements (sections, points, etc.) within the perspective, as well as enabling connections with other entities.

Database fields are assigned to a logical data group as the third level of the road database. These data fields have distinct properties that should correspond to the type of information being stored, including real numbers, integers, text, tables and more.

The database stores various types of information such as inventory data including road, kilometre marker, network nodes, road maintainers, network information and section indications. Construction data like pavement data, width data, road geometry and structures are also stored. Load data, condition data, traffic data, climate data are stored in the form of records within the data fields. Within the road database, key figures are controlled, assessed and derived through formula and filter transformations for a portion of the data. The outcomes of this data processing and control act as inputs for the analysis system VIAPMS_AUSTRIA [52].

VIAPMS_AUSTRIA comprises the following components:

- Road condition assessment procedure
- Road condition forecast
- Generating alternative section-specific maintenance strategies
- Cost-Benefit Analysis for the assessment of measures
- Heuristic optimization method

The application of the optimization data analysis method results the "optimized urgency ranking." This list includes analysed road sections (maintenance segments) with assigned maintenance measures aligned with a specified maintenance budget. The creation of the optimized urgency ranking essentially concludes the objective management of the "Road pavement management" subtask. During the development of construction programs, the "Road Pavement Management (PMS)" subtask is broadened through integration with the urgency ranking of structures (BMS - Structure Management System) and linked to form an overall result (EMS - Maintenance Management System).

Chapter 3: Sensors and Sensor Systems for The Evaluation of Structural Road Conditions

3.1.1. Sensors

A sensor is a device that converts a specific physical property into an electrical signal, often in the form of voltage, current, or charge. Sensors can be passive or active. Passive sensors generate a signal based on input activity without needing external energy. Examples include thermocouples, photodiodes, and sensors using the piezoelectric effect. Active sensors, however, rely on an external power source called an excitation signal. They respond to this signal by producing an output signal. For instance, a resistive strain gauge measures strain using electrical resistance. To measure the sensor's resistance, an external electrical current is applied from a power source [53].

When exploring sensor options, it is important to note that there are both conventional and novel types available. Conventional sensors, for example based on piezoelectric technology have been widely used in various applications. These sensors have been extensively used, providing dependable measurements and proving suitable for numerous scenarios.

In contrast, there are novel sensors based on Micro Electro Mechanical Systems (MEMS) technology that provide unique advantages. These sensors can be installed either wired or wirelessly, offering greater flexibility in monitoring pavement response.

There are a broad variety of sensors used in numerous applications for thorough data collecting. An accelerometer is an automated device that measures acceleration, quantifies vibrations, and determines gravitational forces (inclination). It is employed in various contexts, such as assessing vibrations in vehicles, engines, structures, and security systems. Furthermore, accelerometers are used in electronic devices like 3D games, computer mice, phones, and earthquake monitoring. The different types of accelerometers include Piezoelectric, Piezoresistive, Capacitive and MEMS (Microelectromechanical Systems) Accelerometers. temperature sensors are essential for analysing materials that depend on temperature as well as external factors. They can be found in a variety of shapes, including thermistors, resistance temperature detectors (RTDs) and thermocouples [2]. RTDs and thermistors rely on variations in electrical resistance with temperature, whereas thermocouples employ the Seebeck phenomenon as its basis temperature measurement. Many industrial activities, climate monitoring and weather forecasting utilise these sensors. The second sensors are pressure

sensors, which track changes in liquid or gas pressure. Common types of pressure sensors used in many applications include piezoelectric pressure sensors, strain gauge pressure sensors and capacitive pressure sensors [2]. Using strain-gauge-based strain sensors involves converting the mechanical force parameter into an electrical signal through a four-step process. It begins with the application of force to a component, causing deformation. This deformation is transmitted through a frictional connection to the strain sensor. The strain sensor incorporates a tempering steel spring bellow, experiencing strain on its material surface due to external stress. Strain gauges affixed to the spring bellow's surface measure this strain, converting it into an electrical resistance change. These strain gauges serve as mechanical-electrical converters, generating a voltage change proportional to the strain. Strain sensors are utilized across diverse industries, including structural engineering (for monitoring pavement, bridges, buildings and other structures), materials testing, automotive engineering (for monitoring components such as suspension systems), aerospace and biomechanics. The third sensor referred to as hygrometer, measures the amount of moisture in the air. For HVAC systems, agriculture and environmental monitoring to operate optimally and avoid problems like mold development or moisture-related damage, these sensors are essential. The fourth set of sensors, known as photodetectors or light sensors, gauge the amount of light present in their immediate environment. For applications like autonomous lighting management, ambient light sensing in displays and proximity detection in smartphones, photodiodes and phototransistors are frequently used as light sensor. The fifth type of sensors are Proximity Sensors which detect the presence or absence of an object within a specified range. They are commonly found in mobile devices for touchless interaction and in industrial settings for detecting the position of machinery or objects on a production line. Inductive, capacitive and ultrasonic proximity sensors are widely used variants. The sixth type of sensors are Motion sensors which are used to detect movement or changes in position. They are integrated into various applications, including security systems, gaming consoles, and smartphones for gesture control and screen rotation. The seventh type of sensors are Sound Sensors or Microphones which are used to capture sound waves and convert them into electrical signals. They play a vital role in applications like audio recording, speech recognition and noise monitoring in public spaces. The last type is Image Sensors, which are commonly found in cameras, capture visual information and convert it into digital signals. These sensors are fundamental to photography, surveillance systems and facial recognition technology. MEMS based sensors are another type of sensor technology which is already widely acknowledged to be able to increase system

performance, reliability, lifespan and safety when compared to current conventional wired systems. The integrated CPU provides a more effective method of data interrogation [2].

3.1.2. Overview about Sensors used for Pavement Analysis

Future condition evaluation and early damage identification are important information for road administrations and their different maintenance strategies which can be used to identify distressed pavements or to estimate the remaining fatigue life [54].

Numerous sensors are used to detect road conditions and distresses. In Figure 3.1, typical intrusive sensing technologies for pavement monitoring are shown.

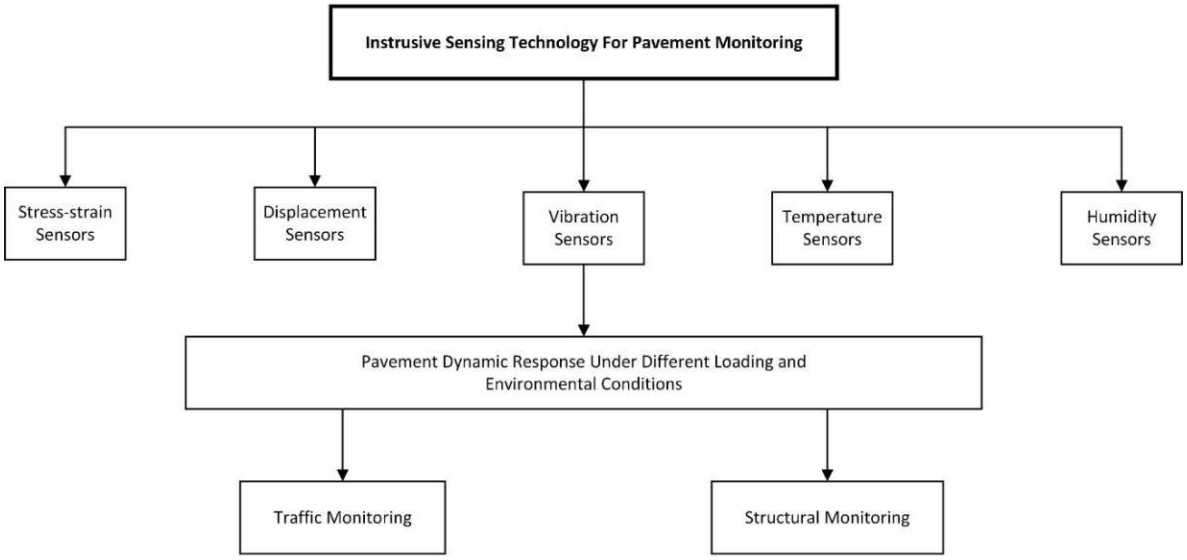

Figure 3.1: Typical Intrusive Sensing Technologies for Pavement Monitoring [6]

For choosing an appropriate sensor it is important to consider the following sections:

• Frequency Response:

Frequency range of the phenomenon or signal you intend to measure is considered. It is crucial to choose a sensor with a frequency response that aligns with the desired range to accurately capture the relevant data.

• Environmental Conditions:

Operating environment determines which sensor will be deployed. Evaluation of factors like temperature, humidity, vibrations or potential exposure to harsh conditions is considered. It is crucial to ensure that the selected sensor is specifically designed to withstand and operate reliably in the anticipated environmental conditions.

• Accuracy and Precision:

Accuracy refers to how close its measurements are to the true values, whereas precision refers to its ability to consistently reproduce measurements. it is important to select sensors that offer the required level of accuracy and precision for the specific application.

• Cost:

Cost of the sensor is a crucial practical factor. It is necessary to strike a balance between the desired capabilities of the sensor and the available budget for acquiring, installing and maintenance.

• Compatibility and Integration:

Sensor output should be compatible with your data acquisition system or software. It is important to ensure that integration is feasible, or plan for any necessary conversions for adaptations.

Sensors embedded into the pavement can be used as part of a road condition monitoring system for measuring and monitor some of the required in-situ data. Therefore, electronic, mechanical and economic aspects must be considered for using these sensors appropriately. For example, the sensor material must be compatible with asphalt or concrete and the construction methods. The sensors are often more brittle than aggregates, stiffer than asphalt and more prone to breakage. Furthermore, sensors are subjected to high temperatures and pressures throughout the construction and asphalt mixing processes. As a result, the sensors require a housing composed of materials that can withstand high temperatures and heavy loads without impairing the ability to sense [55].

Previous pavement instrumentation projects have shown some drawbacks of conventional wired piezoelectric sensors such as high cost, low reliability, complexity of field instrumentation, etc [9]. Furthermore, conventional sensors typically have a relatively large size, many external wires and they are very pricey. Therefore positioning numerous sensors of various types to obtain continuous data can very likely result in logistical issues and possible structural damage. Additionally, it is necessary to install data gathering equipment near to the pavement which may create complex issues among other things such as power supply, data storage and transmission. On-site office buildings are typically set up beside the test track in projects like MnROAD and Virginia Smart Road. This condition is not possible for highways but an on-site data collecting system for a test track may not encounter such issues. The use of

SHM for paving systems is constrained by all limitations of wired conventional piezoelectric sensors.

MEMS sensors are more affordable per unit and smaller than a conventional sensor providing the ability to increase in-pavement array density enabling more data to be collected. Additionally, a highly integrated multifunction sensor that can measure many parameters at once including for example temperature, Relative humidity and strain may be created using MEMS technology. The installation costs may be further decreased by lowering the number of sensors required with this multipurpose installation [2].

The most common sensors used for monitoring the status of roads are strain sensors and inertial sensors such as accelerometers and gyroscopes. Gyroscopes and accelerometers can be used separately or in an inertial measurement unit (IMU). In an Inertial Measurement Unit (IMU), gyroscopes convey details regarding the object's rate of rotation in three-dimensional space. Simultaneously, accelerometers within the IMU offer insights into alterations in velocity and the direction of gravity. Integration of data from both gyroscopes and accelerometers is commonly achieved through a sensor fusion algorithm. IMUs are often grouped depending on the technology, features and target applications of their accelerometers and gyroscopes [56, 57].

In addition to acceleration sensors and strain sensors, temperature sensors, humidity sensors, and various other types of sensors are also employed.

Strain sensors are mainly based on the piezoresistive effect, piezoelectric effect or fiber-optic sensing principles. Piezoresistive strain sensors use materials that change their electrical resistance when subjected to mechanical strain. But piezoelectric sensors generate electrical signals when mechanical stress is applied to them. Fiber-optic sensors on the other hand, utilize changes in the light transmission properties of optical fibres due to strain.

When vehicles pass over, the pavement materials undergo deformation or strain is deduced due to the applied load. Strain sensors are embedded, attached to the pavement surface layers or with them to measure small deformations. By monitoring the strain distribution, engineers can understand how the pavement structure responds to traffic loads and external forces.

Strain sensors are essential components of Structural Health Monitoring (SHM) systems for pavements. SHM involves continuous or periodic monitoring of the structural integrity and performance of pavements over time. Strain data collected by sensors provide valuable

information about the load-bearing capacity, stiffness and overall health of the pavement. This lead to identify early signs of damage or degradation. Last but not least, Strain sensors help analyze the distribution of loads on the pavement surface. By understanding load distribution, engineers can optimize pavement designs and maintenance strategies to reduce the risk of localized failures and extend the pavement lifespan. Besides, sensors are capable of providing real-time data, allowing immediate detection of critical events, such as overloading or excessive deformation. Real-time monitoring enables prompt response to potential issues enhancing the safety and reliability of pavements.

Beside other Influences it is important to consider additional variables that may affect pavement particularly modulus of the viscoelastic asphalt layer such as vehicle speed and pavement temperature. Random vehicle loads in contrast, with different vehicle kinds, speeds and load pressures which might result in random mechanical reactions should also be considered as key inputs and recognized throughout the modulus assessment process. In order to accurately evaluate the modulus and record the data on random vehicle loads and pavement temperature, a certain sensor configuration should be created [58]. The suggested sensor arrangement for real-time modulus assessment which comprises of an input sensing module for random loads, an output sensing module for mechanical reactions and an environmental sensing module for pavements is fully described by Am, et. Al 2021 [58].

The vehicle moving load is considered as the external excitation which is employed for modulus assessment in pavement health monitoring system. This is similar to the impulsive force exerted by Falling weight deflectometer (FWD) to complete the back calculation of the pavement moduli. The vehicle load is random in contrast to the well-known load form of FWD as seen by the varied vehicle type, load pressures and speeds [59].

Sensors are often part of local or global monitoring system that requires additional systems besides the sensors. A complete monitoring system consists of three main components which are as follows [60].

- Embedded sensing devices linked to an ad hoc data acquisition system
- Post-processing of potentially enormous amounts of data coming from the sensors
- A user-friendly interface displaying the overall road network conditions and alerting in case maintenance is required.

Thus creating a methodology for the inverse computation of pavement mechanical performances is just as crucial as having a device that is compatible with the pavement itself. The final tool is intended to aid in decision-making on pavement maintenance measures.

3.2. Accelerometers

3.2.1. Introduction

One of the most popular sensors for measuring stresses, vibrations and shocks are accelerometers. An Accelerometer is a device that monitors velocity change or rate of a mass that is attached to a spring in one or more directions. They are often mounted directly to the vibrating structure (or inside) and in response to acceleration mechanical energy is converted to electrical signal. The gravitational constant is used to describe acceleration which is 9.81 m/s^2.

Frequently utilized kind of accelerometers in industrial applications and on road pavements are piezoelectric accelerometer.

Piezoelectric accelerometers are an essential component in pavement monitoring systems, offering valuable insights into the dynamic behaviour and structural performance of roadways. By converting mechanical forces into electrical signals, piezoelectric accelerometers provide real-time data on the pavement response to traffic. This enables engineers to assess durability, identify potential issues and optimize maintenance strategies. One of the significant advantages of using piezoelectric accelerometers is their ability to analyse dynamic loads from moving vehicles. The sensors capture dynamic forces exerted by passing vehicles. This can be used to determine the impact of heavy trucks or high-speed traffic on fatigue life and overall performance. Real-time data provided by piezoelectric accelerometers is used for quick detection of potential issues such as overloading or uneven load distribution. This capability allows critical situations to be addressed promptly enhancing road safety and maintenance efficiency [61].

Piezoresistive accelerometers are the premier type for shock testing due to their strain gauge technology. While they require amplifiers and temperature compensation, they offer a wide bandwidth, low noise, and can feature gas/fluid damping for protection against internal resonant frequency. Their DC coupling allows output integration for velocity and displacement calculation during shock events. However, piezoelectric accelerometers are preferred for vibration testing [61].

Another type of acceleration sensor consists of MEMS based Sensor elements. MEMS-based sensors typically consist of miniaturized mechanical sensing components that are manufactured on silicon chips. The most distinguishing features of a typical MEMS sensor are incredibly small size and embedded microprocessor, or CPU. This type of sensor has a much lower price than other sensors due to the materials used and integrated interconnection. This type of sensor is mainly used in the automotive industry and consumer electronics. MEMS sensors could potentially be used to enhance the existing structural health monitoring (SHM) capabilities of pavement systems, with minimal worry about inherent compromising properties. Many vehicles have MEMS based gyroscopes and accelerometers for various different applications such as Airbag deployment. They detect changes in acceleration and convert them into electrical signals that are processed further. Some research project used car-mounted MEMS-Sensors or similar MEMS-Sensors mounted in smartphones for detecting road irregularities and unevenness [61].

Table 3.1 offers a reference table suggesting suitable accelerometer types for various applications [61].

Table 3.1: Which accelerometer types work best for different testing applications

Application	Piezoelectric	Capacitive MEMS	Piezoresistive
Static Acceleration	✓	✓	✓
G-Force		✓	✓
Seismic	✓		
Low Frequency Vibration (<1Hz)	✓	✓	✓
General Vibration (5Hz to 500 Hz)	✓	✓	
High Frequency Vibration (>500Hz)	✓		
Genera Shock (<100Hz)	✓	✓	✓
High Impact Shock (<250Hz)	✓		✓
Extreme Shock (>1000Hz)			✓

Piezoelectric accelerometers offer a wide frequency range, capable of measuring both low-frequency vibrations caused by slow-moving vehicles and high-frequency impacts from heavy traffic or road irregularities. This broad spectrum allows for a comprehensive assessment of the pavement response under various loading conditions. In some pavement monitoring systems, piezoelectric accelerometers are integrated with other sensors, such as strain gauges, temperature sensors, and GPS units. Combining multiple sensors enables engineers to collect

multi-parameter data, providing a more holistic understanding of the pavement structural behaviour and environmental influences.

3.2.2. Piezoelectric Sensors

Piezoelectric sensors can function as sensitive accelerometers by directly utilizing the piezoelectric effect, with a focus on vibration level detection and tracking temporal fluctuations in acceleration. In terms of their mounting, piezoelectric accelerometers are typically mounted on or embedded within the pavement surface. They can be installed directly onto the pavement layer or placed in small shallow holes known as boreholes to ensure a firm and secure attachment. The sensors must be strategically positioned to capture representative data on traffic loads and pavement responses.

Direct and inverse piezoelectric effects are two ways that piezoelectric materials can function. The capacity of a material to convert mechanical strain into electrical charge acting as a sensor is known as the "direct piezoelectric effect". The capacity to convert an applied electric potential into mechanical strain energy acting as an actuator is known as the inverse piezoelectric effect [38].

Piezoelectric resonators can be utilized to create vibrating elements that can be used as gyroscopes or accelerometers. The idea of a piezoelectric accelerometer was first developed in 1964 when it was discovered that applying stress alters a quartz material to oscillate with resonance frequency [62]. Aoyagi et al. [63] introduced a unique approach for acceleration sensing based on the alteration in capacitance brought about by a change in fringing field. This was coupled in an interdigitated capacitor parylene proof mass situated next to a bulk PZT substrate with a high dielectric constant [63].

Piezoelectric acceleration frequently employs lead zirconate titanate (PZT) sensing components which generate an electric charge or output when subjected to acceleration. PZT which has a strong piezoelectricity and a high dielectric constant is the most widely used commercially available piezoelectric ceramic material for making self-powered sensors [64]. Due to its high dielectric constant and electromechanical coupling coefficient, the latter is particularly well suited for applications embedded into the pavement. PZT on the other hand, deform in an uncoordinated manner because they are stiffer and more brittle than the asphalt mixture [64].

A stretching procedure that directs the polymer chains in a certain direction gives another type of piezoelectric sensor, the polymer PDVF. Despite having a lower piezoelectric coefficient (about one-tenth that of PZT) its properties make it more desirable for use as a sensor. The sensors have a minimal energy need yet continuous operation is neither practical nor beneficial. The answer is to run the systems in standby-active modes so that an accumulation of charge system may quickly gather the energy required for operation. Understanding how, when and for how long the sensor must operate is a challenge for effective data collection [64].

In applications where vibration and shock are present, piezoelectric accelerometers outperform capacitive MEMS or piezoresistive accelerometers due to their extremely low noise levels. Piezoelectric accelerometers can be triaxial or single axis with sensitivity ranging from high for seismic applications to low for shock testing. There are even certain varieties that can withstand harsh conditions . Piezoelectric accelerometers cannot monitor the gravity vector or persistent accelerations due to their AC coupling which is a significant drawback. However due to inherent decay characteristics it poses difficulty in integrating the data for velocity or displacement information. But due to their performance advantages, piezoelectric accelerometers are frequently used in industrial testing applications [65].

3.2.2.1 Advantages of Piezoelectric Sensors

Piezoelectric acceleration sensors offer several advantages in pavement monitoring, making them a valuable choice for assessing structural health and performance of pavements. They include higher sensitivity, wide frequency range, fast response, durability, lightweight, lower power consumption, wireless capabilities, cost-effectiveness, easy integration and Non-Destructive Testing.

Piezoelectric acceleration sensors are highly sensitive to even small accelerations and vibrations. This sensitivity allows them to capture and measure subtle changes in pavement behaviour, including minor deformations or dynamic loads caused by passing vehicles. In terms of frequency range, they have a broad range enabling them to capture both low-frequency and high-frequency vibrations. This characteristic is essential in monitoring various types of road conditions and traffic loads, providing a comprehensive understanding of pavement responses [66].

Piezoelectric acceleration sensors have rapid response times, allowing them to record instantaneous changes in acceleration accurately. This real-time data acquisition is crucial for detecting sudden impact events or dynamic load variations which aides in identification of

critical situations. They are also compact and lightweight making them suitable to install and integrate into pavement structures. Their small size also minimizes the impact on the pavement mechanical properties ensuring that the sensor installation does not affect the overall performance of the road.

Piezoelectric accelerations are designed not only to withstand harsh environmental conditions such as temperature fluctuations, moisture exposure and mechanical shocks but also consume minimal power during operation. This makes them energy-efficient for continuous monitoring applications. Their robustness ensures reliable and long-lasting performance in outdoor applications like pavement monitoring, whereas their lower power consumption allows for extended monitoring periods without frequent battery replacements.

Many piezoelectric acceleration sensors are equipped with wireless communication capabilities, enabling remote data transmission and real-time monitoring. This feature simplifies data collection and reduces the need for physical access to the sensors for maintenance or data retrieval. Compared to some other advanced sensing technologies, piezoelectric acceleration sensors are relatively cost-effective. This affordability makes them accessible for deployment in large-scale pavement monitoring projects contributing to more comprehensive infrastructure assessment.

Piezoelectric acceleration sensors can be easily integrated with other monitoring systems such as strain sensors, temperature sensors and GPS units. This leads to gather multi-parameter data for a more comprehensive analysis of pavement performance [66]. Application of piezoelectric acceleration sensors in pavement monitoring is non-destructive meaning it does not cause damage to the pavement structure during data collection. This advantage is crucial for routine monitoring and evaluation of existing roadways without causing additional wear or disruption.

3.2.2.2 Disadvantages of Piezoelectric Sensors

While piezoelectric sensors offer various advantages for pavement monitoring but there are some disadvantages that should be considered when using them in this application. The following are some of the key disadvantages.

Piezoelectric sensors have a limited dynamic range which means very high or very low accelerations may not be accurately measured. In pavement monitoring where vehicles of different sizes and weights travel at varying speeds, dynamic range limitation could result in some acceleration data being outside the measurement range. Performance of sensitivity to temperature can also be affected by temperature variations. Changes in ambient temperature

can cause shifts in the sensor output, leading to potential inaccuracies in the measured data. Temperature compensation techniques may be required to mitigate this effect [67].

Piezoelectric sensors are susceptible to noise interference, which can impact the accuracy of the collected data. External factors like electromagnetic interference (EMI) or mechanical vibrations from nearby equipment may introduce noise into the output. Piezoelectric sensors can be sensitive to rough handling or excessive mechanical shocks. During installation and maintenance, care must be taken to avoid damaging the sensors, as any physical damage can lead to inaccurate readings or complete sensor failure.

Environmental factors such as moisture and humidity, can impact long-term performance of piezoelectric sensors. In outdoor pavement monitoring, exposure to weather conditions may lead to gradual degradation of the sensor sensitivity and accuracy. Installation of piezoelectric sensors can add extra mass on the pavement structure. Although it is small but may affect stress distribution and alter the behaviour of the monitored area. Sound design and installation is necessary to minimize these effects [67].

Piezoresistive sensors must be used with appropriately designed sensing chips and must be applied with understanding of potential causes of errors. One of the most significant sources of errors can be considered to be rotational alignment inaccuracy during manufacture and installation. The cleanliness of the silicon substrates that were utilized and the oxygen levels in the silicon samples are additional variables that could significantly affect variability [62].

3.2.3. Piezoresistive Acceleration Sensors

Though piezoresistive accelerometer may sound similar to the Piezoelectric accelerometer, not to be mistaken, they are pretty different:

Piezoelectric acceleration sensors make use of the phenomenon where piezoelectric materials generate an amount of electric charge on their surfaces when exposed to a force. This charge is directly proportional to the applied force. When these surfaces are contacted, the accumulated charge can be released and transformed into an electrical voltage.

In piezoresistive acceleration sensors, the deformation of the material resulting from the displacement of the seismic mass within the suspension is employed to measure the displacement. In the simplest configuration, the suspension consists of a flexural beam onto which the piezoresistive elements are applied.

Piezoresistive accelerometers are typically manufactured with short, rigid flexures and proof masses that deflect out of the plane. The acceleration-induced strain in these flexures causes shifts in the outputs of embedded piezoresistive Wheatstone bridges on their top surfaces. To ensure the durability of these devices, they usually require bonded glass or silicon covers, as well as overtravel tabs positioned above and below the proof masses to prevent flexure breakage when exposed to mechanical shocks [68].

The use of single short flexures in piezoresistive accelerometers offers advantages because they concentrate the induced strain onto the piezoresistive sense elements. In contrast, the common quad-supported topology employed in planar capacitive accelerometers would not be suitable for piezoresistive devices. This is because the induced strain would be distributed across the four legs, ultimately reducing sensitivity. As a result, constructing long flexures in piezoresistive accelerometers is generally discouraged [68].

Piezoresistive sensors must be used with appropriately designed sensing chips and must be applied with understanding of potential causes of errors. One of the most significant sources of errors can be considered to be rotational alignment inaccuracy during manufacture and installation [69].

Jaeger et al. [70] demonstrated how temperature changes and measurement errors can significantly affect the accuracy of the findings made during the calibration and use of piezoresistive stress sensors. The objective of this section is to ascertain how sensitive the manufactured sensing chip is to alignment and rotational defects that can have an impact on the sensor output signal. An alignment error of roughly 4.5° can cause a 2% acceptable inaccuracy in the sensor output signal. As a result, it can be said that the existing sensor design has a low sensitivity to rotational errors within 4.5° misalignment. Non-linear nature of the induced error brought on by the rotational misalignment is also highlighted.

3.2.3.1 Advantages and disadvantages of Piezoresistive Sensors

The Piezoresistive accelerometer offers several advantages and disadvantages [68]:

Advantages:

1. Ideal for speed and displacement applications due to its DC outputs, which effectively minimize integration and double integration errors in comparison to sensors featuring AC output.

2. Capable of measuring frequencies as low as 0 Hz.

3. Can accurately measure static angles.

4. Provides a differential output signal.

5. Piezoresistive sensors demonstrate heightened sensitivity, enabling them to detect minute variations in pressure, force, or acceleration.

Disadvantages:

1. Ineffective for dynamic applications.

2. Constrained operating temperature range due to internal electronics.

3. Limited bandwidth, confined to the low kHz range.

4. Piezoresistive sensors may be susceptible to overload situations, which could result in potential damage or a decrease in accuracy.

3.2.4. MEMS accelerometers

MEMS accelerometer sensors are microelectronic devices designed with comb-like structures, typically mounted on a printed circuit board (PCB). Sensing components in MEMS accelerometers, including capacitors, piezoresistors, or piezoelectric materials, can translate the motion of the proof mass mechanically into an electrical signal. Each type of MEMS, including capacitive MEMS accelerometers, piezoresistive MEMS accelerometers and piezoelectric MEMS, offers unique advantages for measuring acceleration and vibration in different applications. In SHM, replacing pricey piezoelectric sensors with more accessible MEMS sensors is a significant trend.

A MEMS accelerometer initially transforms pavement vibrations into an analog voltage signal (Colibrys, Inc., n.d.). This voltage signal undergoes filtration and the resulting output is subsequently sampled at specific rates by an analog-to-digital converter integrated into the microprocessor. These samples are transmitted efficiently using a low-power, time-division multiple access (TDMA)-based protocol via the radio transceiver [71].

Both analogue voltage outputs and a digital signal with a duty cycle inversely proportional to acceleration are produced by the device. A surface micromachined polysilicon structure (the sensor) is typically put together on top of a silicon wafer, Thin Films include materials such as silicon dioxide (SiO2), silicon nitride (Si3N4) and polysilicon, Metal Layers like aluminium or gold, Piezoresistive Material like polysilicon and Piezoelectric Material like lead zirconate titanate (PZT).

Polysilicon springs that provide resistance against acceleration forces suspend the sensor surface above the silicon wafer. Deflection of the structure in reaction to acceleration is measured using a differential capacitor which consists of central plates coupled to the moving component and independent stationary plates. The capacitor becomes unbalanced by the acceleration-induced beam deflection and generates an output square wave whose amplitude is proportional to acceleration. After this signal has been corrected, phase sensitive demodulation methods are used to identify the direction of the acceleration. Each pin corresponding to x and y axes receives a digital output from a duty cycle modulator stage.

Capacitive accelerometers are mostly referred to as MEMS accelerometers. Capacitive MEMS accelerometers are also used in smartphone and they are by far the smallest and cheapest alternatives for accelerometers. Capacitive MEMS accelerometers are the favoured option for electrical engineers since they can be installed directly on printed circuit boards. Capacitive MEMS accelerometers are popular because of their small size and inexpensive cost but their data quality is substantially poor at higher frequencies and amplitudes [65]. Generally, for diagnostic applications that call for lower noise over wider frequency ranges and bandwidths beyond 10 kHz, noise performance is typically not low enough to meet their needs. Currently, low-noise MEMS accelerometers are available, but their bandwidth is only a few kHz and their noise density ranges from 10 $\mu g/\sqrt{Hz}$ to 100 $\mu g/\sqrt{Hz}$. Despite this restriction, condition monitoring product designers still use MEMS accelerometers in their new product conceptions, even if their noise performance barely satisfies their requirements [72]. Two distinct analog MEMS accelerometers, namely the SD1221-005 by Silicon Designs and the MS9002.D by Colibrys, underwent evaluation concerning their noise density and power consumption (Bajwa et al., 2017). Despite the SD1221-005 exhibiting a lower noise density, the MS9002.D was chosen over the SD1221-005 due to its superior suitability for embedded wireless applications attributed to its lower power consumption [71].

MEMS accelerometers are DC-coupled and a great option for human-based applications. They are also a suitable choice for health monitoring of pavements due to their low cost and power consumption [65].

MEMS accelerometers are appropriate for low-energy vibration monitoring applications due to their small size, reliability in a variety of frequencies and ability to function in a variety of environmental conditions [39]. Quantitative Accelerated Life Testing (QALT) method has been developed by Bâzu et al. to investigate the dependability of commercially available

MEMS accelerometers. The QALT process was created as an application-driven test plan which integrated a temperature test with vibration and tilt testing enabling two different forms of mechanical stress to be measured. At temperatures up to 145°C, the accelerometers were tested at a fixed frequency. A single-channel, low-noise Texas Instrument 16-bit ADC that can sample an analogue input between 0 and 5 V at a rate of up to 1000 kHz and a dual-axis ADXL210 accelerometer was used with digital outputs of 1500 Hz and amplitude of 6g. The test results demonstrated outstanding dependability for vibration and tilt testing at high temperatures. A worst-case scenario was created since there were no failures even after 200 hours of vibration testing at 145°C. This strategy predicted a failure after 201 hours of vibration monitoring at 145°C, with the moving accelerometer fatigue fracture being viewed as the most likely failure source [39].

3.2.5. Evaluation algorithms for measured signal

In general, using inverse analysis to deduce pavement layer attributes is the primary goal of the study of the recorded accelerations. The three phases that make up the strategy herein proposed for reaching this goal are.

- Calculating the acceleration history at the sensor position while simulating the driving vehicle on a pavement model.
- Reveal and "separate" impact of the moving load from other vibration sources but the observed acceleration history must be smoothed.
- By changing the model parameters to match the calculations against the smoothed data, it is expected that the computed layer attributes best reflect the in-situ pavement state at the moment of measurement.

In this chapter, we will explore the fundamentals of accelerometer measurements, which involve capturing acceleration data and understanding how to process and analyse it. Accelerometers are devices used to measure acceleration and we will delve into how these measurements can be further utilized, such as integrating the data to calculate displacements or deformations caused by the acceleration.

3.2.5.1 Double Integration

This technique is based on the basic connection between vertical displacement and acceleration. Acceleration *a(t)* can be used to express pavement velocity *v(t)* and vertical displacement $y(t)$:

$$v(t) = v(0) + \int_0^t a(\tau)d\tau \tag{4-3}$$

$$y(t) = y(0) + v(0)t + \int_0^t \int_0^\xi a(\tau)d\tau d\xi \tag{5-3}$$

where $v(0)$ and $y(0)$ are dependent on the pavement's initial state and can be set to zero if it was at rest. The projected vertical displacement unexpectedly wanders when the observed acceleration is simply doubly integrated. The measurement inaccuracies at low frequencies are disproportionately amplified by the integration procedure, causing a significant vertical displacement drift. Since the pavement returns to rest once the weight has passed, the estimate defies physical principles. However, the anticipated ultimate vertical displacement is expected to be 50 µm rather than zero. A common approach in the literature to account for drift is to estimate the drift by fitting a polynomial and deducting it from the doubly integrated signal [87, 88]. While the following Algorithm 2 uses a somewhat more straightforward approach.

3.2.5.2 Constrained Least-squares Estimation

With the help of constrained least-squares estimation, this approach discretizes the link between acceleration and vertical displacement. In terms of pavement velocity $v(n)$ and vertical displacement *y(n),* the measured acceleration $a(n)$ may be expressed as follows. *T* is the interval between time t_{n-1} and time t_n respectively.

$$v(t_n) = \frac{y(t_n) - y(t_{n-1})}{T} \tag{6-3}$$

$$a(t_n) = \frac{v(t_n) - v(t_{n-1})}{T} = \frac{y(t_n) - 2y(t_{n-1}) + y(t_{n-2})}{T^2} \tag{7-3}$$

Rewriting in matrix form,

$$\overbrace{\begin{bmatrix} a(t_n) \\ a(t_{n-1}) \\ \vdots \\ a(t_0) \end{bmatrix}}^{a} = \frac{1}{T^2} \overbrace{\begin{bmatrix} 1 & -2 & 1 & 0 \\ 0 & 1 & -2 & 0 \\ \vdots & \vdots & \vdots & \vdots \\ 0 & 0 & 0 & 0 \end{bmatrix}}^{M} \overbrace{\begin{bmatrix} y(t_n) \\ y(t_{n-1}) \\ \vdots \\ y(t_0) \end{bmatrix}}^{y} \tag{8-3}$$

Imposing the beginning and final constraints on the pavement state, solve for *y* by minimizing the mean-squared error between *a* and the measurements a_m.

$$\begin{aligned} y^* &= \arg \min_{\underbrace{y|Cy=d}} \|a - a_m\|^2 \\ &= \arg \min_{\underbrace{y|Cy=d}} \|My - a_m\|^2 \end{aligned} \tag{9-3}$$

Lagrange multipliers or common numerical algorithms such *lsqlin* in *MATLAB* can be used to solve the least squares problem with linear equality requirements. Assuming that the pavement is at rest before to and following the application of the load will result in zero initial and final conditions in our example. Using *k* samples at the start and *m* samples at the final, the rest time can be defined as follows:

$$C = \begin{bmatrix} I_{k*k} & 0_{k*(n+1-k)} \\ 0_{m*(n+1-m)} & I_{m*m} \end{bmatrix}, d = \underbrace{[00\ldots0]^T}_{k+m} \tag{10-3}$$

3.2.5.3 Model-Based Estimation

Pavement-vehicle interaction model created by Bajwa et al served as the inspiration for this algorithm [89]. When the measured response can be represented by a family of functions *f (k; t)* parametrized by *k*, this approach is most appropriate. It is possible to choose the right family of functions using experimental results or a pavement response underlying model. The noise-corrupted measured acceleration is used by the previous two algorithms to directly estimate the pavement displacement.

Algorithm 3 initially de-noises the acceleration readings $a_m(t)$ before integrating the acceleration $a(t)$ twice to determine the displacement $d(t)$. *Considering* $a_m(t) = a(t) + \varepsilon(t) = f(k;\ t) + \varepsilon(t)$ where $\varepsilon(t)$ is a vector of unidentified model parameters and the measurement error or noise at time *t and k*. It is possible to estimate the acceleration $a(t)$as follows.

$$k^* = arg \rightarrow \min_k \int_{-\infty}^{\infty} (a_m(t) - f(k-t))^2\, dt \tag{3-11}$$

$$a(t) = f(k^* - \tau) \tag{12-3}$$

$$y(t) = y(0) + \int_0^t \int_0^\xi f(k^* - \tau) d\tau d\xi$$

Considering that $y(0) = 0$ indicates that the pavement was at rest at time *t = 0*,

$$y(t) = \int_0^t \int_0^{\xi} f(k^* - \tau) d\tau d\xi \tag{13-3}$$

The best accurate estimate was obtained using Algorithm 3 by curve-fitting. However, this was partially due to the right function family being employed to describe pavement acceleration. With the same three parameters as the following function, the Mexican hat function *f(k,t)* was selected to represent the Ricker wavelet family.

$$m(t_n) = -\alpha \left(1 - \frac{t_n^t}{\sigma^2}\right)^{e^{\frac{-t_n^t}{2\sigma^2}}} + \varepsilon(t_n) \tag{14-3}$$

The reaction for subsequent axle loads can be decoupled using algorithm 3, which is also the least sensitive to the selected time window.

At several points in the pavement construction, acceleration was measured and recorded in a digital file. The following equations can be used to numerically double integrate the recorded acceleration to determine deflections as defined in [90]:

$$vc_{(i)} = vc_{(i)} + \frac{a_{(i-1)} + a_{(i)}}{2} \Delta t \tag{15-3}$$

$$dc_{(i)} = dc_{(i-1)} + \frac{vc_{(i-1)} + vc_{(i)}}{2} \Delta t \tag{16-3}$$

where $a_{(i)}$represents the acceleration at the i_{th} sample. $c_{(i)}$ indicates the computed velocity there and $dc_{(i)}$ denotes the calculated deflection.

Nevertheless, double integration amplifies the original signal low frequencies like a filter. When there is pavement acceleration, it amplifies little baseline offsets in the acceleration such as errors or distortions in the reference level of motion. It transforms them into unacceptably large drifts in the estimated deflection. Thus, a quick and effective corrective technique to get rid of the drift was suggested [90]. The approach determines the drift in the computed deflection under the assumption that it is zero when mechanical stress of tire is absent. This presumption is accurate both before and following the tire load arrival at the measurement site. Although the drift is unknown between the two instances, it may be predicted using a spline interpolation. Experience has demonstrated that methods for linear baseline correction such as the one described in [91], are ineffective for approximating the random drifts that result from the double integration of road accelerations. As a result, a nth-order polynomial function is

employed. The corrected deflection is obtained by subtracting the polynomial function from the computed deflection.

3.2.5.4 Wave Propagation Algorithm

When striking a pavement structure vertically on its surface, three varieties of stress waves emerge. These encompass longitudinal waves, Transverse waves and Rayleigh waves. In this context, our attention is directed towards longitudinal waves, often referred to as compression or P-waves, which primarily travel in a vertical downward direction [93]. Stress waves exhibit two potential states based on their amplitude.

- Elastic, causing reversible deformation exclusively.
- Inelastic, involving irreversible deformations.

The advancing wavefront on the other hand, consistently pertains to an elastic wave due to its swifter pace compared to inelastic waves. In this context, accelerometers are positioned both at the upper and lower surfaces of the targeted layers. Their purpose is to ascertain the time of flight, denoted as Δt, for the advancement of a vertical longitudinal wave traversing through these layers. By employing the measured Δt values, it becomes possible to calculate the velocity of the longitudinal wave, denoted as v_L. Here, h represents the thickness of the relevant layer.

$$v_L = \frac{h}{\Delta t} \tag{17-3}$$

The determination of the elastic stiffness of the layer through its longitudinal wave velocity is enabled by two practical presumptions.

I. The layer is conceptualized as a macro homogeneous substance.
II. Longitudinal wave is treated as a bulk wave (as opposed to a bar wave) [93].

Longitudinal bulk waves exhibit similarity to waves propagating through infinite media, where lateral deformation is constrained. Longitudinal bar (extensional) waves resemble waves propagating through slender rods, allowing lateral deformation [94]. Given these conditions, the subsequent relationship between the elastic stiffness tensor component $C1111$, the material's mass density ρ, and vL emerges [93]:

$$C_{1111} = \rho v_l^2 \tag{18-3}$$

The subsequent standard relation of isotropic elasticity enables the calculation of the modulus of elasticity E

$$E = C_{1111}\frac{(1+\nu)(1-2\nu)}{1-\nu} \tag{19-3}$$

3.3. Strain Sensors

3.3.1. Introduction

Strain (ε) is used to describe the relative change in length, often caused by mechanical stress [102].

$$\varepsilon = \frac{\Delta l}{l_0} \tag{27-3}$$

Here, l_0 represents the initial length, and Δl signifies the absolute alteration in length. When the material lengthens due to strain, it usually concurrently becomes slimmer. The lateral strain can be defined as follows:

$$\varepsilon_q = \frac{\Delta \mathrm{d}}{d_0} \tag{28-3}$$

The ratio of lateral to longitudinal strain is known as the Poisson's ratio:

$$\nu = -\frac{\varepsilon_q}{\varepsilon} \tag{29-3}$$

For small deformations, strain is proportional to mechanical stress. The constant of proportionality is known as the modulus of elasticity:

$$E = \frac{\sigma}{\varepsilon} \tag{30-3}$$

Strain gauges (SGs) are the delicate elements employed in various forms within sensors, such as for gauging weight, pressure, mechanical stress, acceleration, or displacement. Rarely do they serve the purpose of measuring strain itself. Most strain gauges consist of a winding metal layer situated on a substrate, often a polyimide film. To provide protection for the metal layer, it is also encased with a protective film. Typically, the strain gauge is affixed to the measurement object by employing an adhesive, such as epoxy resin or cyanoacrylate glue. The strain state of a material is not a scalar quantity. When analysing a planar surface element, it can experience stretched along one direction while being concurrently compressed along

another. The measurement using strain gauges is affected by various temperature effects, fatigue and creep of the adhesive layer [102].

The ability to study pavement reaction to moving loads over time and to validate the design-phase assumptions is made possible by strain measurements of the pavement which is of significant interest [103]. It may be feasible to foretell the occurrence of fatigue or rutting events by tracking the evolution of strain in the pavement over time. High tensile stresses at the base of the asphalt layers brought on by continuous traffic loads and climate effects reduce the pavement overall bearing capacity. Rutting which is characterized by a permanent pavement deformation can result from repeated compression loads brought on by vehicle movements [104].

Between 2003 and 2006, the National Centre for Asphalt Technology (NCAT) carried out a number of instrumentation studies. The aim was to explore connection between vehicles and pavement as well as how this affected pavement degradation [105]. These investigations used Geokon 3500 Earth Pressure Cells (EPCs) and Horizontal Asphalt Strain Gauges from Construction Technology Laboratories Inc (CTL). Vertical stress and horizontal strain were quantified on asphalt concrete (HASG). The Virginia Smart Road project instrumented 12 flexible pavements [106]. The researchers placed Geokon 3900 EPC to detect vertical stress at the layer interfaces and Dynatest Strain Gauges to assess horizontal strain of asphalt concrete.

Using the vertical stress and the stiffness of the asphalt concrete, the deformation of the material can be estimated. However, the Hot Mix Asphalt (HMA) stiffness is strongly influenced by the pavement age, temperature profile and frequency of loading. These factors make the output quite challenging to be accurate [107].

In road construction, various types of strain sensors are employed to monitor the stresses and deformations of roads. Some of the common strain sensors used in road construction will be discussed below:

3.3.2. Vertical Gauges

A vertical strain gauge, specifically designed to evaluate and track the vertical strains and deformations experienced by road structures, this type of strain gauge is strategically positioned in a vertical orientation on the surface of the structure. This positioning enables precise

detection of changes in length or deformation along the vertical axis. To gauge vertical stresses in the base, subbase and subgrade an earth pressure cell is employed. Two circular stainless-steel plates are joined at their edges by welding. To fill the small space between the plates fluid is employed. When vertical load is placed on top of the fluid it becomes strained. Within the stainless-steel tubing a pressure transducer is mounted. The data acquisition system detects the electrical signal (often voltage) that the transducer converts from the fluid pressure [108]. The sensitive component of the vertical asphalt strain gauges is held in place by two circular plates. The bottom plate job is to hold the sensor in place, while the top plate distributes the weight evenly across the centre bar. Additionally, this particular sort of sensor has a sharp spike that can be placed into the underlying layer [109]. A scheme of a vertical asphalt strain gauge is given in Figure 3.2.

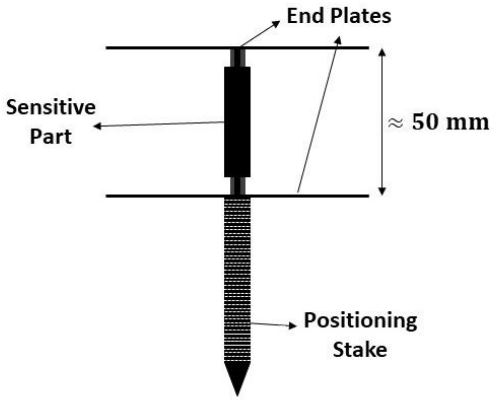

Figure 3.2: Schematics of a vertical asphalt strain gauge

Mechanistic-Empirical Pavement Design Guide (MEPDG), a recently developed tool calculates the total rutting by adding up the deformations of all trial pavement layers. The trial section is prepared for construction if all distresses including rutting fall within the standard. Therefore, to verify MEPDG for local circumstances, vertical deformation (or strain) is measured as presented by Md Rashadul Islam et al [108]. The sensor is kept in place without tilting using the bottom plate. The applied force is distributed evenly across the sensors by the top plate. To achieve the appropriate density, HMA is placed in between these two plates and manually compressed. It can resist temperatures up to 205 °C and includes braided lead wire coated with Teflon polymer to reduce electrical noise.

The compressive stress in the road structure, particularly in the unbound layers, is measured using pressure cells. These gadgets' modes of operation rely on their attributes. In reality, there are primarily two categories of pressure cells, hydraulic and diaphragm-based. The first one is

made up of two steel plates that have been arranged to create a cavity between them which is filled with liquid. Strain gauges are used to monitor the induced liquid pressure which correlates to the applied load. A rigid ring that supports a diaphragm makes up the diaphragm cells. A strain gauge measures the diaphragm's deflection which is caused by the application of load [93]. Al-Qadi et al. [110] recommended a technique for the installation. For the sensor to be in the horizontal position after being inserted into the excavation of the unbound layer. Levelling must be verified before building work begins and the previously dug material is finally used to cover the sensor.

3.3.3. H – Gauges

Horizontal asphalt strain gauges are dedicated sensors utilized for measuring and analyzing strains occurring within asphalt surfaces, such as roadways and pavements. The sensor H shape helps to improve their anchor in the asphalt medium. The centre bar can have one to four active strain gauges coupled in direct configurations to contain. The centre bar edges are each joined to a metal strip. A schematic representation of a horizontal asphalt strain gauge is given in Figure 3.3. Since significant tensile loads are concentrated here and might result in fatigue crises, they are often positioned towards the base of the bituminous layers [109].

Similar to those described in the preceding section [108], the operation concept and compatibility with asphalt materials and building stages are also shared. To allow the positioning stake during installation, a hole must be drilled. To fill the hole and cover the area, sand binder combinations are used. The sensor is then carefully inserted into the hole until the bottom plate makes contact with the surface. The suppliers often advise first removing the top plate so that you may apply the asphalt mix all around the gauge. Then replacing it so that the mix covers the sensor and following that paving and compacting could begin. In terms of statistics, H-gauges have a higher survival rate than vertical asphalt strain gauges [109].

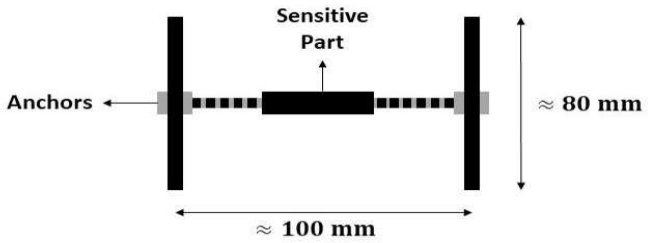

Figure 3.3: Schematics of an H-gauge

3.3.4. Fiber Optics

Fiber optic sensor (FOS) is a device that detects certain amounts of strain using an optical fiber that is coupled to a light source. Due to their compact size, flexibility, embeddability and immunity to electromagnetic interference FOSs constitute a viable technology to gather essential information regarding the pavement conditions [111]. Additionally, FOSs provide local or distributed strain measurements with excellent precision (resolution of around ±1 με).

Vertical deflection of a road pavement is measured using linear variable differential transformer (LVDT). These devices transform the relative displacement from a mechanical reference into an output voltage. A reference rod needs to be secured deep enough for the deflection caused at minimal surface loads. The most advanced multi-depth deflectometers (MDD) can measure deflection at many places along the pavement structure. Whereas single-layer deflectometers (SLDs) can only measure the deflection of a single layer of the pavement. Before installing the LVDT and the upper plate, it is necessary to complete a core for the positioning of the rod and sealing. Finally, some asphalt must be used to protect the plate [112, 113]. Due to their infinite resolution, these instruments can deliver readings that are very exact. Zhou et al confirmed the viability of using the Wuhan Heavy Duty Machine Tool Factory casting facility. MEMS high-temperature optical fiber F-P acceleration sensing system was tested in an industrial setting. The detecting probe was rigidly connected to the casting cavity because it was immersed in the casting sand which was roughly at 1300 °C. The sand mold was cast using a vibration motor in order to improve the quality of the foundry goods during the cooling of the casting steel. A signal demodulation system with an industrial control computer was then used to track the casting vibration status in real time throughout the cooling process [114].

Modern fiber optic sensing technologies have evolved quickly to fill the gaps left by electrical sensors. The optical fiber Bragg grating (FBG) sensor, the most frequently used fiber optic sensor in engineering has been extensively studied for structural health monitoring of diverse infrastructures [115-116]. Its distributed sensing capabilities, small weight, resilience to electromagnetic interference, high accuracy, sensitivity and capacity for survival make it a desirable sensor[117]. A fiber Bragg grating (FBG) acts as a distributed Bragg reflector within a short segment of optical fiber. It reflects specific wavelengths of light while transmitting others, accomplished by a periodic variation in the refractive index of the fiber core, creating a wavelength-specific dielectric mirror. The Bragg wavelength is sensitive to strain, meaning that any strain causes a shift in the Bragg wavelength. By measuring this wavelength shift, the

strain can be deduced. The long-term study of the performance of a pavement might use an FBG sensor. Wang and Tang [118] examined the bare FBG sensors for pavement monitoring in 2005 employing a pair of fiber gratings for simultaneous detection of pavement stresses and temperatures. However, a glass-based bare FBG sensor is particularly vulnerable to breakage during the demanding pavement building process [119]. Contrarily, the usage of glass fiber reinforced polymer (GFRP) material has shown to be a durable material for civil applications. It has improved the ruggedness of FBG sensors by packaging and protecting them [120, 121]. The GFRPFBG sensor invention opens up possibilities for a dependable fiber optic sensor for ongoing pavement condition monitoring.

3.3.5. Geophone

Geophones are sensors that gauge the pavement's displacement velocity when it is subjected to shifting stresses. Thus, the deflection response may be obtained simply once integrating the signal. A mass that is connected to a spring and enclosed in a coil make up the gadget (Figure 3-4). When the geophone moves, the coil and magnet both move in relation to it. As a result, a voltage that is proportionate to the displacement velocity as determined by the geophone is induced in the coil [122,123]. Measurements are only feasible above a minimal frequency because geophones often exhibit a nonlinear response and an attenuation of the recorded displacement amplitude beneath the natural frequency [124].

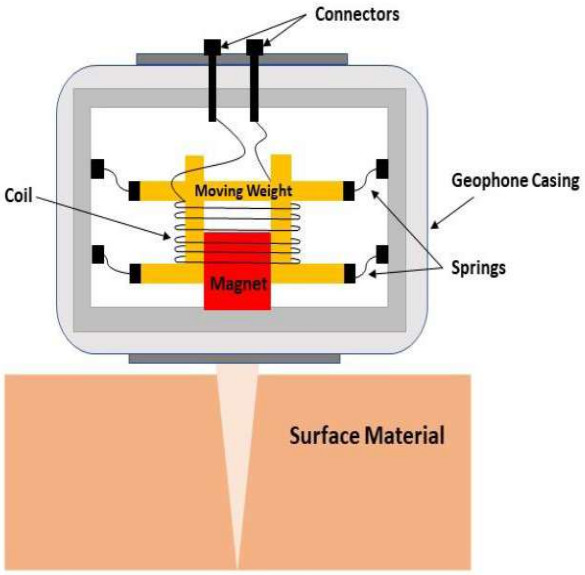

Figure 3.4: Geophone

3.4. Temperature Sensors

3.4.1. Introduction

Monitoring the temperature in road construction is crucial for Material Properties (such as asphalt, concrete, and aggregates), Workability, density and compaction of materials (is essential for the road's stability and load-bearing capacity), Preventing Issues (such as freezing or excessive heat, can negatively impact the road's structural integrity) and Longevity.

Temperature sensors operate on diverse physical phenomena that change with temperature variations. Here are several of the most common measurement principles for temperature sensors:

Thermoresistive sensors: Some materials change their electrical resistance with the temperature. Platinum resistance thermometers (Pt100) demonstrate a foreseeable change in resistance with temperature. Pt thin films are employed as a sensing layer. Thin layer enables cost-effective production despite high raw material costs. Platinum is a good compromise between high resistance (10.6 μΩcm), excellent TCR Temperature Coefficient of Resistance (3927ppm/°C) and exceptional material properties. Pt thin film structured on Al2O3 ceramic using photolithography [102].

Thermoelectric sensors (Thermocouples): Thermocouples employ the thermoelectric phenomenon, in which a voltage is generated due to the temperature contrast between two different metals or alloys. This voltage is directly correlated to the temperature difference, enabling temperature measurement through two effects: Seebeck and Peltier. The Seebeck effect is the occurrence of contact voltages due to different chemical potentials. The Peltier effect occurs when an electric current is passed through a thermoelement, causing energy to transfer from one junction to the other [102]. The most wildly used probes for measuring pavement temperature are thermocouples. Thermocouple types K, E or T are suitable for embedding in pavement since they may be used from subzero to extremely high temperatures. But they are less precise than the following technologies in the range of 0.5 to 5 °C [109].

CMOS-basierte Temperatursensoren: Temperature sensors based on CMOS technology are devices produced using Complementary Metal-Oxide-Semiconductor (CMOS) technology, which is a highly prevalent approach in the semiconductor industry. These sensors make use of CMOS circuits to detect and record variations in temperature. CMOS-based temperature sensors offer several advantages such as cost-effectiveness, low power consumption (making

them suitable for battery-operated applications), integrated circuit functionalities, and good linearity (often providing a linear response to temperature changes, crucial for accurate measurements) [102].

Bimetallic Strips: Bimetallic strips are composed of two layers of metal with distinct coefficients of thermal expansion. When the temperature changes, this leads to the bending or deformation of the strip, which can be utilized for temperature measurement [102]. Linear length expansion:

$$\frac{\Delta l}{l} = \alpha \Delta T \qquad (31-3)$$

These diverse measurement principles offer a broad range of possibilities for temperature measurements across various applications, depending on precision needs, temperature ranges and environmental circumstances.

3.4.2. Thermochron iButton

Temperature measurement and storage are features of Maxim Integrated Products has been developed with trade name Thermochron iButton. This affordable and dependable temperature sensor contains a secured memory section and a wide temperature range thermometer (14 to 185°F). It can hold up to 2,048 temperature measurements and record time and temperature at user-defined intervals of up to 255 minutes (Maxim Integrated 2014). If the internal battery can ensure a minimum of two years of operating duration at room temperature, the monitoring period can be increased to 340 days. This depends on the maximum measurement interval. To guarantee that it operates effectively in the concrete environment, the iButton sensor is also covered by a tough stainless-steel covering.

The iButton temperature sensor large memory, extended battery life, tough packaging and affordable price are key benefits. For temperature monitoring of new concrete during construction, field projects have employed iButtons. For instance, the Des Moines International Airport used iButtons to track the temperature history of freshly laid concrete. Texas Department of Transportation used iButtons in a demonstration project in 1999. The iButton does not require a continual connection with the laptop because it has its own memory system, unlike the MEMS digital humidity sensor [2].

3.4.3. Radio-Frequency Identification (RFID) Temperature Tag

An RFID Temperature Tag is a specialized type of Radio-Frequency Identification (RFID) tag that is designed to monitor and transmit temperature-related data. These tags are commonly used in various industries and applications where temperature monitoring is crucial, such as pavement health monitoring, large-scale structures like dams and environmental monitoring These active wireless RFID tags incorporate MEMS-based temperature sensors and advanced ultra-high frequency (UHF) RF technology, enabling real-time data collection and storage [2]. the RFID tag comprises an internal temperature logger for capturing concrete temperature at predefined intervals, as well as a built-in battery for power. The presence of an antenna within this tag facilitates communication with the Pro device, allowing for tag identification, data extraction, and adjustment of time intervals. Through interaction with the portable Pro device, the collected temperature data could be seamlessly transferred and stored for subsequent concrete maturity calculations using the PCC (Portland Cement Concrete) maturity concept. Consequently, this RFID tag proved highly suitable for concrete temperature monitoring [2].

This tag boasts the capability to transmit and receive data at distances of up to 100 feet (30 meters) from the handheld device or up to 300 feet (100 meters) from a fixed interrogator. Its remarkable operational lifespan, exceeding six years, can be attributed to its low power consumption. Within this system, the i-Q32T RFID tag can be divided into two components: an embedded probe and an extended probe. The embedded probe represents the temperature logger installed within the i-Q32T tag. However, for deep pours and large concrete structures, an RFID tag can be equipped with a stainless-steel temperature probe. This extended probe allows for temperature measurement at considerable depths below the concrete surface. Nevertheless, even with an extended probe attached, an i-Q32T tag with an antenna can still be placed at the surface to transmit data [2].

The most important advantages of RFID tags are their low cost, extensive communication range, durability in concrete, and low power consumption.

3.5. Humidity Sensors

3.5.1. Introduction

It has been shown that an excess of moisture in the road structure accelerates pavement distress and reduces road-bearing capacity. As a result, it is important to plan and include drainage

systems into the road which can be effective over the duration of the pavement. Monitoring the moisture content at various depths on the road structure can provide access to information about the drainage systems and record mechanical characteristics of the pavement [129, 130]. Humidity can be quantified through two methods: absolute humidity and relative humidity. Absolute Humidity is characterized as the proportion of the water vapor mass present in the air relative to the air volume. Relative Humidity is defined as the proportion of the moisture content in the air compared to the maximum (saturated) moisture capacity the air can retain at a same given temperature and pressure of the gas. Relative humidity (RH) stands as one of the most frequently measured parameters in both industry and everyday situations. Traditionally, microporous thin sheets and thin plates of piezoelectric quartz sensors have been employed to measure RH. These materials operate based on alterations in luminescence and oscillation frequency, respectively, to achieve sensing. A range of humidity sensors exists, categorized by sensing mechanisms, sensing materials, sensor design, fabrication technologies, and applications. These sensors are classified as capacitive, oscillating, resistive, gravimetric, impedimetric, thermo elemental, hydrometric, or integrated optical, depending on their method of sensing. Studies indicate that optical fiber sensors demonstrate optimal performance in severe weather conditions [131]. For pavement purposes, humidity sensors like MEMS Humidity Sensors, capacitive sensors or resistive sensors with suitable protective measures are frequently employed to oversee moisture levels and guarantee the structural stability of the pavement. These sensors contribute to the control of aspects such as road safety, longevity, and overall performance in diverse environmental conditions.

3.5.2. MEMS-Based Relative Humidity and Moisture Sensors

Bridges, pavements and buildings are exposed to degradation processes over time which can be accelerated by excessive moisture content. High chloride concentrations are transferred by moisture from saltwater, rain, soil, snow and floods which causes steel reinforcing rebars to corrode. Additionally, moisture transfer encourages harmful chemical reactions including carbonation and the alkali-aggregate reaction as well as chemical degradation [132]. Norris et al. (2008) experimentally and analytically evaluated the application of nanotechnology/MEMS to monitor the temperature and internal relative humidity of concrete. They employed microcantilever beams and moisture-sensitive thin polymer for this purpose. Embedded wireless MEMS and nanotechnology-based sensors have the potential to create self-sensing. This was reported by a recently released feasibility study by Saafi et al. [132]. Concrete

structures can benefit if early occurrence of tiny cracks is detected. Moreover, measurement of the rate of temperature, moisture, chloride, acidity and carbon dioxide levels could reflect a loss in structural integrity.

Yang et al. [133] used the Sensirion® SHT71 digital humidity sensor, a commercial off-the-shelf MEMS device that can detect temperature and relative humidity (RH). The commercial MEMS digital humidity sensor an innovative device that combines sensor elements and signal processing circuitry on a silicon chip using MEMS technology.

To provide a completely calibrated digital output, commercial MEMS digital humidity sensor incorporates components paired with signal processing circuitry on a silicon chip. The capacitor of a MEMS sensor is constructed as a special capacitive sensor element made of paired conductors to detect humidity and monitor temperature. A polymer dielectric that separates these conductors may absorb or release water according to the relative humidity of the surrounding environment, changing the capacitance of the capacitor. A "micro-machined" finger electrode system with various protective and polymer cover layers also serves as the capacitance for of this MEMS sensor. It may concurrently shield the sensor from interference. However, MEMS sensors must be linked to a data reader such as evaluation kit EK-H4 and a computer. Both constantly require power (battery) supply, to continually monitor and store measurement data. Therefore, the development and integration of a wireless communications sub-system into MEMS digital humidity sensor was the main emphasis of this work [13]. The wireless transmission and reception ends are the two components of a designed wireless system. Data is sent from MEMS sensor into wireless transmission device via the wireless transmission end. The computer wireless receiving end is utilized to download data without the usage of a cable. To communicate between the transmission and receiving ends, microcontrollers and XBee-PRO modules are needed [133].

RH is calculated using an electrical circuit by determining the capacitance difference. A "micro-machined" finger electrode system with various protective and polymer cover layers also serves as the capacitance for the chip of the MEMS sensor. This may concurrently shield the sensor from interference. However, MEMS humidity sensors must be attached to an evaluation kit EK-H4 data reader and a computer. They need a constant power supply to continually monitor and save measurement data. Temperature and humidity on a concrete pavement (JPCP) in a US-30 highway section near Ames, Iowa, USA, were monitored using this sensor (described in section 4-11) [133].

3.5.3. LC Water Content Sensor

It is crucial to keep an eye on the moisture levels in water-permeable transportation infrastructure. In order to be reliable over the long term, it is critical to precisely calculate the water demand. Unwanted moisture can cause peeling and debonding of the asphalt and aggregate particles in asphalt mixes. A wireless and passive embedded sensor was developed by Ong et al. (2008) [134] for monitoring the moisture content of civil engineering materials. This included items such sand, subgrade soil and concrete in real-time.

The LC sensor will be useful for tracking water levels in asphalt concrete pavements. That is made of a composite composition comprising fine and coarse aggregates, asphalt binders and porosities. Throughout the asphalt pavement useful life water that is being accumulated. This is due to precipitation, snowmelt, subterranean water tables and runoff strips from asphalt cement during coarse aggregates which compromises the pavement structural integrity. The asphalt pavement water or moisture content can be monitored by the LC sensor enabling for efficient management, rehabilitation and maintenance [134]. In addition, Ong et al. (2008) identified a number of potential uses for the LC sensor in transportation engineering projects. This included monitoring water trapped in pavement substructures at base, subbase, subgrade and pile structures. It can lead to frost-heave issues, subsurface erosion, pavement depression and loss of structural integrity.

The sensor employed a planar inductor-capacitor (LC) circuit embedded within test samples for remote water content measurement. It tracked changes in the sensor's resonant frequency via a loop antenna. Water, having a higher dielectric constant than the samples, increased the circuit's capacitance, lowering the sensor's resonant frequency. This allowed for efficient water content monitoring [134].

The zero-reactance frequency Fz is at which the imaginary portion of the impedance (reactance) goes to zero. The resonant frequency F0 is the frequency at which the real component of the impedance (resistance) is at its highest. The sensor is represented by an inductor and capacitor that are serially coupled in order to connect F0 and Fz to the inductor and capacitor. In order to simulate capacitive loss, the capacitor is additionally connected in parallel with a resistor as shown in Figure.3.5 [134].

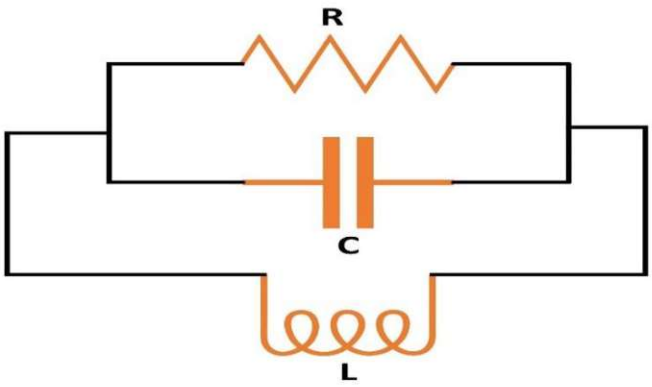

Figure 3.5: The Sensor Is Modeled As An Inductor L And Capacitor C Connected In Series

$$f_0 = \frac{1}{2\pi\sqrt{LC}} \tag{32-3}$$

$$f_z = \frac{1}{2\pi}\sqrt{\frac{1}{LC} - \frac{1}{R^2C^2}} \tag{33-3}$$

Accordingly, the capacitance of the capacitor is greatly increased by the presence of water, which lowers the sensor resonant frequency as given in (32-3). The electrically conductive water also causes the capacitor capacitive loss to rise which lowers *R*. Equation (33-3) shows that the sensor's resonance frequency is only reliant on the capacitance as the inductance is constant during the experiment. This is used to monitor changes in the dielectric constant. On the other hand, the zero-reactance frequency is a function of capacitance and resistance. This relies on the substrate conductivity and dielectric constant respectively. To increase measurement precision, the zero-reactance frequency can also be monitored in addition to the resonant frequency [134].

The LC sensor offers cost-effective and reliable roadway condition monitoring. Its affordability, wireless, passive design (no battery lifetime problems), durability and portability make it superior to other monitoring sensors, especially RFID (the radio-frequency identification)-based ones that are more prone to electrical component failures [134].

3.5.4. Capacitive Humidity and Moisture Sensors

Hydrophobic polymers and other organic materials find use in crafting capacitive humidity sensors. These sensors exhibit greater durability compared to equivalent resistive humidity sensors, given their ability to handle significant water vapor condensation under high humidity

conditions and operate effectively at relatively elevated temperatures, up to around 200°C. Capacitive thin-film humidity sensors are responsive to RH variations as their operation hinges on the dielectric constant value of the active layers. The performance of capacitive humidity sensors is influenced by three primary factors, encompassing the electrode's surface area, polarization of the dielectric material, and the separation distance between the electrodes [131]. MK33 Capacitive Humidity Sensor and the Hydro-Probe II Moisture Sensor are two probe-based moisture sensors that have been developed. They may be used to monitor internal RH in concrete [2]. Due to great solvent and hot water resistance, MK 33 capacitive sensor may be placed directly into a concrete mixture. The Hydro-Probe II Moisture Sensor measures RH in concrete using digital microwave moisture measurement. This Sensor may be immediately inserted into plastic concrete much as the MK 33 Capacitive Humidity Sensor to offer accurate RH reading. Other probe-based moisture sensors such as Time Domain Reflectometry (TDR) and the Stevens Hydra Probe are frequently employed in soil moisture monitoring. However, RH profile versus pavement depth cannot be provided by these probe-based moisture sensors [2].

3.5.5. Smart Dust

A "Smart Dust" wireless sensor network was designed by Pei et al [135, 136] to monitor pavement temperature and moisture content in order to identify ice road conditions. The system was created using sensor network devices that are readily available. Based on sensor readings, a dry, wet, frozen and other pavement surface states classification algorithm was created and included into the sensors. Three different types of sensors were chosen to interface with the Mica 2 motes employed in their study based on the suggested methodology to identify ice road conditions. The Crossbow "Smart Dust" wireless network third-generation mote module is represented by Mica 2 motes.

3.6. Energy Supply

For traffic management and road maintenance, the information on traffic and structural state may be obtained by using accelerometer sensors for analysing the dynamic reaction of the pavement.

Monitoring time might be separated into short-term and long-term period, depending on the type of measurements. Test conditions heavily depend on the durability of the sensors and energy supply. A longer monitoring period is typically preferred even if it can be obtained. A

short-term period may just last a few months while a long-term period may last many years. The time between data measurements might range from a few seconds to many hours. However, short periods might deliver more detailed data while using more power. Hence it is important to find a balance between the length of the data-measuring interval and battery life. One tactic is to modify the interval as circumstances change[73].

The damage is not assessed directly on specimens since the modern monitoring methods do not call for the removal of pavement samples. It is rather explored through monitoring of pavement characteristics such as elastic modulus or acoustic qualities. The majority of the sensor properties, such as packaging, energy supply system, materials are influenced by these variables [74].

One of the biggest barriers to the broad adoption acceleration sensors and systems is the availability of electricity over a long period. Commercially available sensors are often powered by battery which prevents continuous and long-term usage. Regularly replacing batteries due to their limited lifespan, which typically lasts about 1 to 2 years (Lajnef et al., 2011) and even as short as four months for lightweight batteries (Nataf and Festor, 2013), proves to be both costly and impractical. A solution lies to use energy harvesting from ambient. For example, mechanical energy that automobiles send to the surface of the road with piezoelectric materials capable of converting this energy into electricity and vice versa [74].

Asphalt pavements can see millions of vehicles passes over the course of their useful life. Moving cars subject the pavement to stress, strain, deformation and vibration. The effect of the car weight also causes the pavement to experience strain and kinetic energy. However, these energies are lost as wasted thermal energy in the pavement increasing the likelihood of pavement degradation. Researchers have recently started looking for new technology to harvest such mechanical energy. The most promising technology is piezoelectric based approach as it can turn stress into energy [75]. Using piezoelectric material significant mechanical energy of the pavement can be captured. The ability of the piezoelectric material is to transform stress into electric charge. A powerful electric field can be used to polarize a piezoelectric material that is electrically neutral. However, there a strong polarization will remain when the electric field is dissipated. On the polarization surface, free charges are absorbed to keep the material electric neutrality. When a force is applied, the substance deformation changes the strength of the polarization causing some free charge to be released in order to maintain the electric neutrality [75].

When the truck volume is greater than 600 V/h, as demonstrated for the 1+2 type truck, the potential mechanical energy can exceed 150 kW for one kilometre of one-lane asphalt pavement. In addition, different PZT-based transducers are investigated in this study for harvesting energy from asphalt pavement. The PZT piles are extremely durable and have a great energy collecting efficiency. If the transducers are physically inserted in the pavement, the total amount of energy that may be extracted is little. Later, a pavement generator prototype construction was developed. According to estimates, a single lane of asphalt pavement may provide more than 50 kW of energy [75].

Assuming the PZT is oriented vertically at the 3rd axle the energy generated through external stress can be computed by:

$$U_E = \frac{1}{2} d_{33} g_{33} T_3^2 At \tag{1-3}$$

$$T_3 = \frac{\sigma A_c}{nA} \tag{2-3}$$

$$A_c = \frac{\pi(h+d)^2}{4} \tag{3-3}$$

U_E: the energy harvested from the pavement for single PZT in Kw

T_3: the stress on the top of PZT

A: the area of PZT

T: the thickness of PZT

A_c: the effective load area

n: the number of PZT piles used in one generator

h: the embedding depth of generator

d: the diameter of one tire print

An analysis of the PZT piles employed in the pavement generator considers their quantity, shape and electric potential. For 0.04 m2 of pavement, 8–16 PZT piles are advised. Increasing the number of PZT piles reduces the individual pile area but raises fabrication costs. Conversely, excessively thin PZT piles risk generator instability under dynamic vehicle loads. To balance stress, displacement, costs, and structural stability, it's advisable to consider using

8-16 piles for a single pavement generator. To reduce the electric potential on the pavement generator, a multilayer PZT structure and a round shape for the pile section are suggested [75].

in another study, in addition to power management energy harvester circuit is developed to accomplish long-term monitoring. Solar harvesting is a helpful option when considering a typical SHM situation where sensors are put out in the open on buildings or bridges. In optimal environmental conditions, a solar panel can produce a power density ranging from 15 to 100 mW/cm^2. Let's consider a solar panel with a surface area of 120 mm × 60 mm. Assuming a worst-case scenario with only 4 hours of full solar light and factoring in a 25% loss from recharge and storage circuitry, we can expect an average daily power generation of approximately 3.24 Wh. This daily energy intake from the solar panel is two orders of magnitude greater than the power consumed by the connected device [76].

Energy conservation techniques such as the one described above, are fundamentally important from the perspective of sensor lifespan for battery-powered devices. This provides a monitoring duration sufficient for pavement monitoring purposes. For wireless sensors and systems, several different procedures have been developed in an effort to conserve energy and extend longevity [77]. The situation is different for self-powered devices where these algorithms enable the most effective use of the energy produced but only have a little impact on its longevity. The deterioration of the sensor itself determines their capacity to survive rather than the availability of energy anymore. As a result, their longevity cannot be determined only by how efficient they are with energy. This must be determined through experimental testing and long-term full-scale implementations.

A wireless sensor accuracy and power use are negatively correlated and both are influenced by the sampling rate and transmit power levels [78]. The sensor lifespan is extended by lowering these two factors, but the accuracy is jeopardized. For this reason, the sensor intermittent operation enables improved energy economy while keeping high-quality data.

The use of energy harvesting architecture is limited and calls for a comparable energy saving technique. The voltage generated by the piezoelectric transducer cannot be directly utilised by the sensor in the road pavement environment. It is characterized by intermittent voltage spikes and the energy of a single event is insufficient to power the sensor. The answer is to store this random energy created by the pressure exerted by cars and anticipate the right time to release it [79].

3.7. Data transmission

To prevent inadvertent data loss, daily data collection and backup are desired. However this may change depending on the circumstances and factors like weather, cost or distance.

In applications where sensor connectivity to a remote transmission system via cable connections is acceptable, it's common for both data transmission and power supply to the sensors to be facilitated through these cable connections. In wired transmission, sensors are directly linked to a data acquisition device or a central hub using a cable, which can be either traditional copper or fiber optic. Data is transmitted from the sensors to the acquisition device via the cable. Wired systems typically offer reliable and swift data transmission, although limited in range by the physical constraints of the cable.

For other applications, cable connections to individual sensors may be impractical or infeasible, necessitating data communication between sensors and a remote transmission system via wireless or optical interfaces [5].

Wireless transmission is ideal for applications where a wired infrastructure isn't feasible or when flexible installation is required. In wireless transmission, sensor data is transmitted wirelessly using radio waves to a receiver. LoRa (Long Range) is a wireless technology crafted for Internet of Things (IoT) applications, offering extensive range with minimal power consumption. Utilizing a modulated chirp signal technique, LoRa ensures exceptional transmission reach, even in challenging environments like buildings or areas with dense vegetation. Sensors send data packets to LoRa gateways periodically or in response to events, which subsequently relay the data to a central server or cloud platform.

LoRaWAN (Long Range Wide Area Network) is based on the LoRa protocol and was designed as an extension specifically for use in networks. The difference between LoRa and LoRaWAN lies in the fact that LoRa refers to the physical layer technology enabling wireless communication over long distances, whereas LoRaWAN is the communication protocol defining the standards and functionalities for the communication and management of IoT devices over a LoRa-based wireless network. It offers a very long range (typically between 10 to 70 kilometres), making it ideal for applications that require communication over large distances. A LoRaWAN network consists of gateways that enable communication between end devices (sensors or actuators) and a central network server. Some reasons for using LoRaWAN include: Unlicensed frequency bands, Open-source technology, Good indoor coverage, Low power consumption.

While wireless systems offer flexibility, they may be subject to greater susceptibility to interference based on the environment and conditions, in contrast to wired systems [80].

Local wildlife and extreme weather should not be allowed to damage the on-site data acquisition system (DAS) or power supplies. However, a moving vehicle mounted with a DAS can be utilized for data collecting provided wireless sensors are employed. Reliable wireless transmission technology that can provide a potent signal and remove electronic interference is necessary for achieving this aim as shown in Figure 3.6 [80].

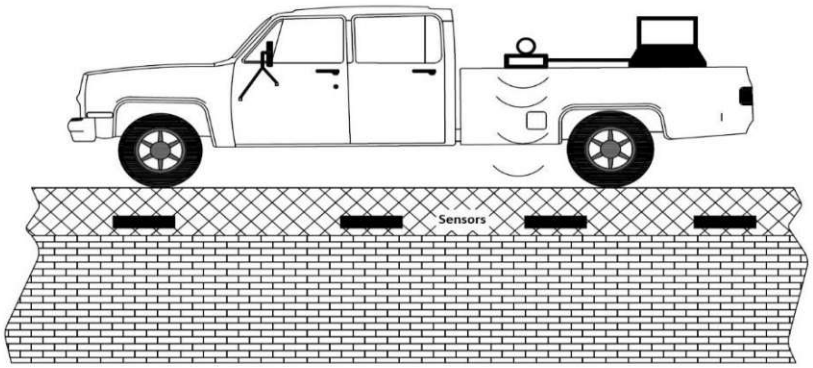

Figure 3.6: Radio Frequency (RF) Reader Mounted on A Moving Vehicle [80]

Simultaneous Sensing and Actuating Smart Antenna Element is a design developed by Das et al. (SSASAE). The single microstrip antenna that is dispersed on a piezoelectric substrate and coupled to digital and analogue components forms the foundation of the design. The design may dynamically stimulate the structure being monitored since the piezoelectric substrate enables it to work as both a sensor and an actuation device. The microstrip antenna is operated by a remote reader and is constructed of a number of patterned narrow metal strips printed on a subsurface layer of the SSASAE. Depending on the polarization orientation chosen these strips can transmit electromagnetic waves in one of two directions. This functionality allows for the control of the device using information that is modulated into both orthogonal polarization directions of a single wireless signal. The device becomes an actuator with information from one polarization orientation, while information from the other polarization orientation seeks measurement data from the device serving as a sensor. When acting as a sensor, the gadget modulates the voltage from the piezoelectric component onto the frequency carrier of the remote reader and sends it to a data-acquisition unit [81].

In order to monitor composite constructions, Jung et al. [82]report the invention of a wireless sensor based on RFID technology. A flat loop antenna is printed onto a polymer substrate for

the sensor. The energy from the reader drives an electrical current via the antenna. The remainder of the circuit is then momentarily powered using this stored current. A multiple channel ADC and a low-power microprocessor is used to form the sensor processing unit. Multiple sensors provide measurement data to the ADC, which then prepares it for the microcontroller. The microcontroller then uses amplitude modulation to send the digital data by modulating data onto the remote carrier frequency of the reader.

Electronics, Radio Frequency Identification (RFID) and antenna components are delicate and brittle. And can melt at low temperatures. They are therefore unable to thrive on their own on asphalt pavement since it experiences tremendous temperatures and pressures during construction. Epoxy resins are extremely flexible and have a relatively high melting point and can thus be utilized to protect the sensor electronics. On the other hand, the piezo experiences an induced axial loading when the epoxy is stressed. Therefore, selecting the right epoxy resin to create the spherical case is crucial. The epoxy and the host material should be compatible with rigidity (HMA). Epoxy can be used to achieve stiffness compatibility if it has a lower stiffness than the host material [83]. The concept of a RFID-based wireless sensor capable of recording maximum displacement and strain values of a structural part is proposed by Mita and Takahira [84]. The sensor is constructed of two blocks holding a straight, thin with 0.291 mm diameter fluorocarbon wire. The second block is permitted to travel down a linear track while the first block remains immobile. The moving block generates a force greater than the static friction between the stationary block and the thin wire when there is displacement in the structure being monitored. The wire is gently pulled away from the stationary block by this force. The highest displacement of the structure that is being evaluated is represented by this distortion. There is no power source needed for this part of the sensor [84]. A capacitor and an inductor linked in series is one of the techniques used by Mita and Takahira to measure maximum displacement of the gliding block following the distortion. A block constructed of two coaxial aluminium pipes with a dielectric substance sandwiched between them serves as a capacitor in this design. As the maximum displacement varies, so does the block capacitance. The frequency of the LC circuit changes as a result of the change in capacitance. The tuned frequency of the wireless transmission is closely correlated with the frequency of the LC circuit when the LC circuit is inductively connected to an RFID reader. As a result, any variations in frequency picked up by the reader may be converted into the maximum displacement value recorded by the sensor [84].

Continuous and precise localization of the observed events is crucial given the rigorous road surface monitoring. Under a variety of driving conditions, both standalone GPS receivers and those built into smart devices are susceptible to partial or total failures. To effectively address inertial navigation system (INS) geo-referencing drifts and errors, integrated GPS/INS positioning systems must be appropriate and dependable. Additionally, the majority of standalone GPS receivers or integrated positioning systems run at 1 Hz, but high-resolution geo-referencing is required to correctly pinpoint the identified road irregularities when traveling at high speeds [85].

To offer timely and appropriate maintenance and repairs for the degraded roads, municipalities must accurately geo-reference the monitored road anomalies. Otherwise, attempts to discover road irregularities would be ineffective. The most well-known navigation and georeferencing technology overall is GPS. Located in orbit, GPS is a satellite navigation system that provides date and time data. Anywhere on or near the planet where there is a line of sight to four or more GPS satellites is accessible to this data regardless of the weather. GPS offers various customers a variety of crucial worldwide features. The US government maintains this system and provides GPS services without any charges or requirements to anybody with access to a GPS device [86].

3.8. Research Projects of Sensors and Sensor Systems for Structural Health Monitoring of Pavements

3.8.1. Introduction

A sensor system is a comprehensive unit comprising various components, including sensors, data acquisition systems (DAQ), power supply units, and, when needed, signal processing units. This integrated approach offers several advantages: it facilitates seamless interaction between components, enhancing efficiency and reliability; it allows for customization to specific application requirements, ensuring more accurate measurements; it simplifies installation and maintenance by integrating power supply and data acquisition; and it often enables continuous monitoring and real-time data acquisition, crucial for swift decision-making and early issue detection in various applications.

3.8.2. Research Projects about Development of Accelerometer Sensors

The effective distribution of money for infrastructure maintenance and development projects depends on the use of new and affordable techniques to automatically monitor structural health of pavements. A long-term monitoring system that would use an ultra-low power sensor as its foundation to assess the status of roads remotely was proposed by KC Enriquez [59]. Their study looked at how to use a straightforward method to extract maximum displacement values from the acceleration information gathered by ADXL202 MEMS accelerometer. The program was created to execute the accumulation phase of a double numerical integration approach in order to reduce the power consumption of the sensor computer core. The host computer was given the task of performing all multiplication operations required to transform the algorithm output to displacement values expressed in inches. To test the functionality of the method, a reconfigurable sensor prototype based on the Xilinx XC3S250E Spartan 3E FPGA was created and subjected to sinusoidal vibration. The features of sinusoidal vibration posed some difficulties for determining peak-to-peak displacement. It was reported that the sensor prototype was effective in producing values proportional to displacement at frequencies between 5 and 30 Hz.

A method to collect samples proportional to acceleration has been developed for the Xilinx XC3S250E using Verilog Hardware Description Language with the use of functional flexibility of FPGAs. Figure 3.7 shows a flow diagram that summarizes the accumulation process. The Verilog software measures the duration of pulse T1 using a counter as seen in the diagram. This counter begins at the rising edge of the accelerometer's DCM output and is increased while this signal is strong. The value is recorded into register T1 at the input pulse falling edge and is utilized to compute an acceleration-related value that is kept in register ACCEL. Before the subsequent DCM pulse is met, the counter is reset. According to equation 26-3, each time a new value proportional to acceleration is calculated, the value is added to the VEL accumulator to acquire velocity. The new value in VEL is added to the DISP accumulator to obtain displacement. The program records the maximum and minimum displacement values attained after each accumulation cycle using the registers MIN DISP and MAX DISP. Time is measured via a second counter that is only increased at the rising edge of the DCM output. When the timer reaches 1000, the 24-bit result is written to the USBMOD4 the registers are then cleared. A peak-to-peak displacement value is calculated by summing the contents of the registers

storing the maximum and minimum values. The Verilog method generates a 24-bit displacement proportional figure as its final output [92].

$$x = \Delta t^2 \sum_{i=0}^{n-1} v(t)_i + a(t)_{i+1} \tag{20-3}$$

The integration procedure is then finished by multiplying these displacement data points by the relevant constants in MATLAB. Relegating all multiplication operations to a host computer would further reduce the power consumption of the computational core of the sensor. This is due to the amount of current consumed by the FPGA depending on the logic design of the device [92].

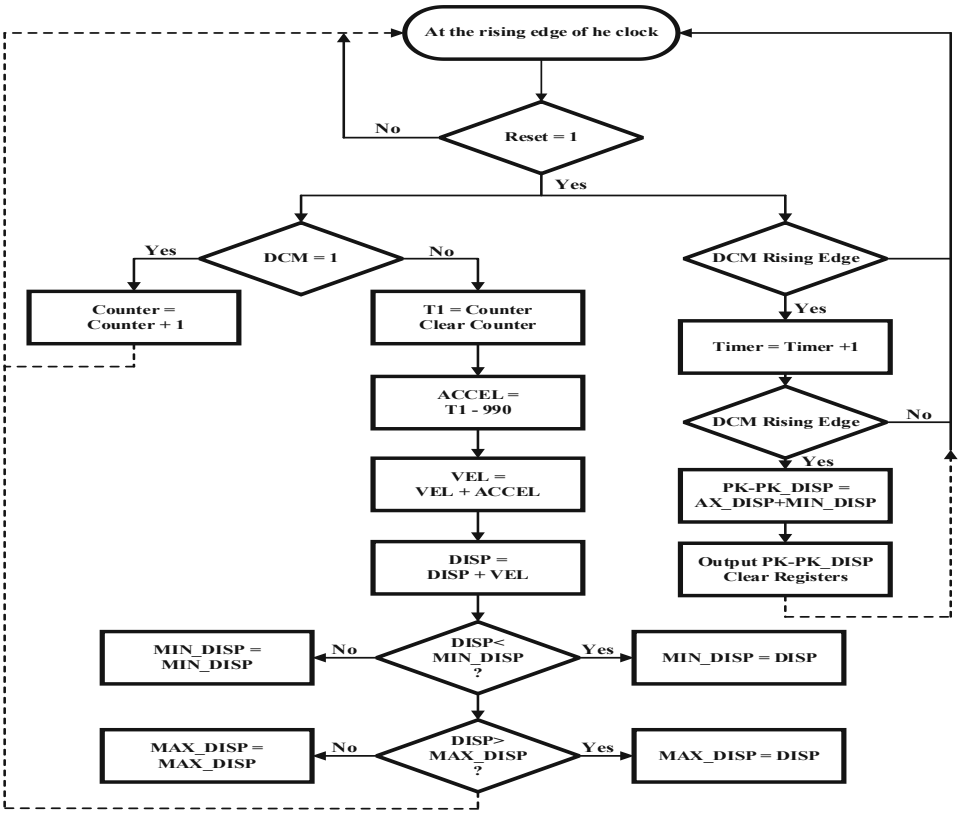

Figure 3.7: Verilog Algorithm to Perform Accumulation [92]

In another research project, a test structure with frequency-sweep sine excitation was used to validate the effectiveness of the MEMS accelerometers and the use of embedded local processing procedures. Mounted on a lateral shaker table, the five-story aluminium test building vibrates for 60 seconds at frequencies ranging from 0.23 Hz to 3 Hz. The structure theoretical model was well matched by the time domain and frequency response data. Additionally, it was discovered that the ADXL210 frequency response function was less noisy than that of the piezoelectric accelerometers utilized in the test [59].

The authors recognized that using batteries to power the monitoring device has limits based on the outcomes of further experiments conducted to confirm specific components. Together, the design sensor

interface and processing core used around 250mW of power, while the overall device used about 1.7W while transmitting. A 9V battery can power the circuit by itself for 20 hours. The Proxim RangeLAN2 can transmit for up to 2.25 hours and sleep for up to 4 hours. These findings persuaded the authors that power consumption is an important design factor that needs to be reviewed in upcoming prototypes [59].

The creation of a wireless device the size of a palm to track vibration in bridge structural components is described by Chung et al. [98]. The prototype primary objective was to verify how well the low-power ADXL202 and Silicon Design 2210 MEMS accelerometers function in SHM applications. The design of each of the monitoring units incorporated one of the two MEMS accelerometers in question. An analogue to digital converter, a microcontroller and an RS232 serial port to interface with a commercially available wireless transmitter were used.

The effectiveness of both sensors was first verified in the lab environment and the devices were then tested on a pedestrian bridge on the campus of the University of California Irvine (UCI). A 10mg sinusoid operating at 2 MHz was used to activate both accelerometers during a shaking table test in the lab. The SD 2210 performed considerably better at accelerations below 0.5mg according to time history graphs. Static noise of the ADXL202 and its related components which was close to 3mg was attributed to the performance disparity. The SD 2210 static noise level was measured at 1mg. Lateral and torsional motion as well as vertical displacement and acceleration on the field were also measured. This was carried out using ADXL202, SD 2210 and a PCB393C tethered sensor which were mounted in the centre and on each side of a pedestrian bridge. The frequency domain analysis of the structural reactions were measured on three successive impulse excitations delivered to the middle span of the bridge. The experiment revealed that the peaks of the modal frequencies detected by the conventional sensor and a simulation model closely matched the peaks of the modal frequencies detected by the two wireless sensors. The authors concluded that both accelerometers are effective in detecting vibrations in this research despite variations in noise and bandwidth. Additionally the performance of the wireless transmission was verified at 150m distance [98].

Lynch et al.[99, 100] designed a wireless modular monitoring systems (WiMMS) and suggested a dual-core architecture to alleviate the power consumption of his system. The revised architecture of the computational core features two processors. A 8-bit Atmel AT90S8515 AVR microcontroller and a 32-bit Motorola MPC555 PowerPC microprocessor while the sensor interface and wireless communication circuitry are unaltered. Figure 3.8 displays the functional diagram for the revised design. The 8-bit Atmel microcontroller handles data-acquisition and general operating functions and was chosen because of its low cost, power efficiency and processing capacity. The 32-bit Motorola microcontroller has the capacity to execute floating-point calculations swiftly. It also has 448 Kbytes of flash ROM and 26 Kbytes of RAM responsible for carrying out the complex data interrogation [101].

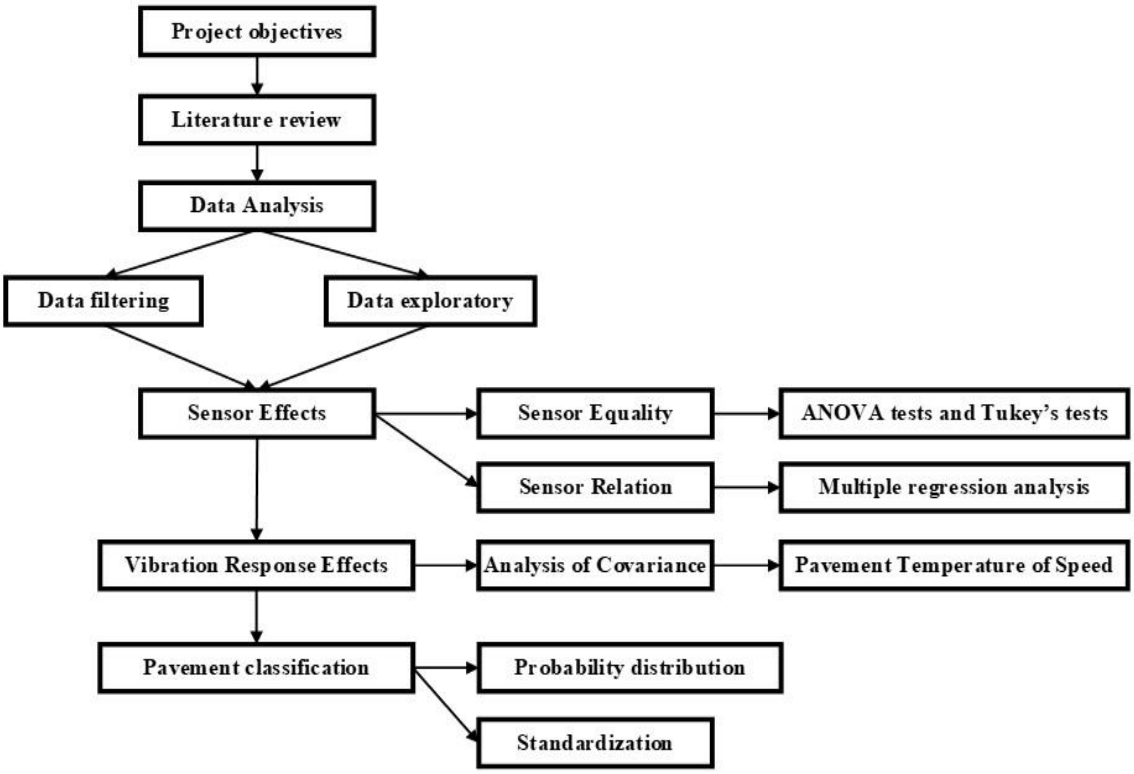

Figure 3.8: Methodology of The Research [101]

3.8.3. Pavement Temperature Based on Low-Cost Sensors and V2I Communications

Jorge Godoy and his team conducted research on a road pavement monitoring system utilizing temperature probes with V2I (vehicle-to-infrastructure communication). The development of this monitoring system was driven by the goal of reducing the time required for routine testing while enhancing the precision of temperature measurements within the pavement's inner layers [128].

Temperature probes were strategically placed at critical locations, enabling the continuous measurement of pavement temperature at various depths. Simultaneously, a dedicated platform on the auscultation vehicle was designed to gather data from nearby probes on request, utilizing a V2I system integrated with embedded probes and wireless communication, as illustrated in Figure 3-9.

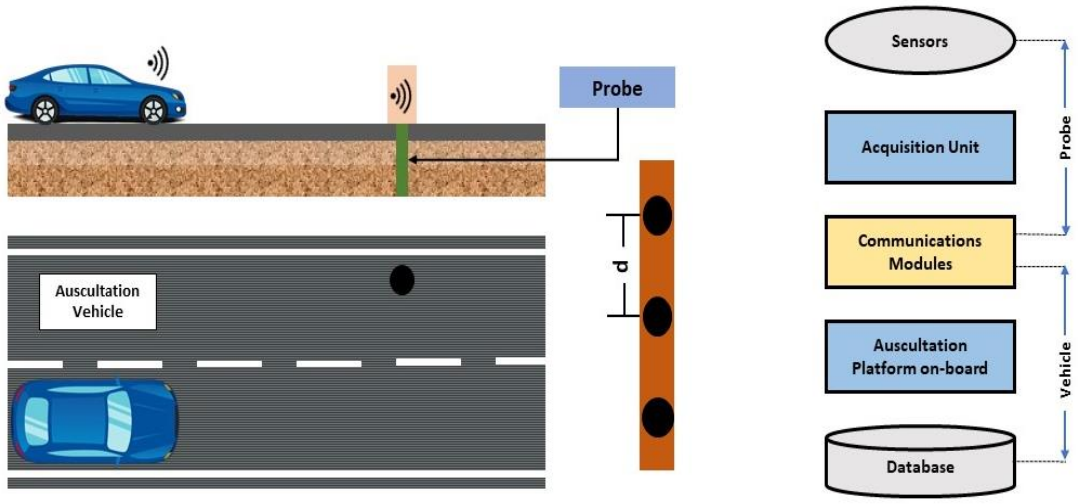

Figure 3.9: Conceptual design of the proposed monitoring system

The probes consist of two primary components: temperature sensors and a WSN (Wireless Sensor Network) node. The node periodically gathers data from the sensors and remains in a standby state until it receives a transmission order. Two operational modes are proposed in this context: (i) instant measurement and (ii) data collection.

The data collected during the tests were utilized to validate the development of a neural network-based model for predicting pavement temperature. Results obtained from one year of testing demonstrate the feasibility of the proposed solution for road monitoring applications. The study also confirmed that as the depth of the layer increases, the model's performance deteriorates, as it cannot accurately capture the signal phase-out caused by the thermal diffusivity of the road, which is dependent on pavement materials [128].

3.8.4. Fraunhofer Sensorsystem

The feasibility of deploying highly miniaturized autonomous microsystems with sensors capable of receiving, processing, storing and transmitting data was investigated by Fraunhofer Institute. The goal was to assess the structural condition of roads. For this purpose, the sensor systems are intended to be integrated into the road infrastructure. Wireless and bidirectional communication with the microsensor systems is essential, utilizing electromagnetic waves. Ideally, the sensor size should align with the grain size which requires a revolutionary approach to miniaturization compared to existing systems. The objective was to record strain, stress, temperature, humidity, salinity and position of the sensor within the road infrastructure. Key parameters for evaluation include sensitivity, long-term stability, selectivity, installation size, interface and particularly power consumption [5].

The sensor system is integrated directly into the road structure, either into the asphalt base layer to detect disturbances and damage or into lower layers for concrete roads to detect early damage. The size of the sensor system matches the grain size of the base layer. In the case of asphalt roads, installation takes place during road construction without the need for additional compaction by rollers [5].

If only measuring mechanical parameters like strain, pressure stress and acceleration is of interest for a road, sensors for temperature and humidity can be easily omitted.

The sensors must be externally mounted due to the required external contact. For future small-scale production, the RFID (Radio-Frequency Identification) sensor system will be implemented in an LTCC (Low Temperature Cofired Ceramic) housing. LTCC refers to glass ceramic foils used as casings for microsystem-produced systems. This technology offers the capability to produce an extremely robust and cost-effective material. The advantages of LTCC include the direct integration of resistors, inductors, and capacitors components, as well as high resistance to mechanical and thermal stress [5]. "In Figure 3-10, you can see a cross-section of the the system:

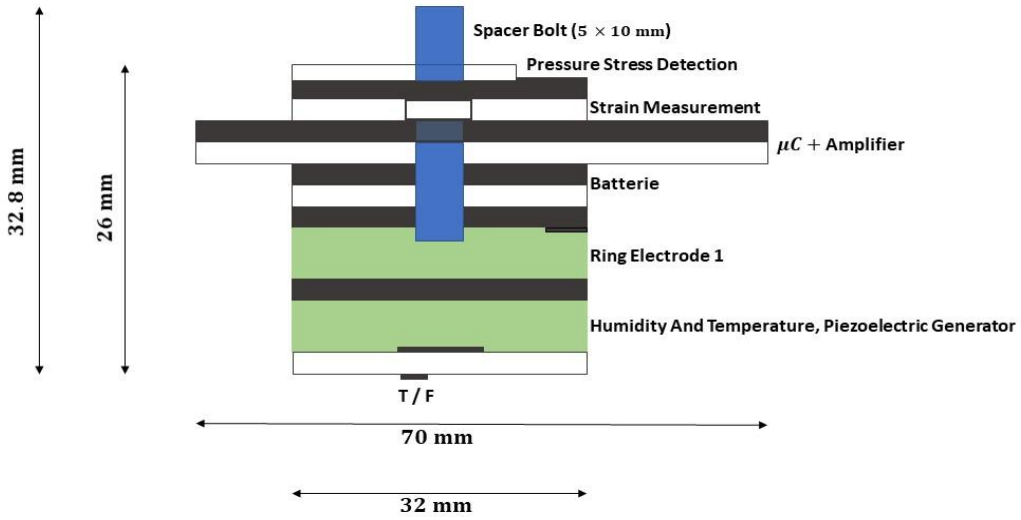

Figure 3.10: Sensor system according to Fraunhofer IPM

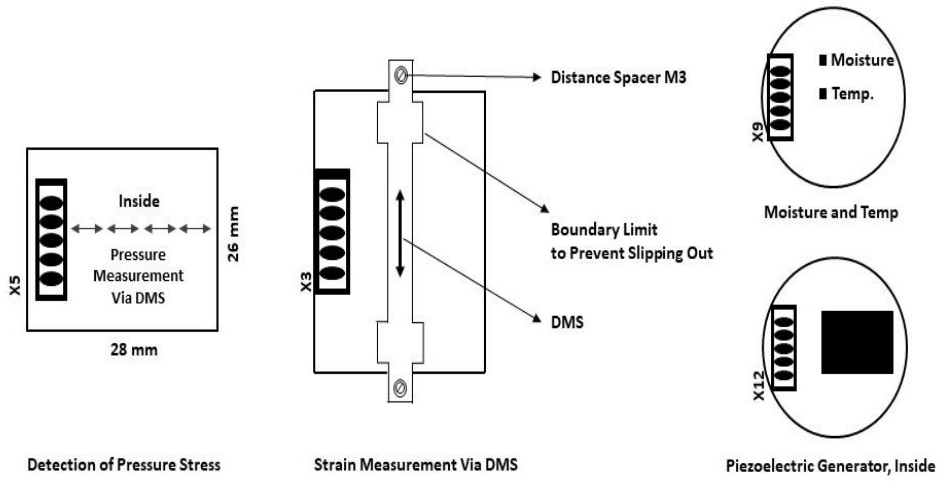

Figure 3.11: structure of the overall system

3.8.5. Sensor Self-Powered Wireless Sensors (SWS)

The sensors can be embedded into the pavement to track the statistics of localized strain. The SWS may be used for ongoing infrastructure monitoring, according to research from a prior FHWA-funded study [125]. The main goals of that project were to manufacture the sensor electronics and create a packaging solution that could endure loads and environmental factors for pavement deployment. Research was conducted on creating a system for estimating the pavement's remaining fatigue life and producing missing data from a set of observations using a traditional statistical technique [54]. SWS has a number of benefits, however there would be a considerable information loss. As a function of cumulative duration at each load level, a portion of the detected data is really compressed. Due to this flaw, it is challenging to comprehend the data produced by SWS [126]. The SWS-based damage detection method entails three main stages: (1) structural simulation using the finite element method (FEM); (2) data generation and feature extraction based on the outputs of the SWS memory cells; and (3) establishing a plausible correlation between the probability density function (PDF) parameters obtained from strain distribution and damage progression. The FE simulations were used to first design a damage scenario for the specified pavement structure. For the data capture points, the cumulative time of occurrences at predefined strain levels is then calculated (sensors). Damage indicators were developed using the strain distribution in each sensor node. In addition, the inherent locality of structural deterioration presents a significant obstacle to the implementation of wireless sensors. As a result, sensors nearby the damaged area are more affected than those farther away. The only method now in use to reliably identify damage at

any point in a structure is to evenly deploy sensors throughout it [125, 127]. Reasonably, the precision of damage detection increases with the proximity of the sensors to the notch. When potential sensors are placed distant from the damage being inflicted, the sensor may not be able to detect damage or the findings may not show a meaningful trend. To increase the performance of damage detection by spatial measurements across an area, more effective technique was created. Based on this, it was determined to utilize the "group effect," or information produced by a collection of sensors. In this instance, the group effect will aid in damage detection even if one sensor is unable to detect it [125]. Preliminary investigations revealed that there was no solid correlation between the damage development and the PDF parameters average, range, minimum, maximum, skewness and kurtosis.

Lajnef et al [80] created and put to the test a sensor system made up of a brand-new wireless self-powered sensor that could detect damage and load history for pavement structures for pavement monitoring. Each sensor node has the ability to record and continually monitor the amounts of dynamic strain in the host pavement structure. A basic radio frequency (RF) reader that could be operated manually or placed on a moving vehicle was used to read the sensor. The roads may be regularly monitored to find changes in structural integrity that can hint to a future crisis manifestation. It also enable more precise scheduling of preservation operations by directly equipping service trucks with inexpensive RF transponders. The sensor chips and receiver were designed and put through successful lab testing. A building project in the USA was used for the installation and testing of a prototype of such technique. Finally, a sensor-specific data interpretation method was developed employing cumulative restricted compressed strain data stored. the sensor memory chip was used to forecast the remaining fatigue life of a pavement structure. There were no cables or wires used in this method. The sensors may be installed quickly and simply with this system using the current installation process [80].

3.8.6. self-powered wireless sensor (SWS) with non-constant injection rates

A "self-powered wireless sensor" is a sensor device capable of functioning independently without relying on external power sources like batteries or wired connections. These sensors are engineered to generate their own energy for conducting sensing operations and wireless communication.

Michigan State University (MSU) has pioneered a novel piezo-based self-powered wireless sensor (SWS) designed for the detection of bottom-up cracking in asphalt concrete. This innovative sensor combines piezoelectric transducers with an array of ultra-low-power floating gate computational circuits. When embedded within the pavement system, it continuously monitors localized strain statistics. The data recorded on-board these sensors can be retrieved using radio frequency (RF) technology. SWSs are categorized into two classes based on their floating-gate properties: constant injection and non-constant injection rates. The primary distinction lies in the data output format of these sensors. There is limited research on the utility of SWS with constant injection rates for Structural Health Monitoring (SHM) [137].

The newly developed MSU sensor incorporates seven memory cells to track cumulative strain events induced by mechanical loading. Its sensing mechanism involves two main phases: energy harvesting from the structure under load using a piezoelectric transducer and recording cumulative voltage (corresponding to strain) events via the sensor electronics.The strain injection rate parameter is a critical sensor property that regulates the rate of change of sensor strain over time. Alavi et al. demonstrated that a sensor with a constant injection rate produces an output histogram that follows a Gaussian distribution.

The analysis was conducted in two stages. Initially, a numerical model was developed to ascertain the structural response of the beam under various damage scenarios. Strains were extracted at the sensing node, followed by the development of a MATLAB script to calculate cumulative loading for each gate and damage state [137].

The results indicated that strain amplitude increases with the notch size, consequently leading to higher measured voltage from the piezoelectric transducer.

3.8.7. Infrared spectrometers, high resolution RGB cameras and laser scanner FOR ROAD CONDITION MAPPING

The University of Applied Sciences in Stuttgart outfitted vehicles with sensors to gather mobile data. These sensors include an RGB camera, a laser scanner, and a GNSS-assisted inertial navigation system integrated onto a van-mounted platform. Additionally, a Polytec spectrometer is equipped with an integrated artificial light source within its spectrometer head [138].

The spectrometer comprises three main components: the sensor head, responsible for collecting and directing light into the polychromator; the polychromator, which disperses the incoming

light into various wavelengths; and an SMA (SubMiniature version A) fiber connector that connects the polychromator to the sensor head. In this research, the spectrometer's sensor head is positioned at the rear of the vehicle to maintain a close proximity (30 to 50 cm) between the sensor and the road surface.

Infrared spectrometry is utilized to assess surface material deterioration and pavement conditions, particularly due to aging. High-resolution RGB imaging facilitates automatic detection of asphalt cracks and serves as a reference for spectrometry data. Laser scanning is employed to identify road geometry irregularities and pavement issues like potholes and ruts. Ultimately, these individual findings are integrated into a comprehensive assessment framework, collectively contributing to the analysis of pavement conditions. All mapping sensors are synchronized with a navigation sensor to collect geo-referenced data [138].

Initial classification outcomes are derived through unsupervised analysis of the spectrometer data. These clusters can be associated with various factors such as new and aged asphalt, illustrating the promising utility of spectral information in road condition mapping.

Chapter 4: Research Projects in Condition Monitoring of Pavements Using Instrumented Test Tracks or Test Sections

4.1. Introduction

In pavement instrumentation applications, the sensitivity of sensors is paramount importance, particularly considering the low displacement and acceleration levels involved. A review of numerous instrumented parts is suggested in this section. Furthermore, it provides detailed insights into the description, installation, and functionality of instrumentation deployed across different road surfaces to gauge pavement response to loading. The section also delves into the recorded strains, detailing the data acquisition process used to determine the vertical compressive stress pulse induced by passing trucks at diverse locations beneath the pavement surface. These datasets were instrumental in determining the influence of factors such as temperature, speed, and tire inflation pressure.

4.2. Field-Testing Site an motorway A10 in south of Salzburg, motorway A3 in south of Vienna and Expressway S31

Valentin Donev et al. [93] conducted research on the instrumentation of field-testing sites aimed at dynamically characterizing the temperature-dependent stiffness of pavements and their respective layers.

This study serves two primary objectives:

1. To gain and share insights into the instrumentation of both rigid and flexible pavements during their new construction.

2. To present the initial data obtained from dynamic testing conducted at the innovatively equipped field-testing sites.

To achieve this goal, one rigid and two flexible pavement structures are outfitted with three types of sensors: temperature sensors (Pt 100), asphalt strain gauges, and accelerometers.

Three different types of pavement structures commonly employed on Austrian motorways and expressways were equipped with instrumentation.

4.2.1. The Three Field-Testing Sites

Field-Testing Site #1 on Motorway A10:

Field-testing site is a concrete slab on the motorway A10, south of Salzburg. The width and the length of the slab amount to 3.50 m and 5.00 m, respectively, see Figure 4.1.

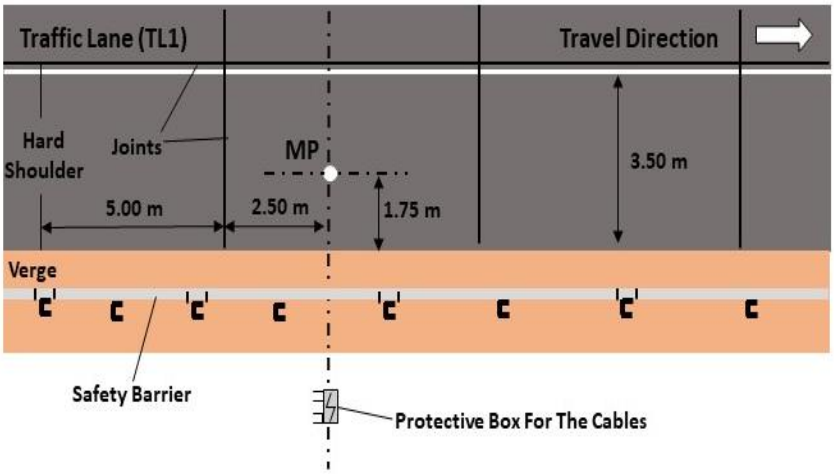

Figure 4.1(a): Field-testing site #1

The pavement structure is illustrated in Figure 4.2.

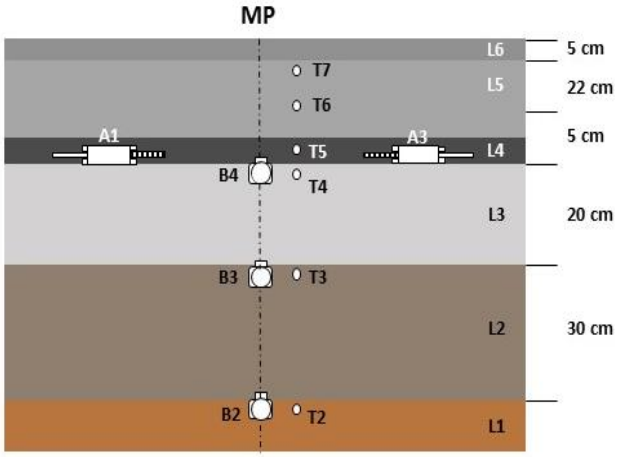

Figure 4.2: The pavement structure

Table 4.1: The layers of the pavement structure A10 motorway

Layer	Thickness (cm)
L6: Top-layer concrete	5
L5: Bottom-layer concrete	22
L4: Asphalt base course	5
L3: Cement-stabilized granular layer	20
L2: Lower unbound granular layer	30
L1: Subgrade	-

As depicted in Figure 4.1(b), six temperature sensors (T2–T7) were positioned at the interfaces between adjacent layers and at the midpoint of the lower concrete layer. Additionally, three accelerometers (B2–B4) were mounted along a vertical axis passing through the central measurement point (MP) for FWD testing. This allows for in situ stiffness characterization of layers L2 and L3. Furthermore, four strain gauges (A1–A4) were affixed to the base of the asphalt layer [93].

Field-Testing Site #2 on Motorway A3:

Field-testing site is a flexible pavement on the motorway A3, south of Vienna. Two ostensibly identical FWD measuring points were instrumented, spaced approximately 70 meters apart from each other, as illustrated in Figure 4.3.

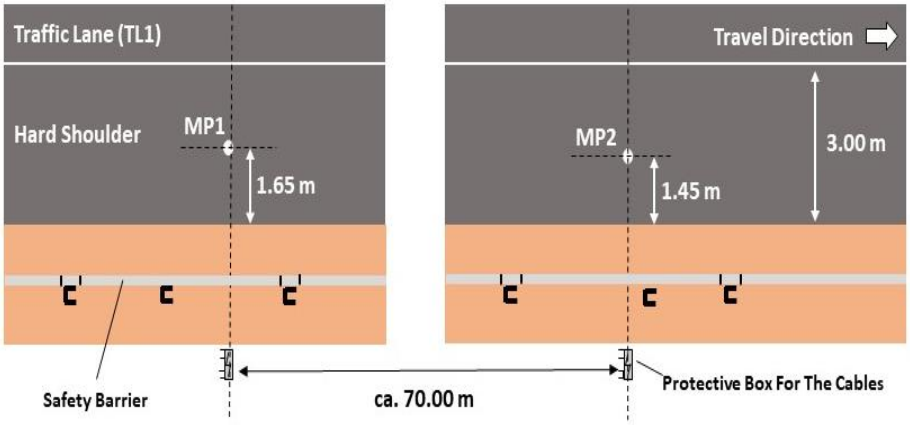

Figure 4.3: Field-testing site #2

The pavement structure is illustrated in Figure 4.4.

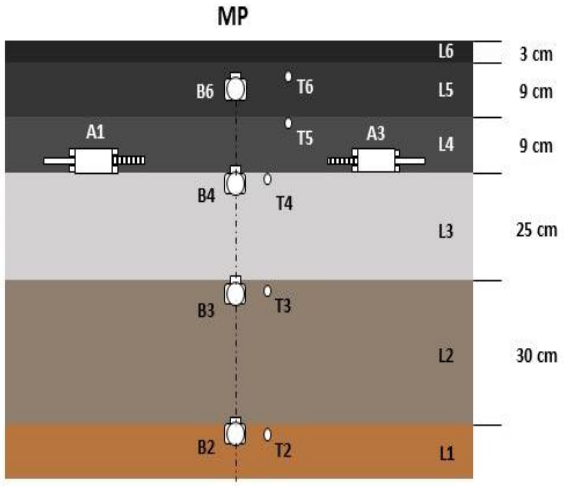

Figure 4.4: The pavement structure

Table 4.2: The layers of the pavement structure A3 motorway

Layer	Thickness (cm)
L6: Asphalt surface course	3
L5: Asphalt binder course	9
L4: Asphalt base course	9
L3: Cement-stabilized granular layer (lean concrete)	25
L2: Unbound granular layer (Angular aggregates)	30
L1: Subgrade	-

As illustrated in Figure 4.2b, sensors were embedded at various depths. Five temperature sensors (T2–T6) were positioned at all interfaces between adjacent layers. Four accelerometers (B2–B4 and B6) were mounted along a vertical axis passing through the measurement points (MP) for FWD testing. This allows for in situ stiffness characterization of layers L2 and L3 as well as of the sandwich layer consisting of the asphalt base and binder courses (L4 and L5). Additionally, two asphalt strain gauges (A1 and A3) were installed at the base course's bottom [93].

Field-Testing Site #3 on Expressway S31:

Field-testing site #3 represents a flexible pavement located on the expressway S31 in the federal state of Burgenland. Due to the lack of a hard shoulder, the FWD measuring point was positioned in the centre of the right lane (TL1), as shown in Figure 4.5.

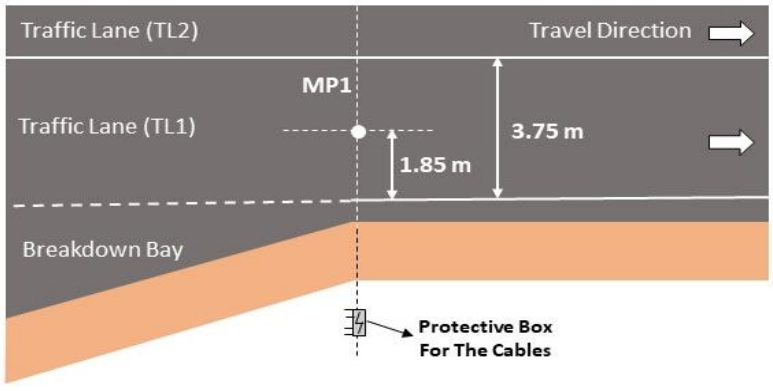

Figure 4.5: Field-testing site #3

The pavement structure is illustrated in Figure 4.6.

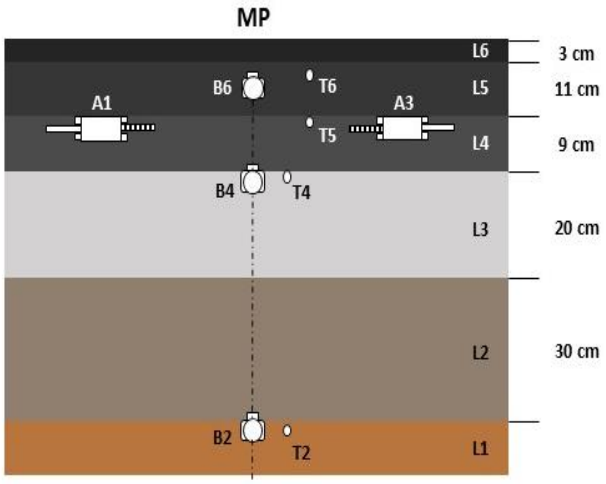

Figure 4.6: The pavement structure

Table 4.3: The layers of the pavement structure S31 expressway

Layer	Thickness (cm)
L6: Asphalt surface course	3
L5: Asphalt binder course	11
L4: Asphalt base course	9
L3 Upper unbound granular layer (Basalt))	20
L2: Lower Unbound granular layer (Rounded aggregates)	30
L1: Subgrade	-

Sensors were implanted at various levels within the pavement layers. Specifically, temperature sensor T2 was positioned at the junction of the subgrade (L1) and the lower unbound layer (L2), while T4 was situated between the upper unbound layer (L3) and the base course (L4). Additionally, T6 was placed between the binder course (L5) and the surface course (L6). Another temperature sensor, T5, was installed at the boundary between the base and binder courses, as depicted in Figures 4.3(b). three accelerometers (B2, B4, and B6) were strategically placed along a vertical axis aligned with the central measurement point (MP) for Falling Weight Deflectometer (FWD) testing, mirroring the locations of T2, T4, and T6. This allows for in situ stiffness characterization of two sandwich layers. They consist of the unbound materials (L2 and L3) and of the asphalt base and binder courses (L4 and L5). Additionally, two asphalt strain gauges (A1 and A3) were meticulously embedded within the base course, as illustrated in Figure 4.3(b) [93].

4.2.2. Installation of sensors

In previous pavement applications, two primary types of accelerometers have been predominantly utilized: integrated electronics piezoelectric (IEPE) and microelectromechanical system (MEMS) accelerometers.

To install the lowest sensors B2 and T2, an excavator was utilized to access the interface between the unbound layer L2 and the subgrade L1. These sensors were embedded using quick-setting cement mortar, serving the dual purpose of preventing displacement or cable disconnection and shielding them from potential damage caused by direct contact with large aggregates. Similarly, sensors B3 and T3 were installed at the interface between L2 and L3 in the same manner. For the installation of high-temperature accelerometers (B4 and B6), openings for the sensors and cable grooves were created in the cement-stabilized or lean concrete layers. Prior to paving, the sensors were covered with loose asphalt mixture and compacted carefully using a hand tamper. To install accelerometers between two asphalt layers (B6), openings for the sensor and cable grooves were made during the construction of the lower asphalt layer using steel dummies and pipes as placeholders. These placeholders were later removed, allowing for the insertion of the sensor and cable into the prepared openings and grooves.

In this study, three methods of asphalt strain gauge installation were tested:

1. Cut, Install, and Cover after Asphalt Placement (Field-testing #1 on the A10):

Advantages: Accurate sensor positioning, low potential for construction damage.

Disadvantages: Rapid asphalt cooling caused installation stress and progressively increased difficulty in handling the material.

2. Installation in a Fixation Tool before Asphalt Placement (Field-testing #2 on the A3):

Advantage: Sensors remained in desired positions during asphalt layer installation and compaction.

Disadvantage: Despite protective measures, only two out of four sensors functioned after construction.

3. Use of Steel Dummy Place-Holders for Real Sensor Placement (Field-testing #3 on the S31):

Advantage: Dummy placeholders safeguard real sensors from excessive compaction loads, enabling accurate positioning.

Disadvantage: Limited to installing strain gauges at the top of asphalt layers in its current form.

4.2.3. Findings

Valentin Donev et al. [93] found that the Pt100 temperature sensors and IEPE accelerometers used in their study are suitable for installation in various pavement layers. They demonstrated resilience against high temperatures and compaction forces during asphalt layer construction. However, sensor overload during hot-state roller compaction of asphalt layers was a significant issue encountered. To mitigate this, the authors suggest using steel dummies as placeholders in hot asphalt layers immediately after construction to prevent sensor damage and ensure reliable data collection for future pavement monitoring.

Additionally, sledgehammer tests, utilizing strikes on a metal plate transmitted through a rubber pad, effectively quantify elastic wave travel time through various pavement layers. Stiffness measurement using elastic wave propagation theory is feasible when there is full-face contact of layers beneath the impact point. In rigid pavements, these tests detect partial loss of contact between concrete slabs and lower layers, affecting measured deflections during testing. In flexible pavements, seasonal variations in Falling Weight Deflectometer (FWD) results primarily stem from temperature-induced stiffness changes in asphalt layers, with other layers exhibiting smaller stiffness variations.

4.3. Test Track at A1 motorway in Switzerland

Tests were conducted at a monitoring site located along the A1 motorway, which connects Zurich and Bern in Switzerland. Table 4.4 provides information on the geometry and materials used in the full-depth structure, categorized as per classification [87].

Table 4.4: Thickness and materials of the pavement layers of the A1 motorway

Layer	Thickness (mm)	Material
1	40	Stone mastic asphalt (maximum aggregate size 11 mm)
2	70	asphalt concrete base course (maximum aggregate size 22 mm)
3	120	asphalt concrete base course (maximum aggregate size 32 mm)
4	95	Asphalt concrete subbase course (maximum aggregate size 22 mm)

To conduct the tests, nine accelerometers were positioned 40 mm below the pavement surface. These sensors were strategically arranged in a triangular pattern to measure the deflections caused by a truck and to assess the consistency of results along the longitudinal axis.

Furthermore, the pavements response to the load was measured using three magnetostrictive deflectometers positioned in a line perpendicular to the vehicle's direction of movement. These deflectometers matched the positions of the accelerometers and measured the differential vertical deformations at three different depths within the structure relative to the base cap, which was situated 40 mm below the pavement surface [87]. Two trucks, one with two axles and another with three axles, were driven across the site at three different speeds: 20 km/h, 50 km/h, and 70 km/h. Double integration was used to determine deflections from the measured accelerations caused by moving load. Subsequently, the computed deflections were compared to both the measured and theoretical deflections. The deflections derived from acceleration demonstrated a reasonable qualitative correlation with those obtained from the magnetostrictive deflectometers. It was also determined that the method loses its effectiveness when dealing with low-intensity induced accelerations. Accelerometers are unsuitable for use with slow-moving, lightly loaded vehicles passing at a substantial distance from the sensor's location [87].

4.4. Test Track in The Jurmu

Ryynänen et al [139] studied a low-volume asphalt road that had sensors installed such as displacement transducers and near-surface accelerometers.

The Jurmu test road can be found in the northern region of Finland, specifically in Taivalkoski. In Finland, asphalt pavements typically feature robust unbound layers and relatively thin asphalt surfaces. You can refer to the pavement structure of the Jurmu test road in the provided table 4.5 for more details. Temperature and moisture sensors, pressure cells (P1, P2, P3), displacement transducers, and accelerometers (A1 to A7) were installed in the pavement to monitor both environmental and load-induced pavement reactions, as illustrated in Figure 4.7.

Table 4.5: Jurmu test road pavement structure

Layer	Thickness (mm)
Asphalt concrete , AC	50
Crushed aggregate	170
Scarified old surface	130
Natural gravel with gobbles	200
Rock layer	300

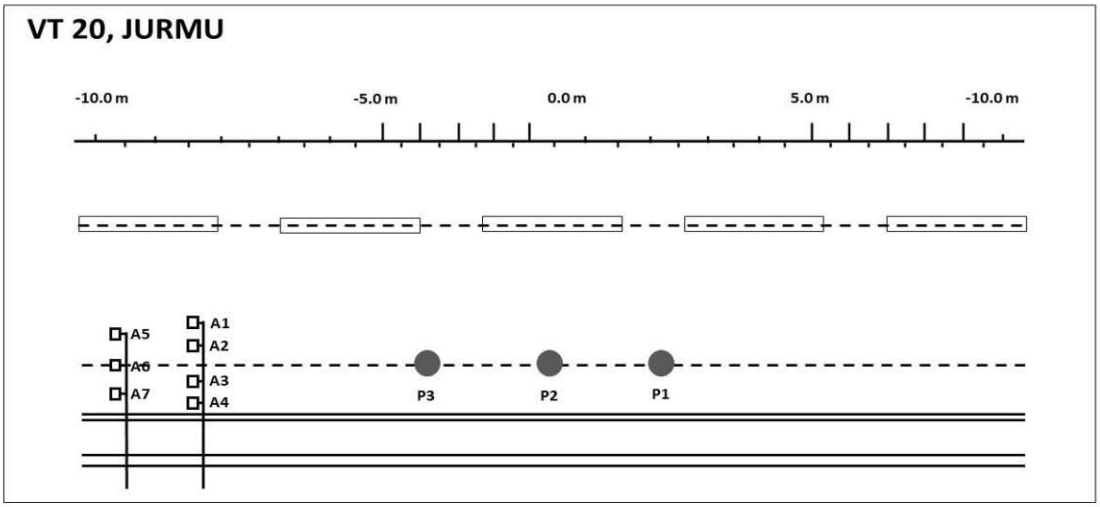

Figure 4.7: Plan view of the instrumented pavement

As depicted in Figure 4.7, the accelerometers were positioned in two transverse rows. The pressure cells were strategically placed at intervals of approximately 2 meters at various depths. Specifically, P1 was situated within the crushed aggregate layer at a depth of 0.13 meters from the pavement surface, P2 was positioned in the scarified layer at a depth of 0.29 meters, and P3 was located at the base of the natural gravel layer at a depth of 0.54 meters [139].

A truck with known weight and dimensions was driven over the gauge array in loading trials at various speeds and trajectories. To calculate deflections, measured accelerations were double-integrated with regard to time. According to the reports, computation adjustments were required to counteract data drift. Nevertheless, there was a difference between deflections estimated from accelerations and the displacement transducers observations. A layered elastic pavement model was employed to match the deflections. However, the resultant moduli felt implausible and nonlinearity was added to the model for extra support. The key insights stemmed from load testing the pavements using trucks of known weights, which followed various paths at different speeds on the road. Precise knowledge of the truck weights allowed for the calculation of pavement responses. Likewise, it was feasible to reverse-engineer the pavement loading by analysing the measured pavement responses [139].

4.5. Accelerated Pavement Tests at IFSTTAR (the French National Institute for Transport and Safety Research)

In an experiment at the IFSTTAR accelerated pavement testing (APT) facility, two geophones (GS11D and ION models) and two accelerometers (Silicon Design and MEMSIC models) were embedded within a pavement structure. Additionally, an anchored deflectometer was installed

as a reference point to measure deflection response. The IFSTTAR APT facility is an outdoor circular test track with a 40-meter diameter and a central loading system, consisting of four loading arms, each capable of carrying loads up to 13 tons (Figure 4.8). Dual wheels were used in this experiment, resulting in a tire-pavement contact stress of 0.6 MPa. The sensors were placed in one of the six test sections of the carousel, which was a 22-meter-long pavement section consisting of an 11 cm thick asphalt concrete layer and a granular base. The diagram in Figure 4.9 illustrates the locations of the geophones, accelerometers, and anchored deflectometer within the pavement section [140].

The geophones and accelerometers were positioned 1 cm below the pavement surface, at the centre of the wheel path. The anchored deflectometer comprised an LVDT connected to a rod anchored at a depth of three meters, measuring the total vertical displacement between the pavement surface and the bottom of the fixed rod.

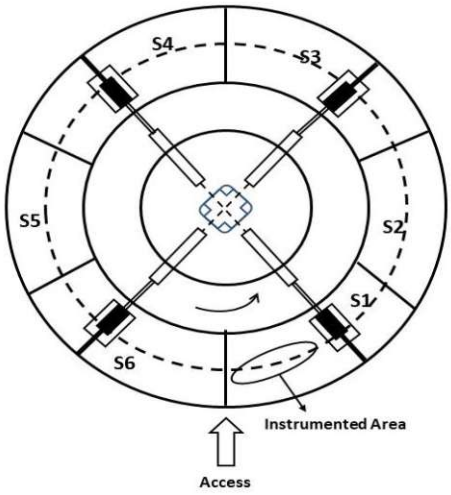

Figure 4.8: APT section dimensions

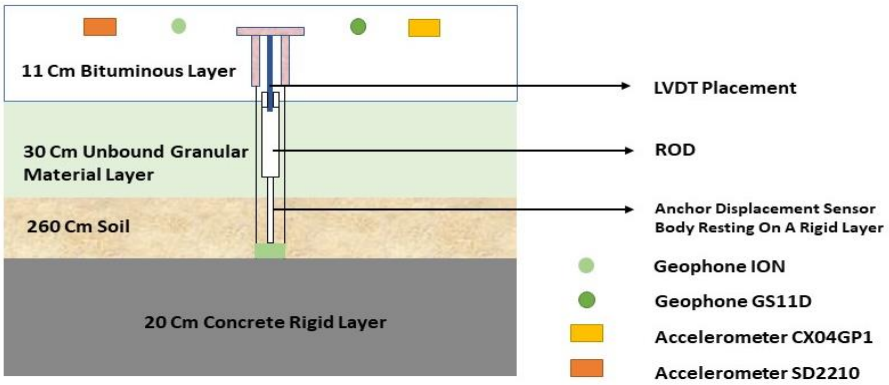

Figure 4.9: Instrumented pavement structure

Tests were conducted under various conditions involving different speeds and wheel positions relative to the sensor locations. These tests encompassed three load levels (45 kN, 55 kN, and 65 kN), speeds ranging from 6 m/s to 20 m/s, and surface temperatures of 19 °C to 20 °C. In each test scenario, deflection measurements were taken with both geophones and accelerometers, and these measurements were compared to those obtained with the anchored deflectometer.

The deflection data collected from the accelerometers and geophones were used to back-calculate pavement layer moduli through the Alize pavement design software, which incorporates a back-calculation tool. This analysis resulted in realistic back-calculated moduli, suggesting that the measured deflection data are accurate enough for this type of analysis and for monitoring pavement layer moduli.

The analysis revealed that the error percentages between the signals from the geophones, accelerometers, and the reference anchored deflectometer were relatively low for all tested sensors and conditions, with the highest error reaching 13.7%. Particularly, for the 55 kN and 65 kN load levels, the mean error values across all transducers were similar and very satisfactory, ranging from 3.55% to 5.03% [140].

4.6. Virginia Smart Road

Between 1998 and 1999 Virginia Department of Transportation built a 3,2 km long test track as part of a research project [110]. The pavement test road on the Virginia Smart Road consists of various sections, including flexible pavement, continuously reinforced rigid pavement, and jointed plain rigid pavement. In total, there are 12 flexible pavement sections, each approximately 100 meters long. The first seven sections are situated on a raised fill, while the remaining five are in a cut. For these sections, a variety of wearing-surface mixes were used, including five different SuperpaveTM mixtures, an open-graded friction course (OGFC), and Stone Matrix Asphalt (SMA). In all sections, there's a hot mix asphalt (HMA) base. Nine sections incorporate an open-graded drainage layer (OGDL) with a 75mm thickness, which is stabilized using asphalt cement in seven sections and Portland cement in two sections. Additionally, a Portland-cement-treated aggregate (CTA) base with a thickness of 150mm is used in ten sections. Above the subgrade in all sections, there's an unbound aggregate subbase layer with thicknesses varying from 75 to 175mm. Furthermore, certain sections also include various geosynthetics and reinforcing steel nettings [110]. Twelve 100-meter portions were monitored across the full length by installing various types of sensors at various depths. The

instrumentation was done while the building was being constructed. Pressure cells, thermocouples, TDR (Time Domain Reflectometry) probes, resistivity probes, H-shaped strain gauges and vibrating wire strain gauges were combined and planted.

RST (Resistive stress transducers) pressure cells were chosen for the purpose of measuring vertical compressive stress across all pavement layers within the Virginia Smart Road. These pressure cells come in two distinct sizes:

1. Pressure cells positioned within the upper layers of the pavement structure have a 150mm diameter and a measurement capacity of up to 690kPa.
2. For the base layers and subgrade, larger pressure cells with a diameter of 225mm were employed, capable of measuring up to 414kPa.

Multiple pressure cells were strategically installed at various locations within different layers of the Virginia Smart Road pavement.

In the Virginia Smart Road pavement sections, temperature measurement was accomplished using T-type thermocouples. These thermocouples are composed of a paired constantan and copper wire, which are twisted, stranded, and shielded. Before installation, all thermocouples were enveloped within geosynthetic material and positioned in the desired locations beneath the pavement material.

To measure moisture content in pavement systems, this study utilized time-domain reflectometry (TDR). Two TDR soil moisture measurement instruments were employed: CS610 and CS615. The CS610 features three parallel conducting rods, each measuring 300mm in length, spaced 22mm apart. In contrast, the CS615 TDR probe comprises two parallel conducting rods, also 300mm in length, with a 32mm separation between them.

The Dynatest PAST-II-AC strain gauge is designed as an "H" shaped precision transducer, purpose-built for measuring strains within Hot Mix Asphalt (HMA). This strain gauge is fully encased within a strip of glass-fiber reinforced epoxy, a material known for its relatively low stiffness but high flexibility and strength characteristics. To guarantee effective mechanical connection to the HMA material once it's installed, both ends of the epoxy strip are firmly attached to stainless steel anchors.

The Geokon model VCE-4200 Vibrating Wire Strain Gauge was chosen for installation in both the subgrade and the cement-stabilized aggregate layers of the pavement sections. Unlike

traditional electrical resistance or semi-conductor strain gauges, the key advantage of the vibrating wire strain gauge lies in its utilization of frequency, rather than voltage, for the output signal. After calibration, these vibrating wire strain gauges were subsequently filled with a thin layer of sand [110].

A data gathering system and developed software were installed to complete the monitoring system. The DaqBook 200 for the acquisition of static data and the Wave Book 200 for the gathering of dynamic data with moving loads made up the data acquisition system. The following programs were developed.

- Smart Wave for post-processing and presenting
- SmartAcq for data collecting
- Smart Organizer for managing raw data

The acquisition carried out during compaction demonstrates that vibrations result in increased longitudinal and transverse horizontal strains. In addition, vibration frequency might be determined by carefully examining the data obtained from the sensors. To evaluate pavement reactions under various loadings and environmental factors, an experimental design with a vehicle of specified loading was conducted. The pavement was overloaded by running multiple passes at four different speeds eight, twenty four, forty and seventy two kilometres per hour. Three different tire pressures of 724, 655 and 552 kPa were used. Results showed that temperature and speed had an impact on the reaction in terms of strain. Finally, to compare the experimental and computational results, a finite element model was employed to describe pavement behaviour. It was discovered that a viscoelastic calculation that accounts for the actual bonding circumstances at the intersections between road layers may more accurately forecast the behaviour of the pavement.

4.7. Test Track in Deyang, China

A 900-meter-long road in Deyang was instrumented to examine the strain response of asphalt pavement under various axle configurations, axle loads, speeds and pavement temperatures. Three distinct pavement configurations commonly employed in China, labelled as semi-rigid (S1), inverted asphalt pavement (S2), and compound asphalt pavement (S3), were chosen for analysis. This was constructed on a 4-lane, 2-way road each 300 meters long. Table 4.6 outlines the composition and materials utilized in each pavement type.

Table 4.6: Pavement structures

Layer	S1	S2	S3
Upper layer	4 cm SMA-13	4 cm SMA-13	4 cm SMA-13
Middle layer	6 cm AC-20 C	6 cm AC-20 C	6 cm AC-20 C
Underlying layer	8 cm AC-25 C	8 cm AC-25 C	8 cm AC-25 C
Base	25 cm Cement stabilized crushed stone (Cement)	10 cm Asphalt + 20cm Gradation aggregate	20 cm Asphalt
Subbase	25 cm Cement stabilized crushed stone	20 cm Cement stabilized crushed stone	30 cm Cement stabilized crushed stone

Strain gauges were put in place at the bottom of the asphalt layer underneath in order to measure the strains there. Four strain gauges were inserted into each of the three pavement constructions in Figure 4-7 to measure the transverse and longitudinal stresses [141]. It should be noted that strain gauges are situated at the left side of the centre lane, as established by the survey findings based on wheel track and rutting location (Figure 4.10).

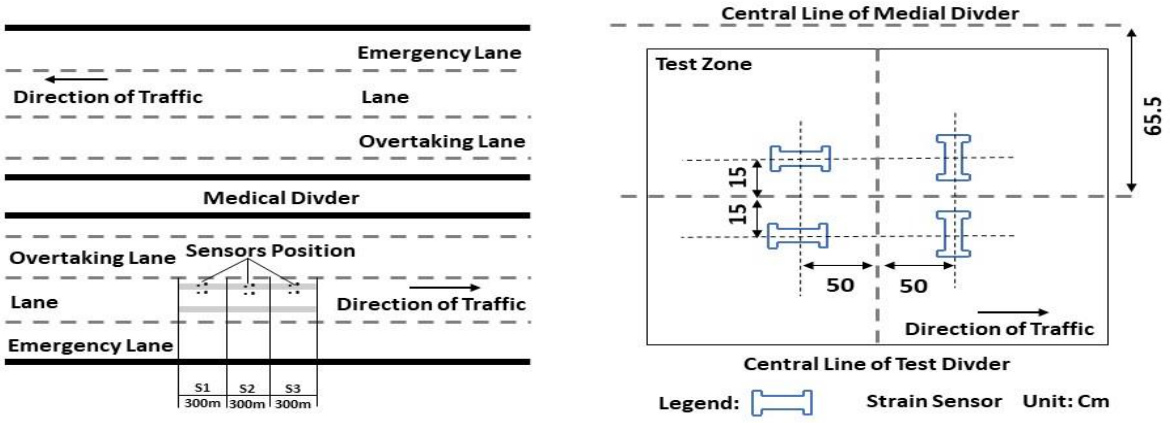

Figure 4.10: Strain Gauge Instrumentation Layout. (A) Overall Layout of Sensor. (B) Specific Layout Mode of Strain Gauge

To conduct load tests, two common types of large trucks from China that could clearly harm the structure of the pavement surface were used.

Truck type 1 single rear axle configuration

Truck type 2 tandem rear axle configuration as shown in 4.11. Three levels of axle load were chosen for each truck type based on the rear axle configuration. Normal, overload and extreme overloading. A single rear axle design has axle loads of 98, 138 and 177 kN whereas a tandem

rear axle one arrangement has axle values of 177, 255 and 334 kN. Within a tolerance of 1.0 kN, the axle load calibration error range is regulated.

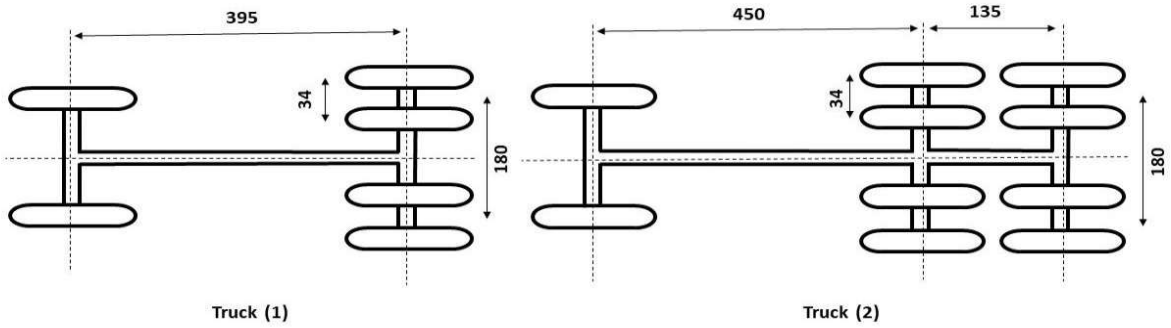

Figure 4.11: Test Trucks (Unit: Cm)

As shown in Table 4.7, tests were conducted at two distinct speeds depending on the axle arrangement and axle load. Measurements were taken at Three distinct temperatures (12, 21, and 43 C) and two different sets of speeds were used for truck passages. Average value is utilised as the equivalent temperature of the pavement structure for each season. Temperature measurements are collected at the surface, inside and at the bottom of the surface layer.

Table 4.7: Experimental Variables and Levels

Variable	Level (No. of Levels)
1 (Lower-Limit)	1(6.1)
Test Trucks	Type 1, type 2 (2)
Axle Load	98,138 177 kN (Truck 1) 177,255, 334 kN (Truck 2) (3 For Each Axle Type)
Speed	Single Axle Load $\leq$ 138 kN, Tandem Axle Load $<$ 255 kN (20, 30, 40, 80 Km hr^{-1}) Single Axle Load $>$ 138 kN, Tandem Axle Load $\geq$ 255 kN (20, 30, 40, 60 Km hr^{-1}) (4 for Each Axle Load)
Pavement Temperature	Winter (12°C), Spring (21°C), Summer (43°C) (3)
Pavement Type	S1, S2, S3 (3)

The findings demonstrated that: 1) S2 pavement exhibits the highest sensitivity to temperature fluctuations, whereas semi-rigid pavement (S1) displays the least dependency on temperature. 2) Strain increases with higher axle load, decreases with high speed, and rises with increased temperature. So, a high loading condition coupled with a high temperature might hasten the development of fatigue damage. 3)'Due to the viscosity characteristics of asphalt material, the impact of truck 2 on the pavement would result in strain accumulation, leading to a greater

strain response compared to truck 1. Finally, strain responses were predicted using a multivariate regression model, and it was discovered that the numerical and experimental findings matched well [141].

4.8. Test section in the state of Maine

The aim of this research project is to offer an overview of the instrumentation employed in Maine's first fully instrumented flexible pavement test section, share valuable insights derived from the utilization of this instrumentation, and present the results of the testing conducted thus far. The selected test segment for this project comprises a portion of Route 15 that traverses Guilford, Maine [142].

For the measurements described in this section, the following sensors were used. It consists of twelve asphalt strain gauges, six asphalt thermocouples, four soil strain gauges, four soil pressure cells, six soil moisture gauges, 24 soil thermocouples and two frost resistivity probes. A schematic of the layers and instruments for the test section shown in Figure 4.12.

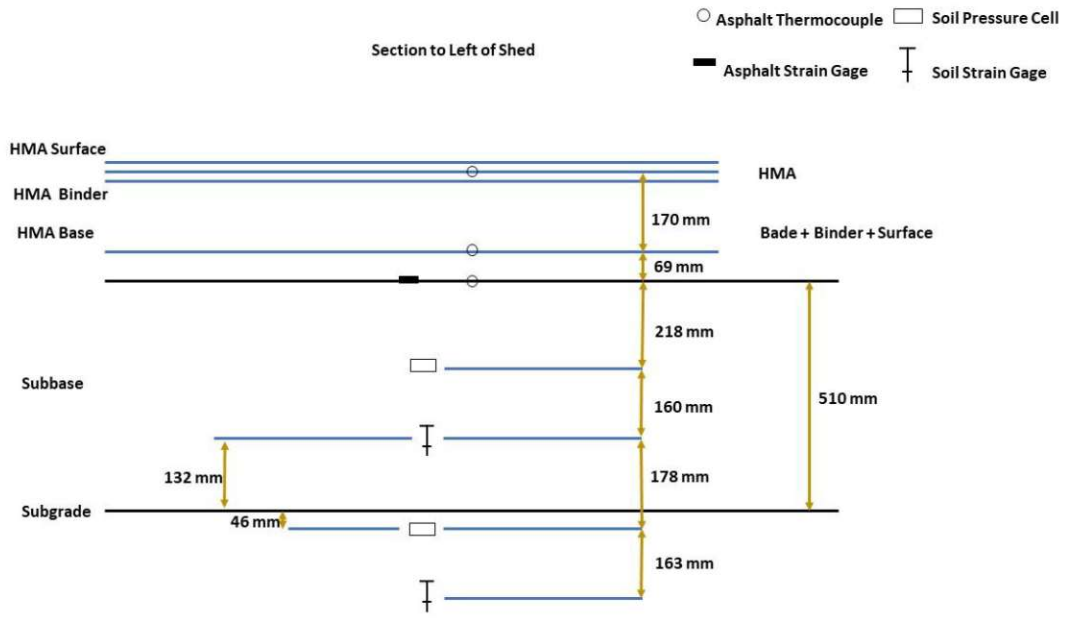

Figure 4.12: Schematic of layers and instruments (Subbase and subgrade instruments were installed in two sections, while HMA strain gauges were installed in four sections)

A separate data collecting system was attached to each type of sensor. It was designed for dynamic and static data collection. This research project demonstrated how installing asphalt strain sensors is very sensitive. The failure rate was high and 3 of the 12 implanted sensors did not survive the building process. By driving a vehicle with a given axle load through a number

of passes, stress and strain measurements were gathered. Three loading cases were considered. To assess the impact of speed and temperature on pavement reaction, each example included truck crossings at five different speeds in a short-range temperature. It was discovered that while speed variation significantly affects the observed strain, duration of loading did not change at various depths. Finally, the experimental design was modelled using an elastic model. For low temperatures and speeds, a strong correlation between experimental and numerical findings was found [109]. The instruments and installation are briefly described in the sections below [142].

The temperatures of the subgrade, subbase and HMA layers were recorded using thermocouples that were inserted at various depths. 20-gauge copper-constantan (Type T) wire pairs were used for thermocouples and each wire pair termination was secured with silicone and a heat-shrink cap. The connection was crimped with a quick tip. The electrical potential created by the bimetal reaction at the wire tip connection is proportional to the difference in temperature between the ends of the wire. with the wire end attached to a readout device with the end being in the ground. The ground temperature may be determined using the readout device reference temperature.

Two strings of 12 Type T thermocouples were used to measure soil temperatures. Each thermocouple string was built using 12-pair wire that was produced by PMC Corporation under the model number TX-212TE/TE061-20U. The thermocouples were mounted on a 2.1 m wooden dowel for each string by threading the wires through holes bored in the dowel at the following intervals. Lowest five thermocouples were placed at 0.3 m and the highest five thermocouples were spaced at 0.5 m. The following six were separated by 0.15 m. The last thermocouple was a flier not one that was inserted through the dowel hole. This thermocouple was built with a longer lead wire so that it could be buried in the ground separately from the other components of the string [142].

The road surface was still at the subgrade level when holes were bored and held open using 7.6 cm diameter PVC pipe prior to the installation of soil thermocouples. The wooden dowel with the thermocouple string was lowered into the hole on the day that the subbase aggregate was being laid. A section of the dowel was left above the subgrade level. The pipe was then retrieved from the hole. Back to the side of the road, the ends of the wires that would be attached to a readout box were routed via a 19 cm PVC conduit. The top thermocouple flyer was placed about 1 m away from the dowel and was covered with extra soil. That was after the subbase

aggregate was backfilled over the PVC pipe and around the exposed piece of the thermocouple string. The thermocouple string was well covered and the standard subbase compaction was finished. The thermocouple flyer on the right side of the instrumented area was not placed far from the remainder of the string while using the identical approach to both thermocouple strings. The top of each string of thermocouples was positioned to be 0.4–0.5 m below completed grade [142].

Using wire from Omega Engineering (TT-T-20 SLE) HMA temperatures were monitored at three depths. This wire was identical to the soil thermocouple wire with the exception that it only had one pair of copper-constantan wires as opposed to 12. That was coated with a robust material that could resist pavement temperatures. Cables temperature-measuring ends were put on the road surface for installation and the sensors were then covered with paving. The cables were underground PVC pipe that was stretched away from the road [142].

From this study, the following conclusions can be drawn:

1) The strain in the HMA layer exhibits a significant delay relative to the fitted model.

2) Time of loading significantly affects tensile strain in the HMA layer, and it can be accurately modelled using a sigmoidal function.

3) at lower temperatures and shorter loading times, tensile strains in the HMA layer closely align with predictions.

4) for the subbase, stresses are consistently underestimated, while predicted strains closely match measured strains. In contrast, for the subgrade, both stresses and strains consistently exceed predicted values, with the disparity growing as loading time and temperature increase.

4.9. The instrumentation of the AA1N highway in France

The instrumentation described is situated along the French four-lane highway A4IN, which runs between Annecy and Chambery [143]. During certain maintenance tasks in 2012, the work was completed. 47 asphalt strain gauges (horizontal and vertical), 12 temperature probes and 2 FBGs sensors were used to instrument two sections. Strain sensors were strategically positioned within the three new pavement layers: the subbase course, the base course, and the wearing course (as illustrated in Figure 4.13).

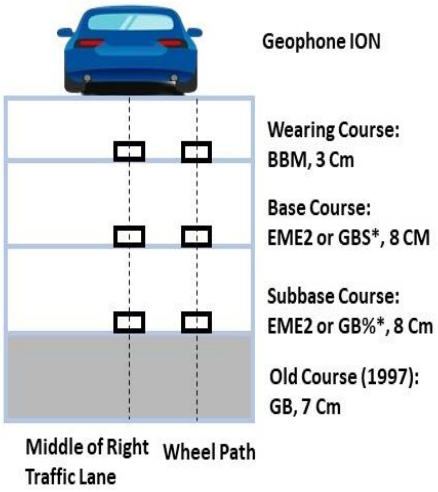

Figure 4.13: The instrumented pavement and the placement of sensors in the transverse direction

For each course, a subset of sensors was installed in the right traffic lane, under the right wheel path, and at the lane's midpoint. The spacing between these two transverse positions was approximately 1.30 meters. These sensors were organized into sets of three to measure longitudinal, transverse, and vertical strain. In each course, two sets were deployed to ensure measurements in both directions, even if some sensors became damaged during the pavement construction process (as shown in Figure 4.14). It's worth noting that no vertical strain sensor could be placed in the wearing course due to its limited thickness.

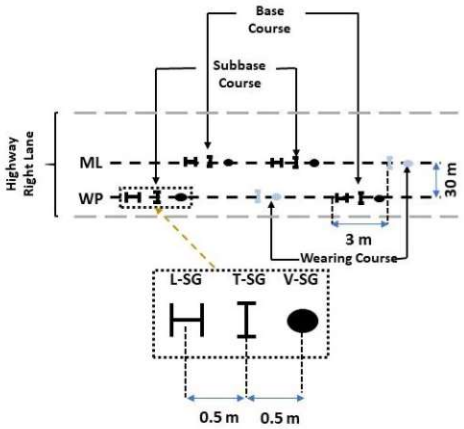

Figure 4.14: Schema of half of the instrumentation on the pavement section

The strain gauges installed in the asphalt pavement under construction experience substantial strains and must maintain resilience over time. Hence, employing field-tested designs utilizing robust materials is crucial for ensuring accurate and reliable long-term data acquisition. Each sensor is composed of four gauges affixed around a vinyl rod, defining the measurement area.

Additionally, two aluminium bars flanking each sensor ensure optimal integration with the asphalt mix. Moreover, sensors placed longitudinally feature a thermistor element adjacent to the gauges, facilitating in-situ temperature measurement across each course.

In the EME2 section, two optical fibers with Bragg gratings were embedded into each course. These fibers are integrated within a geotextile, which not only secures the optical fibers but also ensures good cohesion with the asphalt.

Measurements were conducted on the instrumented pavement using a designated loadbearing truck. The loading truck used is a brine truck typically employed for snow removal. Before each measurement, the load is calibrated by controlling two parameters:

1. Weight of Each Half Axle: The rear axle is rated at 13,000 kg, adhering to the French reference axle standard.

2. Tire Pressure: This is adjusted to ensure consistent load distribution on the pavement surface. Three different speeds were targeted. The experimental design data analysis revealed that truck trajectory and vehicle speed had a significant influence on measured strains in flexible pavements [143].

For each measurement, the transversal position of the truck is recorded. Transversal sand strips are installed at the beginning, middle, and end of the measurement zone to facilitate this. After each truck pass, the distance between the tire footprint in the sand and the sensor line is measured. From this, the distance between the load and sensors can be deduced. The ΔDj parameter is defined as the distance between sensor j and the middle of the rear left axle. This parameter is positive when the load is to the left of sensor j in the traffic direction. To assess the effect of ΔDj on measured strain, the loaded truck takes different trajectories.It is notable that the strain is three times higher when the load is directly above the sensors (25 µm/m) compared to when the load is on either side (8 µm/m) [143].

Regarding the influence of speed, the pavement was loaded at different speeds (10 km/h, 50 km/h, and 90 km/h). The measurement temperature was 23°C, and ΔD was 180 cm (with the right rear axle above the sensors). At a speed of 12 km/h, the maximum strain for the rear axle is 24 µm/m. At a speed of 70 km/h, the maximum strain for the rear axle is 9 µm/m. The effect of speed is significant: an increase in speed from 12 km/h to 70 km/h reduces strain by 2.5 times. This decrease in strain with increasing speed aligns with the viscoelastic properties of asphalt.

4.10. Chongqing International Airport Asphalt Pavement Sensor Network Monitoring

In light of the intricate natural environment and diverse aircraft loadings, the imperative first step in assessing pavement performance is the extraction of critical data from the monitoring database. The dynamic response data of airport pavement, obtained through embedded sensors, can be harnessed to enhance pavement design methodologies, fine-tune mechanical models, and assess pavement performance. A monitoring system was established at the connecting taxiway AG of Chongqi Jiangbei International Airport. This research predominantly relied on Fiber Bragg Grating (FBG) measurement technology, with the utilization of moving average filters and Fast Fourier Transform (FFT) filters in digital signal processing (DSP) for monitoring data processing and dynamic response acquisition [144]. Dong et al. (2018) offers a layout plan of an airport asphalt pavement sensor network for monitoring structural information. Three elements of the sensor matrix may be distinguished.

- Response monitoring group
- Wandering determination group
- Temperature monitoring group

Different types of FBG sensors from two domestic companies were used for response measurement. The SI425 optical sensing demodulator from Micron Optics Inc., connected to the sensors via cable, was employed to collect the monitoring data. A camera was used to capture image information of the aircraft. Collecting data using the demodulator in situ was impractical due to the rigorous operational management of the airport. Alternatively, using high-power wireless access points from TP-Link provided an acceptable solution to transmit response data wirelessly to a permissible region of the airport.

The first group consists of parallel rows of vertical, longitudinal and transverse strain sensors. Pressure cells, vertical, longitudinal and transverse strain sensors were placed at various distances from the centreline. This was carried out according to the main landing gear configuration of most common aircraft with a longitudinal spacing of 0.5 m between sensors of the same row. The goal of the wandering group was to ascertain the aircrafts wandering with its impact on dynamic reaction and distribution. To detect the transverse position of each nose wheel, Seven transverse strain sensors were inserted close to the centreline ranging from 0 to 1.2 m with 0.2 m pitch. To counteract the effects of aircraft weight, the third sensing group

included two temperature sensors that were situated 16 meters from the centreline [144]. Figure 4.15 illustrates the sensor arrangement and the pavement structure at the taxiway.

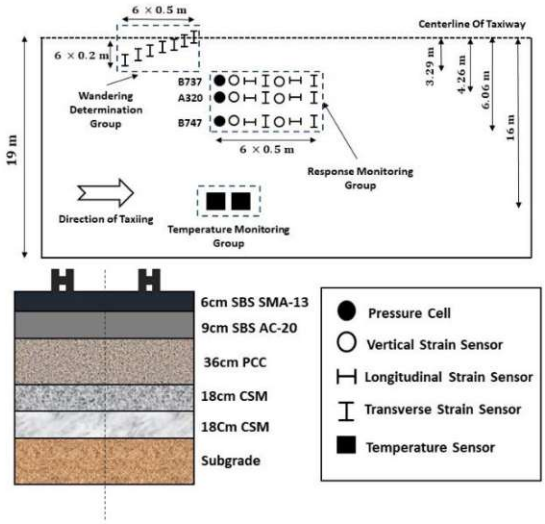

Figure 4.15: Sensor layout and pavement structure

The dynamic response of asphalt pavement is also significantly affected by aircraft speed. The aircraft speed can be calculated by dividing the longitudinal distance between the two sensors by the interval between the longitudinal strain time histories. The duration of the dynamic response exhibits an inverse proportional relationship with speed, following a power function. Furthermore, the forward and backward propagation distances of stress and strain appear to be uncorrelated with taxiing speed.

Using both the signal correlation method and the time difference method, it is possible to calculate the speed of individual passing aircraft. The findings obtained from these two methodologies exhibit strong consistency.

A moving average filter can be employed to denoise the response induced by temperature, while an FFT (Fast Fourier Transform) filter is recommended for eliminating noise from the external environment. Considering the signal sampling theorem, the permissible transverse interval for the wandering determination sensors depends on the geometries of both the nose wheel and the sensors.

Up until this point, the presentation of the influence of temperature and aircraft wheel type has been hindered by the lack of comprehensive monitoring data.

Chapter 5: Conclusion

In conclusion, real-time and long-term monitoring of road infrastructures is very important part of pavement management systems. The ability to assess the current health conditions of pavements empowers allows a strategical of existing pavements planning and execution of different maintenance measures, ultimately enhancing road safety and prolonging the lifespan of these vital transportation arteries. Embedded sensors emerge as a potent tool for tracking pavement deterioration over time, offering a non-disruptive alternative to traditional assessment methods.

In road construction, advanced sensor technologies have enhanced our capability in monitoring and maintaining infrastructure. Various sensing technologies have been explored in the literature to evaluate pavement health. The application of accelerometers, strain sensors, temperature sensors, and humidity sensors provides detailed information regarding roadways' structural health and environmental conditions. Sensors have distinct features with different advantages and disadvantages, which must be seriously considered to optimize their application. While these innovations have the potential to revolutionize infrastructure monitoring, it is crucial to acknowledge the need for further research and development in this field.

Accelerometers and geophones have enabled the assessment of pavement deflection leading to the calculation of resilient modulus through back calculation procedures. These devices, distinguished by their compact size and consistent output measurements offer promising avenues for future exploration. Also, if a sensor malfunctions or breaks, it can be replaced easily. Based on the research projects in Chapter 4, a drawback of these sensors is that they measure acceleration, which must be converted to deflection through mathematical integration. Finding suitable methods to achieve this is still under investigation. High precision, however, often costs dearly, and the large volume of data produced will also require advanced processing capabilities. In addition, calibration is necessary periodically to keep the accelerometers accurate.

The most frequently employed strain sensors are asphalt strain gauges which can be employed either in a horizontal H-gauge configuration or vertically. Their ability to detect minute changes makes them essential for long-term infrastructure management also their smaller size makes them particularly well-suited for large-scale applications. Despite their accuracy, installation of the strain sensors is labour-intensive, mainly in existing structures, and they must be

protected against harsh environmental conditions to prevent damage. Besides, high-quality strain sensors cost a lot. Based on the research by Valentin Donev et al. on motorway A10 south of Salzburg, motorway A3 south of Vienna, and Expressway S31 in Chapter 4, sensor overload during the hot-state roller compaction of asphalt layers was the main issue encountered with strain gauges. To prevent such problems, it is recommended to install a steel dummy as a placeholder in the hot asphalt layers immediately after their construction and just before compaction.

The temperature sensors are easy to install and maintain; they are cost-effective and monitor environmental conditions that affect road materials and structure. Although they provide relevant information on the changes in temperature, they do not express information on the structural stress or damage, hence would require more sensors to achieve full monitoring. Moreover, temperature sensors require regular calibration and could be vulnerable to extremely weather conditions. Humidity sensors are of prime importance in the identification of moisture levels, which might be contributory to structural damage, like corrosion and frost heave. They act as early warning systems to water infiltration and leaks, hence increasing the longevity of road infrastructure. However, the installation of humidity sensors could be tricky, and their accuracy might eventually deteriorate with environmental factors. Regular maintenance will be required in order to ensure their long-term reliability.

MEMS and Wireless sensors represent a cutting-edge solution for infrastructure condition monitoring, providing wireless detection and monitoring capabilities for structural and material-related damage. Notably, wireless monitoring systems offer cost-effective installation, eliminating the need for extensive wiring. MEMS-based sensor systems hold great promise in achieving Smart Pavement Structural Health Monitoring (SHM). Moving forward, several critical areas warrant focused research and attention.

1. **Energy Consumption and Power Harvesting**: Overcoming the limitation of battery life in sensors is essential. Power harvesting technologies such as piezoelectric transducers that convert ambient energy sources like vibrations from passing vehicles into electrical energy, present a promising solution. Further research is needed to make power harvesting practical for widespread commercial adoption. Additionally, efforts should be concentrated on increasing memory capacity and miniaturizing the entire sensor system.

2. **Data Processing and Modelling**: The fluctuation in vehicle type, speed, wheel-load distribution, humidity, temperature and pavement roughness during real pavement monitoring poses significant challenges. To mitigate these impacts effectively, efficient data processing techniques and precise modelling should be developed.

3. **Commercialization of MEMS and Wireless Sensing Technologies**: While MEMS and wireless sensing technologies hold immense potential, many are still in the research phase and have not yet reached commercialization. Future efforts should be focused on bridging this gap leading these innovations to practical and real-world applications.

In conclusion, the field of pavement monitoring through sensing technologies is evolving rapidly offering tremendous benefits for infrastructure management. However, it is clear that continued research and development efforts are essential to address challenges, refine technologies to ensure the successful integration into pavement management systems for safer and more durable roads.

Appendix

List of Figures

List of Tables

References

1. Modares, M. and N. Waksmanski, *Overview of structural health monitoring for steel bridges.* Practice Periodical on Structural Design and Construction, 2013. **18**(3): p. 187-191.
2. Ceylan, H., et al., *Development of a wireless MEMS multifunction sensor system and field demonstration of embedded sensors for monitoring concrete pavements: volume I.* 2016.
3. Zonzini, F., et al., *Vibration-based SHM With upscalable and low-cost sensor networks.* IEEE Transactions on Instrumentation and Measurement, 2020. **69**(10): p. 7990-7998.
4. Girolami, A., D. Brunelli, and L. Benini. *Low-cost and distributed health monitoring system for critical buildings*. in *2017 IEEE Workshop on Environmental, Energy, and Structural Monitoring Systems (EESMS)*. 2017. IEEE.
5. Ina Schumacher , Prof. Dr. Jürgen Wöllenstein. Abschlussbericht der Machbarkeitsstudie zur Entwicklung von Sensoren zur Erfassung des strukturellen Straßenzustands. Fraunhofer-Institut für Physikalische Messtechnik in Freiburg. 2012.
6. Hou, Y., et al., *The state-of-the-art review on applications of intrusive sensing, image processing techniques, and machine learning methods in pavement monitoring and analysis.* Engineering, 2021. **7**(6): p. 845-856.
7. Shuo Yang, et al., Health monitoring of pavement systems using smart sensing technologies. Published by ProQuest LLC (2015).
8. Nils Thorstensen, Unive. -Prof.Dip. -Ing. Dr.techn.Norbert Ostermann, Univ.Ass.Dip.-Ing. Michael Ostermann, Projektass. Dip.-Ing .Johannes Kehrer, Fahrwegispektion Ansatz einer objektiven Zustandserfassung, submitted to obtain the academic degree of master of Engineering Sciences, submitted at the Vienne University of Technology, 2019.
9. Valentin Donev, Univ. Prof. Dipl.-Ing. Dr. techn. Ronald Blab and Univ. Ass. Dipl.-Ing. Dr. techn. Markus Hoffmann, Erhaltungsmanagement Straßenoberbau -Zustandsbewertung und Zustandsprognose, submitted to obtain the academic degree of Master of Engineering Sciences, submitted at the Vienna University of Technology, Faculty of Civil Engineering, 2014.
10. Flintsch, G.W. and K.K. McGhee, *Quality management of pavement condition data collection*. Vol. 401. 2009: Transportation Research Board.
11. Univ.Lektor.Dipl.-Ing. Dr.techn. Markus Hoffmann, Script: Straßenerhaltung und Infrastrukturmanagement, 2019
12. Ahmed Elseicy, Alex Alonso-Díaz, Mercedes Solla, Mezgeen Rasol and Sonia Santos Assunçao, Combined Use of GPR and Other NDTs for Road Pavement Assessment, Remote Sens. 2022, 14, 4336: p. 8-22.
13. Gopalakrishnan, K., et al., *Wireless MEMS for transportation infrastructure health monitoring*, in *Wireless MEMS Networks and Applications*. 2017, Elsevier. p. 53-76.
14. Hu, J.; Vennapusa, P.K.R.; White, D.J.; Beresnev, I. Pavement thickness and stabilised foundation layer assessment using ground-coupled GPR. Nondestruct. Test. Evaluation 2015, 31, 267–287
15. Valentin Donev, Olaf Lahayne, Bernhard Pichler & Lukas Eberhardsteiner. Ultrasonic characterisation of the elastic properties of mineral aggregates used in asphalt mixtures. Institute of Transportation, TU Wien.2023
16. Park, C.-S.; Jeong, J.-H.; Park, H.-W.; Kim, K. Experimental Study on Electrode Method for Electrical Resistivity Survey to Detect Cavities under Road Pavements. Sustainability 2017, 9, 2320.
17. Arbeitsanleitung für Griffigkeitsmessungen mit dem SRM, Forschungsgesellschaft für Straßen und Verkehrswesen (FGSV), FGSV-Nr. 409, ISBN 3-937356-26-6, Köln.
18. Rosario, F., et al. *Sensing road pavement health status through acoustic signals analysis*. in *2017 13th Conference on Ph. D. Research in Microelectronics and Electronics (PRIME)*. 2017. IEEE.

19. Pan, Y., et al., *OBJECT-BASED AND SUPERVISED DETECTION OF POTHOLES AND CRACKS FROM THE PAVEMENT IMAGES ACQUIRED BY UAV.* International Archives of the Photogrammetry, Remote Sensing & Spatial Information Sciences, 2017. **42**.
20. Pan, Y., et al., *Detection of asphalt pavement potholes and cracks based on the unmanned aerial vehicle multispectral imagery.* IEEE Journal of Selected Topics in Applied Earth Observations and Remote Sensing, 2018. **11**(10): p. 3701-3712.
21. Zhang, L., et al. *Study on pavement defect detection based on image processing utilizing UAV*. in *Journal of Physics: Conference Series*. 2019. IOP Publishing.
22. Pan, Y., et al., *Monitoring Asphalt Pavement Aging and Damage Conditions from Low-Altitude UAV Imagery Based on a CNN Approach.* Canadian Journal of Remote Sensing, 2021. **47**(3): p. 432-449.
23. Zhang, C. and A. Elaksher, *An unmanned aerial vehicle-based imaging system for 3D measurement of unpaved road surface distresses 1.* Computer-Aided Civil and Infrastructure Engineering, 2012. **27**(2): p. 118-129.
24. Zhang, K., H. Cheng, and B. Zhang, *Unified approach to pavement crack and sealed crack detection using preclassification based on transfer learning.* Journal of Computing in Civil Engineering, 2018. **32**(2): p. 04018001.
25. Huincalef, R., et al. *An Approach to Automated Recognition of Pavement Deterioration Through Machine Learning*. in *Argentine Congress of Computer Science*. 2018. Springer.
26. Van Der Horst, B., R. Lindenbergh, and S. Puister, *Mobile laser scan data for road surface damage detection.* International Archives of the Photogrammetry, Remote Sensing and Spatial Information Sciences, 2019. **42**(2/W13).
27. Fan, R., et al., *Pothole detection based on disparity transformation and road surface modeling.* IEEE Transactions on Image Processing, 2019. **29**: p. 897-908.
28. Sattar, S., S. Li, and M. Chapman, *Road surface monitoring using smartphone sensors: A review.* Sensors, 2018. **18**(11): p. 3845.
29. Basavaraju, A., et al., *A machine learning approach to road surface anomaly assessment using smartphone sensors.* IEEE Sensors Journal, 2019. **20**(5): p. 2635-2647.
30. Souza, V.M., *Asphalt pavement classification using smartphone accelerometer and complexity invariant distance.* Engineering Applications of Artificial Intelligence, 2018. **74**: p. 198-211.
31. Astarita, V., et al., *A mobile application for road surface quality control: UNIquALroad.* Procedia-Social and Behavioral Sciences, 2012. **54**: p. 1135-1144.
32. Wu, C., et al., *An automated machine-learning approach for road pothole detection using smartphone sensor data.* Sensors, 2020. **20**(19): p. 5564.
33. Vittorio, A., et al., *Automated sensing system for monitoring of road surface quality by mobile devices.* Procedia-Social and Behavioral Sciences, 2014. **111**: p. 242-251.
34. Li, J., X. Zhao, and H. Li. *Method for detecting road pavement damage based on deep learning*. in *Health Monitoring of Structural and Biological Systems XIII*. 2019. SPIE.
35. Aslan, O.D., et al. *Using Artifical Intelligence for Automating Pavement Condition Assessment*. in *International Conference on Smart Infrastructure and Construction 2019 (ICSIC) Driving data-informed decision-making*. 2019. ICE Publishing.
36. Bhatia, Y., et al., *Convolutional neural networks based potholes detection using thermal imaging.* Journal of King Saud University-Computer and Information Sciences, 2019.
37. Wu, H., et al., *Road pothole extraction and safety evaluation by integration of point cloud and images derived from mobile mapping sensors.* Advanced Engineering Informatics, 2019. **42**: p. 100936.
38. Sodano, H.A., D.J. Inman, and G. Park, *A review of power harvesting from vibration using piezoelectric materials.* Shock and Vibration Digest, 2004. **36**(3): p. 197-206.
39. Bâzu, M., et al., *Quantitative accelerated life testing of MEMS accelerometers.* Sensors, 2007. **7**(11): p. 2846-2859.
40. Akyildiz, I.F., et al., *Wireless sensor networks: a survey.* Computer networks, 2002. **38**(4): p. 393-422.
41. Chamanian, S., et al., *Powering-up wireless sensor nodes utilizing rechargeable batteries and an electromagnetic vibration energy harvesting system.* Energies, 2014. **7**(10): p. 6323-6339.

42. Xue, W., et al., *Pavement health monitoring system based on an embedded sensing network.* J. Mater. Civ. Eng, 2014. **26**(10): p. 04014072.
43. Mulholland, P., *Pavement management systems (PMS) for local government; guidelines report.* 1991.
44. Attoh-Okine, N. and O. Adarkwa, *Pavement condition surveys–overview of current practices.* Delaware Center for Transportation, University of Delaware: Newark, DE, USA, 2013.
45. Wolters, A., et al., *Implementing pavement management systems for local agencies*. 2011.
46. Peterson, D., *Pavement management practices. Final report*. 1987, National Research Council, Washington, DC (USA). Transportation Research Board.
47. Shahin, M., et al., *PAVER 5.1 User Manual.* US Army Corps of Engineers, Engineer Research and Development Center, Construction Engineering Research Laboratory, 2010.
48. Shamsabadi, S.S., *Design and implementation of Pavemon: A gis web-based Pavement Monitoring System based on large amounts of heterogeneous sensors data*. 2015: Northeastern University.
49. Shahin, M., et al., *Effect of sample unit size and number of surveyed distress types on pavement condition index for asphalt-surfaced roads.* Transportation research record, 1995(1508).
50. Shahini Shamsabadi, S., *Design and implementation of PAVEMON: A GIS web-based pavement monitoring system based on large amounts of heterogeneous sensors data.* Ph. D. Thesis, 2015.
51. Zhang, Z. and M.R. Murphy, *AWeb-BASED PAVEMENT PERFORMANCE AND MAINTENANCE MANAGEMENT AND GIS MAPPING SYSTEM FOR EASY ACCESS TO PAVEMENT CONDITION INFORMATION.* 2012.
52. Dipl.-Ing. Alfred Weninger-Vycudil, o.Univ.Prof.Dipl.-Ing.Dr.nat.techn. Johann Litzka, Entwicklung von Systemelementen für ein österreichisches Pavement Management System. submitted to obtain the academic degree of Doctor of Technical Sciences, submitted at the Vienna University of Technology, Faculty of Civil Engineering, 2001.
53. Mohammad Fahad, Richard NAGY, Daniel GOSZTOLA. PAVEMENT SENSING SYSTEMS. Civil and Environmental Engineering Vol. 18, Issue 2, 603-630.2022
54. Lajnef, N., et al., *Toward an integrated smart sensing system and data interpretation techniques for pavement fatigue monitoring.* Computer-Aided Civil and Infrastructure Engineering, 2011.
26(7): p. 513-523
55. Di Graziano, A., et al., *Structural health monitoring of asphalt pavements using smart sensor networks: A comprehensive review.* 2020. **7**(5): p. 639-651.
56. Noureldin, A., T.B. Karamat, and J. Georgy, *Fundamentals of inertial navigation, satellite-based positioning and their integration.* 2013.
57. Groves, P.D., *Principles of GNSS, inertial, and multisensor integrated navigation systems, [Book review]*. IEEE Aerospace and Electronic Systems Magazine, 2015. **30**(2): p. 26-27.
58. Ma, X., Z. Dong, and Y. Dong, *Toward asphalt pavement health monitoring with built-in sensors: A novel application to real-time modulus evaluation.* IEEE Transactions on Intelligent Transportation Systems, 2021.
59. Enriquez, K.C., *Characterization Of A Mems Accelerometer For A Highway Health Monitoring Ultra-Low Power Sensor.* 2009.
60. Officials, T., *AASHTO Transportation Asset Management Guide: A Focus on Implementation*. 2011: AASHTO.
61. Steve Hanly. Shock & Vibration Overview. Midé Technology's website.2016.
62. Willis, J. and B.J.P.o.t.I. Jimerson, *A piezoelectric accelerometer.* 1964. **52**(7): p. 871-872.
63. Aoyagi, S., et al., *Surface micromachined accelerometer using ferroelectric substrate.* 2007. **139**(1-2): p. 88-94.
64. Ji, X., et al., *Fabrication and performance of a self-powered damage-detection aggregate for asphalt pavement.* Materials & Design, 2019. **179**: p. 107890.
65. Ji, X., et al., *Fabrication and performance of a self-powered damage-detection aggregate for asphalt pavement. 2019. 179: p. 107890.*
66. Johannes Wagner, Jan Burgemeister. Piezoelectric Accelerometers. Metra Mess- und Frequenztechnik Radebeul.2021.

67. Zakriya Mohammed, Ibrahim (Abe) M Elfadel, Mahmoud Rasras, *Monolithic Multi Degree of Freedom (MDoF) Capacitive MEMS Accelerometers*, Micromachines, 2018.
68. Aaron Partridge, et al., *A High-Performance Planar Piezoresistive Accelerometer*, JOURNAL OF MICROELECTROMECHANICAL SYSTEMS, 2000.
69. Mohammed, A.A., W.A. Moussa, and E. Lou, *High-performance piezoresistive MEMS strain sensor with low thermal sensitivity.* Sensors, 2011. **11**(2): p. 1819-1846.
70. Suhling, J.C. and R.C. Jaeger, *Silicon piezoresistive stress sensors and their application in electronic packaging.* IEEE sensors journal, 2001. **1**(1): p. 14-30.
71. Ravneet Bajwa, Erdem Coleri, Ram Rajagopal, Pravin Varaiya, Christopher Flores. Pavement performance assessment using a cost-effective wireless accelerometer system. Comput Aided Civ Inf. 2020;35:1009–1022. 2020.
72. Ed Spence. What You Need to Know About MEMS Accelerometers for Condition Monitoring. www.analog.com. 2016.
73. Ruiz, J.M., et al., *Computer-Based Guidelines For Concrete Pavements Volume II: Design and Construction Guidelines and HIPERPAV II User's Manual*. 2005, United States. Federal Highway Administration. Office of Infrastructure
74. Di Graziano, A., V. Marchetta, and S. Cafiso, *Structural health monitoring of asphalt pavements using smart sensor networks: A comprehensive review.* Journal of Traffic and Transportation Engineering (English Edition), 2020. **7**(5): p. 639-651.
75. Zhao, H., et al., *Harvesting energy from asphalt pavement by piezoelectric generator.* Journal of Wuhan University of Technology-Mater. Sci. Ed., 2014. **29**(5): p. 933-937.
76. Di Nuzzo, F., et al., *Structural health monitoring system with narrowband IoT and MEMS sensors.* IEEE Sensors Journal, 2021. **21**(14): p. 16371-16380.
77. Nakas, C., D. Kandris, and G. Visvardis, *Energy efficient routing in wireless sensor networks: a comprehensive survey.* Algorithms, 2020. **13**(3): p. 72.
78. Ghosh, S.K., et al. *Power efficient event detection scheme in wireless sensor networks for railway bridge health monitoring system*. in *2014 IEEE International Conference on Advanced Networks and Telecommuncations Systems (ANTS)*. 2014. IEEE.
79. Rault, T., A. Bouabdallah, and Y. Challal, *Energy efficiency in wireless sensor networks: A top-down survey.* Computer networks, 2014. **67**: p. 104-122.
80. Lajnef, N., et al., *Smart pavement monitoring system*. 2013, United States. Federal Highway Administration.
81. Das, N.K., F. Khorrami, and S. Nourbakhsh. *New integrated piezoelectric-dielectric microstrip antenna for dual wireless actuation and sensing functions*. in *Smart Structures and Materials 1998: Smart Electronics and MEMS*. 1998. SPIE.
82. Jung, K.H., J.W. Bredow, and S.P. Joshi. *Electromagnetically coupled embedded sensors*. in *Smart Structures and Materials 1999: Industrial and Commercial Applications of Smart Structures Technologies*. 1999. SPIE.
83. Alavi, A.H., et al., *Continuous health monitoring of pavement systems using smart sensing technology.* Construction and Building Materials, 2016. **114**: p. 719-736.
84. Mita, A., S.J.S.M. Takhira, and Structures, *A smart sensor using a mechanical memory for structural health monitoring of a damage-controlled building.* 2003. **12**(2): p. 204.
85. El-Wakeel, A., *Robust Multisensor-Based Framework for Efficient Road Information Services*. 2020, Queen's University (Canada).
86. Grewal, M.S., L.R. Weill, and A.P. Andrews, *Global positioning systems, inertial navigation, and integration*. 2007: John Wiley & Sons.
87. Arraigada, M., et al., *Evaluation of accelerometers to determine pavement deflections under traffic loads.* Materials and Structures, 2009. **42**(6): p. 779-790.
88. Gindy, M., H.H. Nassif, and J. Velde, *Bridge displacement estimates from measured acceleration records.* Transportation research record, 2007. **2028**(1): p. 136-145.
89. Rajagopal, R., et al., *Sensor network for pavement performance monitoring*, in *Computing in Civil Engineering (2013)*. 2013. p. 97-104.

90. Arraigada, M., M.N. Partl, and S. Angelone, *Determination of road deflections from traffic induced accelerations.* Road materials and pavement design, 2007. **8**(3): p. 399-421.
91. Boore, D.M., *Effect of baseline corrections on response spectra for two recordings of the 1999 Chi-Chi, Taiwan, earthquake*. 1999: US Department of the Interior, US Geological Survey.
92. Chen, W., et al. *Implementation of 2-axis Circular Interpolation for a FPGA-based 4-axis Motion Controller*. in *2007 IEEE International conference on control and automation*. 2007. IEEE.
93. Valentin Donev, et al., Instrumentation of field-testing sites for dynamic characterization of the temperature-dependent stiffness of pavements and their layers, TU Wien, Institut for Transportation
94. Valentin Donev, Olaf Lahayne, Bernhard Pichler & Lukas Eberhardsteiner, Ultrasonic characterisation of the elastic properties of mineral aggregates used in asphalt mixtures. Institute of Transportation, TU Wien.2023
95. Levenberg, E., *Inferring pavement properties using an embedded accelerometer.* International Journal of Transportation Science and Technology, 2012. **1**(3): p. 229-246.
96. Council, V.T.R., *Business Needs for Pavement Engineering*. 2003: Transportation Research Board, National Research Council.
97. Dowling, R., *National Cooperative Highway Research Program (NCHRP) Report 535: Predicting Air Quality Effects of Traffic-Flow Improvements: Final Report and User's Guide. Transportation Research Board.* 2005.
98. Chung, H.-C., et al. *Real-time visualization of bridge structural response through wireless MEMS sensors*. in *Testing, Reliability, and Application of Micro-and Nano-Material Systems II*. 2004. SPIE.
99. Lynch, J.P., et al. *A wireless modular monitoring system for civil structures*. in *Proceedings of the 20th International Modal Analysis Conference (IMAC XX), Los Angeles, CA, February*. 2002. Citeseer.
100. Lynch, J.P., et al. *Field validation of a wireless structural monitoring system on the Alamosa Canyon Bridge*. in *Smart Structures and Materials 2003: Smart Systems and Nondestructive Evaluation for Civil Infrastructures*. 2003. SPIE.
101. Zhang, D., *Using multiple sensors to approach pavement deterioration through multiple regression analysis and distribution fitting*. 2021, Northern Arizona University
102. Silvan Schmid, Sensorik und Sensorsystme, Skriptum von Institut für Sensor- und Aktuaorsystem,2021.
103. Selvaraj, S.I., *Review on the use of instrumented pavement test data in validating flexible pavement mechanistic load response models.* Procedia-Social and Behavioral Sciences, 2012. **43**: p. 819-831.
104. Taher, B.M., R.K. Mohamed, and A. Mahrez, *A review on fatigue and rutting performance of asphalt mixes.* Scientific Research and Essays, 2011. **6**(4): p. 670-682.
105. Timm, D.H., A.L. Priest, and T.V. McEwen, *Design and instrumentation of the structural pavement experiment at the NCAT test track*. 2004, National Center for Asphalt Technology (US).
106. Loulizi, A., et al., *Data collection and management of the instrumented smart road flexible pavement sections.* 2001. **1769**(1): p. 142-151.
107. Islam, M.R., R.A.J.I.J.o.S. Tarefder, and E. Research, *Field measurement of vertical strain in asphalt concrete.* 2013. **4**(2): p. 1-6.
108. Islam, M.R. and R.A. Tarefder, *Field measurement of vertical strain in asphalt concrete.* International Journal of Scientific & Engineering Research, 2013. **4**(2): p. 1-6.
109. Barriera, M., et al., *In situ pavement monitoring: A review.* Infrastructures, 2020. **5**(2): p. 18.
110. Al-Qadi, I.L., et al., *The Virginia Smart Road: The impact of pavement instrumentation on understanding pavement performance.* Journal of the Association of Asphalt Paving Technologists, 2004. **73**(3): p. 427-465.
111. Kara De Maeijer, P., et al., *Fiber optics sensors in asphalt pavement: state-of-the-art review.* Infrastructures, 2019. **4**(2): p. 36.
112. Joshi, S. and S.M. Harle, *Linear variable differential transducer (LVDT) & its applications in civil engineering.* Int. J. Transp. Eng. Technol, 2017. **3**(4): p. 62-66.

113. Saevarsdottir, T., S. Erlingsson, and H. Carlsson, *Instrumentation and performance modelling of heavy vehicle simulator tests.* International Journal of Pavement Engineering, 2016. **17**(2): p. 148-165.
114. Zhou, C., et al., *Study on a high-temperature optical fiber F–P acceleration sensing system based on MEMS.* 2019. **120**: p. 95-100.
115. Hirayama, N. and Y. Sano, *Fiber Bragg grating temperature sensor for practical use.* ISA transactions, 2000. **39**(2): p. 169-173.
116. Maaskant, R., et al., *Fiber-optic Bragg grating sensors for bridge monitoring.* Cement and Concrete Composites, 1997. **19**(1): p. 21-33.
117. Malla, R.B., A. Sen, and N.W. Garrick, *A special fiber optic sensor for measuring wheel loads of vehicles on highways.* Sensors, 2008. **8**(4): p. 2551-2568.
118. Wang, J.-N. and J.-L. Tang, *Using fiber Bragg grating sensors to monitor pavement structures.* Transportation research record, 2005. **1913**(1): p. 165-176.
119. Udd, E. and W.B. Spillman Jr, *Fiber optic sensors: an introduction for engineers and scientists*. 2011: John Wiley & Sons.
120. Zhou, Z., et al., *Techniques of Advanced FBG sensors: fabrication, demodulation, encapsulation and their application in the structural health monitoring of bridges.* Pacific Science Review, 2003. **5**(1): p. 116-121.
121. Zhou, Z., J. Ou, and B. Wang. *Smart FRP-OFGB bars and their application in reinforced concrete beams*. in *Proceedings of the first international conference on structural health monitoring and intelligent structure*. 2003.
122. Nazarian, S. and A.J. Bush III, *Determination of deflection of pavement systems using velocity transducers.* Transportation Research Record, 1989. **1227**: p. 147-158.
123. Liu, P., et al., *Measurement and evaluation on deterioration of asphalt pavements by geophones.* Measurement, 2017. **109**: p. 223-232.
124. Duong, N.S., et al., *Monitoring of pavement deflections using geophones.* International Journal of Pavement Engineering, 2020. **21**(9): p. 1103-1113.
125. Alavi, A.H., et al., *Damage detection using self-powered wireless sensor data: An evolutionary approach.* Measurement, 2016. **82**: p. 254-283.
126. Lajnef, N., et al., *Smart Pavement Monitoring System, Report: FHWA-HRT-12-072.* Fed. Hwy. Administ.(FHWA), Washington, DC, 2013.
127. Sundaram, B.A., et al., *Wireless sensors for structural health monitoring and damage detection techniques.* Current Science, 2013: p. 1496-1505.
128. Jorge Godoy., et al., Smart Sensing of Pavement Temperature Based on Low-Cost Sensors and V2I Communications Sensors 2018, https://doi.org/10.3390/s18072092
129. Salour, F., *Moisture influence on structural behaviour of pavements: Field and Laboratory Investigations*. 2015, KTH Royal Institute of Technology.
130. Arnold, G., et al., *Pavement moisture measurement to indicate risk to pavement life*. 2017.
131. Muhammad Tariq Saeed Chani,Abdullah Mohammed Asiri and Sher Bahadar Khan, *Humidity Sensors Types and Applications,* London, United Kingdom.2023
132. Norris, A., et al., *Temperature and moisture monitoring in concrete structures using embedded nanotechnology/microelectromechanical systems (MEMS) sensors.* 2008. **22**(2): p. 111-120.
133. Yang, S., et al., *Integration of a prototype wireless communication system with micro-electromechanical temperature and humidity sensor for concrete pavement health monitoring.* Cogent Engineering, 2015. **2**(1): p. 1014278.
134. Ong, J.B., et al., *A wireless, passive embedded sensor for real-time monitoring of water content in civil engineering materials.* 2008. **8**(12): p. 2053-2058.
135. Pei, J.-S., et al. *A "Smart Dust"-based road condition monitoring system: performance of a small wireless sensor network using surge time synchronization*. in *Proceedings of the IMAC-XXV Conference*. 2007.
136. Pei, J.-S., et al., *An experimental investigation of applying Mica2 motes in pavement condition monitoring.* Journal of Intelligent Material Systems and Structures, 2009. **20**(1): p. 63-85.
137. Amir H. Alavi et al. A new approach for damage detection in asphalt concrete pavements using battery-free wireless sensors with non-constant injection rates. DOI: 10.1016/j.measurement.2017.06.035. Michigan State University.2017.

138. A.Miraliakbari, M. Hahn, *DEVELOPMENT OF A MULTI-SENSOR SYSTEM FOR ROAD CONDITION MAPPING,* The International Archives of the Photogrammetry, Remote Sensing and Spatial Information Sciences. 2014, USA.
139. Ryynänen, T., T. Pellinen, and J. Belt. *The use of accelerometers in the pavement performance monitoring and analysis*. in *IOP Conference Series: Materials Science and Engineering*. 2010. IOP Publishing.
140. Bahrani, N., et al., *Alternate method of pavement assessment using geophones and accelerometers for measuring the pavement response.* Infrastructures, 2020. **5**(3): p. 25.
141. Ai, C., et al., *Analysis of measured strain response of asphalt pavements and relevant prediction models.* International Journal of Pavement Engineering, 2017. **18**(12): p. 1089-1097.
142. Swett, L., R.B. Mallick, and D.N.J.I.J.o.P.E. Humphrey, *A study of temperature and traffic load related response in different layers in an instrumented flexible pavement.* 2008. **9**(5): p. 303-316.
143. Gaborit, P., et al., *Investigation of highway pavements using in-situ strain sensors.* Sustainability, eco-efficiency, and conservation in transportation infrastructure asset management, 2014: p. 331-337.
144. Dong, Z., X. Ma, and X.J.I.J.o.P.E. Shao, *Airport pavement responses obtained from wireless sensing network upon digital signal processing.* 2018. **19**(5): p. 381-390.